

PCA R&D Serial No. 1883

Structural Thermal Break Systems for Buildings - Heat Transfer Characteristics of Lightweight Structural Concrete Walls

by M. G. VanGeem

ORNL/Sub/84-21006/3

**STRUCTURAL THERMAL BREAK SYSTEMS
FOR BUILDINGS -
HEAT TRANSFER CHARACTERISTICS OF
LIGHTWEIGHT STRUCTURAL CONCRETE WALLS**

**Final Report
by
Martha G. Van Geem**

Report Prepared by

**CONSTRUCTION TECHNOLOGY LABORATORIES, INC.
5420 Old Orchard Road
Skokie, Illinois 60077
under Subcontract No. DE-AC05-84CE21006**

**Prepared for
Building Thermal Envelope Systems and Materials Program
Energy Division
OAK RIDGE NATIONAL LABORATORY
Oak Ridge, Tennessee 37831
Operated by
MARTIN MARIETTA ENERGY SYSTEMS INC.
for the
U.S. DEPARTMENT OF ENERGY
Under Contract No.
DE-AC05-84OR21400**

December 1988

**CR5730/824
I.D. #1993E
2109E**

Printed in the United States of America. Available from
National Technical Information Service
U.S. Department of Commerce
5285 Port Royal Road, Springfield, Virginia 22161
NTIS price codes--Printed Copy: A07 Microfiche A01

This report was prepared as an account of work sponsored by an agency of the United States Government. Neither the United States Government nor any agency thereof, nor any of their employees, makes any warranty, express or implied, or assumes any legal liability or responsibility for the accuracy, completeness, or usefulness of any information, apparatus, product, or process disclosed, or represents that its use would not infringe privately owned rights. Reference herein to any specific commercial product, process, or service by trade name, trademark, manufacturer, or otherwise, does not necessarily constitute or imply its endorsement, recommendation, or favoring by the United States Government or any agency thereof. The views and opinions of authors expressed herein do not necessarily state or reflect those of the United States Government or any agency thereof.

TABLE OF CONTENTS

	<u>Page</u>
TABLE OF CONTENTS.	i
LIST OF TABLES	iii
LIST OF FIGURES.	iv
ABSTRACT	vii
EXECUTIVE SUMMARY.	viii
Scope.	viii
Steady-State Temperature Test Results.	x
Dynamic Temperature Test Results	xii
INTRODUCTION	1
OBJECTIVES AND SCOPE	2
TEST SPECIMENS	5
Wall Construction.	5
Physical Properties of Walls	12
Instrumentation.	12
CALIBRATED HOT BOX TEST FACILITY	18
THERMAL PROPERTIES OF CONCRETE FOR STEADY-STATE TEMPERATURE CONDITIONS	21
Calibrated Hot Box Test Results.	22
Test Procedures	22
Thermal Resistance and Conductivity	22
Steady-State Temperature Profiles	24
Guarded Hot Plate Test Results	30
Test Specimens	30
Test Procedures	32
Test Results	33
Heat Flux Transducer Test Results.	37
Test Procedures	37
Test Results	37
Discussion of Results.	39
DYNAMIC (24-HR PERIODIC) CALIBRATED HOT BOX TESTS	39
Test Procedures	42
Test Results	43
Measured Temperatures and Temperature Differentials	46
Heat Flow	46
Discussion of Test Results	47
Heat Flow Comparisons	47
Thermal Lag	47
Reduction in Amplitude	50
Total Heat Flow	54
Comparisons with other Concrete Walls	57

TABLE OF CONTENTS
(continued)

	<u>Page</u>
DYNAMIC (3-FREQUENCY) CALIBRATED HOT BOX TEST.	62
Test Cycle	62
Data Collection.	64
Test Results	64
Analysis	71
TRANSIENT TEMPERATURE TESTS.	71
Test Procedures.	71
Test Results	73
SUMMARY AND CONCLUSIONS.	75
Steady-State Temperature Conditions.	75
Dynamic Temperature Conditions	76
Limitations.	77
ACKNOWLEDGMENTS.	78
REFERENCES	79
APPENDIX A - CALIBRATED HOT BOX INSTRUMENTATION AND CALIBRATION	
APPENDIX B - DYNAMIC (24-HR PERIODIC) TEMPERATURE TEST RESULTS FOR WALL L	
APPENDIX C - CHARACTERIZING THE DYNAMIC THERMAL PERFORMANCE OF A WALL USING PERIODIC EXCITATION, by Mark Modera, LBL	
APPENDIX D - TRANSIENT TEMPERATURE TEST RESULTS	

LIST OF TABLES

	<u>Page</u>
1. Lightweight Structural Concrete Mix Design	6
2. Summary of Physical Properties for Walls L and S.	13
3. Steady-State Results from Calibrated Hot Box Tests	23
4. Measured Properties of Guarded Hot Plate Test Specimens.	31
5. Steady-State Results from Guarded Hot Plate Tests.	34
6. Steady-State Results for Wall S Measured Using Heat Flux Transducers	38
7. Predicted Thermal Resistance of Walls L and S	41
8. Abbreviations for Heat Flow and Temperature.	45
9. Measured Thermal Lag for Wall L	49
10. Measured Reduction in Amplitude for Wall L	53
11. Total Heat Flow for Wall L	56
12. Concrete Wall Comparisons	59
13. Fourier Transformations for Sine Cycle Data.	72
14. Summary of Transient Test Results for Walls L and S.	74
B1. Dynamic (Periodic) Test Results for NBS Temperature Cycle	B5
B2. Dynamic (Periodic) Test Results for NBS+10 Temperature Cycle	B10
B3. Dynamic (Periodic) Test Results for NBS-10 Temperature Cycle	B15
D1. Transient Test Results for Wall L	D5
D2. Transient Test Results for Wall S	D10

LIST OF FIGURES

	<u>Page</u>
1. Lightweight Concrete Wall with Normal Weight Concrete Strip.	4
2. Reinforcement Details for Lightweight Concrete Walls L and S	7
3. Consolidation of Concrete in Wall Panel Using a Plate Vibrator.	9
4. Wall S Formwork with Fill Material in Place of Normal Weight Concrete Strip	10
5. Reinforcement Placed over First Layer of Concrete for Wall S	10
6. Wall S after Lightweight Concrete Cast and Before Normal Weight Concrete Cast	11
7. Normal Weight Concrete Cast for Wall S	11
8. Wall L Air, Surface, and Internal Thermocouple Locations	14
9. Wall S Air, Surface, and Internal Thermocouple Locations	15
10. Indoor Surface of Wall L Before Calibrated Hot Box Testing.	16
11. Outdoor Surface of Wall L Before Calibrated Hot Box Testing.	16
12. Indoor Surface of Wall S Before Calibrated Hot Box Testing.	17
13. Outdoor Surface of Wall S Before Calibrated Hot Box Testing.	17
14. Mounting of Internal Thermocouple Using Reinforcement as Support	19
15. Mounting of Internal Thermocouple Within Reinforcement Grid	19
16. Calibrated Hot Box Test Facility	20
17. Schematic of Calibrated Hot Box.	20
18. Wall Thermal Resistances Measured by Calibrated Hot Box (ASTM: C 976).	25

LIST OF FIGURES
(Continued)

	<u>Page</u>
19. Steady-State Temperature Profiles Across Wall L.	26
20. Steady-State Temperature Profiles Across Wall S.	28
21. Thermal Conductivity of Lightweight Concrete Specimens	35
22. Thermal Conductivity of Normal Weight Concrete Specimens	36
23. Measured Thermal Conductivity of Lightweight Concrete.	40
24. Climatic Chamber Air Temperatures for Dynamic Sol-Air Temperature Cycles	44
25. Heat Flow for NBS, NBS+10, and NBS-10 Test Cycles	48
26. Definition of Thermal Lag and Reduction in Amplitude	51
27. Definition of Total Measured Heat Flow	55
28. Thermal Lag and M Values for the NBS Test Cycle Applied to Concrete Walls	60
29. Reduction in Amplitude and M Values for the NBS Test Cycle Applied to Concrete Walls	60
30. Total Heat Flow Ratio and M Values for the NBS Test Cycle Applied to Concrete Walls	61
31. Sine Functions with 6, 12, and 24-hr Periods	63
32. Climatic Chamber Air Temperature for Sine Temperature Cycle.	65
33. Measured Temperatures for Sine Test Cycle.	66
34. Heat Flow for Sine Cycle	67
35. Comparison of Wall Surface Temperature Measurement Methods.	69
36. Comparison of Wall Heat Flow Measurement Methods	70
A1. Indoor (Metering) Chamber Energy Balance	A3
B1. Measured Temperatures for NBS Test Cycle	B2
B2. Temperature Differentials for NBS Test Cycle	B3
B3. Heat Flow for NBS Test Cycle	B4

LIST OF FIGURES
(Continued)

	<u>Page</u>
B4. Measured Temperatures for NBS+10 Test Cycle	B7
B5. Temperature Differentials for NBS+10 Test Cycle	B8
B6. Heat Flow for NBS+10 Test Cycle	B9
B7. Measured Temperatures for NBS-10 Test Cycle	B12
B8. Temperature Differentials for NBS-10 Test Cycle	B13
B9. Heat Flow for NBS-10 Test Cycle	B14
D1. Measured Temperatures for Transient Test on Wall L	D2
D2. Temperature Differentials for Transient Test on Wall L	D3
D3. Heat Flow for Transient Test on Wall L	D4
D4. Measured Temperatures for Transient Test on Wall S	D7
D5. Temperature Differentials for Transient Test on Wall S	D8
D6. Heat Flow for Transient Test on Wall S	D9

STRUCTURAL THERMAL BREAK SYSTEMS FOR BUILDINGS -
HEAT TRANSFER CHARACTERISTICS OF LIGHTWEIGHT STRUCTURAL CONCRETE WALLS

by

Martha G. Van Geem*

ABSTRACT

A lightweight structural concrete was developed for use in exterior walls of low-rise residential and commercial buildings. The lightweight concrete has a unit weight of 50 pcf (800 kg/m³), a compressive strength of 2000 psi (13.8 MPa) and a thermal conductivity of 1.6 Btu·in./hr·ft²·°F (0.23 W/m·K). Lightweight concretes have not been previously developed with this combination of low density and moderate compressive strength.

The portland cement concrete developed for this project can be used to combine structural, thermal insulation, and heat storage capacity functions of exterior walls in one element. For many climates this concrete can be used without additional insulation as a complete wall system in low-rise buildings.

Heat transfer characteristics of two 8-in. (200-mm thick), full-size wall assemblies were evaluated using a calibrated hot box (ASTM Designation: C 976). One test specimen, designated Wall L, was an 8-in. (200-mm) thick wall constructed entirely of the newly developed lightweight structural concrete. The second specimen, designated Wall S, was the same as the first except for a 6-in. (150-mm) high normal weight concrete strip running horizontally across the wall at mid-height. The horizontal strip simulates a floor slab extending through an exterior wall.

Overall thermal resistances of Walls L and S, respectively, are 5.2 and 4.7 hr·ft²·°F/Btu (0.92 and 0.83 m²·K/W) at 75°F (24°C). Thermal resistance of Wall S is 11% less than that for Wall L.

Thermal conductivities of concrete used to construct Walls L and S were measured using a guarded hot plate (ASTM Designation: C 177). Average measured thermal conductivity of the lightweight concrete developed for this project is about 1/9th that for normal weight concrete.

Tests for dynamic temperature conditions provide a measure of thermal response for selected temperature ranges. Results from three 24-hour period, sol-air temperature cycles showed that heat storage capacity of the lightweight concrete delayed heat flow through the test specimen. Average thermal lag for the 8-in. (200-mm) thick lightweight concrete wall was 6 hours.

A dynamic cycle composed of three sinusoidal temperature functions was applied to Wall L to investigate an alternative analysis technique. The analysis technique uses hot box test data to determine a time constant and thermal diffusivity of the homogeneous lightweight structural concrete wall.

*Senior Research Engineer, Fire/Thermal Technology Section, Construction Technology Laboratories, Inc., Skokie, Illinois 60077 (312) 965-7500

EXECUTIVE SUMMARY

Scope

A significant amount of energy is lost from conditioned environments of buildings through thermal bridges. Reduction of energy loss can be achieved by providing thermal break materials in place of high conductivity materials that create thermal bridges. The purpose of this project is to investigate lightweight concrete systems for potential use as structural thermal breaks in buildings.

The program was conducted at Construction Technology Laboratories, Inc. (CTL). The project is sponsored jointly by the U.S. Department of Energy (DOE) Office of Buildings and Community Systems, and the Portland Cement Association. It is part of the Building Thermal Envelope Systems and Materials Program (BTESM) in the Energy Division of Oak Ridge National Laboratory (ORNL).

A thermal break is an element made of a material with a high thermal resistance used in place of a material with a lower thermal resistance to reduce energy losses through a building envelope. A thermal break may range in size from a small plastic nail used in place of a metal nail, to a large sheet of insulation used to prevent energy losses through a building foundation. The term "structural" used as an adjective to "thermal break" implies the material has load-bearing capabilities.

The primary objective of this project was to develop a portland cement concrete with sufficient thermal resistance and strength properties to serve as an effective structural thermal break in building envelopes. A concrete was developed with an air-dry unit weight of 50 pcf (800 kg/m^3), a compressive strength of approximately 2000 psi (13.8 MPa), and a thermal conductivity of $1.6 \text{ Btu}\cdot\text{in.}/\text{hr}\cdot\text{ft}^2\cdot^\circ\text{F}$ ($0.23 \text{ W/m}\cdot\text{K}$). The most commonly used concrete,

normal weight concrete, has a density of approximately 145 pcf (2320 kg/m³), a compressive strength in the range of 2500 to 6000 psi (17 to 41 MPa), and a thermal conductivity of 12 to 16 Btu·in./hr·ft²·°F (1.7 to 2.3 W/m·K). Lightweight concretes have not been previously developed with the combination of low density and moderate strength proposed for this project.

Although it is envisioned that the proposed lightweight concrete could be used for many building components, project emphasis is to evaluate the concrete for use in exterior walls for low-rise buildings. The portland cement concrete developed for this project will combine the structural, thermal insulation, and heat storage capacity functions of exterior walls in one element. For many climates the concrete developed can be used without additional insulation as a complete wall system in low-rise buildings.

The project is divided into five major tasks. This is the third of three project reports. The first report* summarized results of Task 1, which was a feasibility study to identify uses for the proposed lightweight portland cement concrete in buildings.

The second project report** summarized results from Tasks 2 through 4. Task 2 included work to select materials and mix designs for the lightweight portland cement concrete and a lightweight polymer concrete. Physical and thermal properties of candidate concretes were determined in Task 3. Casting and surface finishing techniques for the most desirable mixes were developed in Task 4.

*Larson, S. C. and Van Geem, M. G., "Structural Thermal Break Systems for Buildings - Feasibility Study," Oak Ridge National Laboratory Report No. ORNL/Sub/84-21006/1, Construction Technology Laboratories, Inc., Skokie, 1987, 88 pages.

**Litvin, A. and Van Geem, M. G., "Structural Thermal Break Systems for Buildings - Development and Properties of Lightweight Concrete Systems," Oak Ridge National Laboratory Report No. ORNL/Sub/84-21006/2, Construction Technology Laboratories, Inc., Skokie, 1988, 91 pages.

This report describes Task 5 work, which was heat transfer measurements of two full-size wall assemblies constructed of the developed portland cement concrete. One test specimen, designated Wall L, was an 8-in. (200-mm) thick wall constructed entirely of the newly developed lightweight structural concrete. The second specimen, designated Wall S, was the same as the first except for a 6-in. (150-mm) high normal weight concrete strip running horizontally across the wall at mid-height. The horizontal strip simulates a floor slab extending through an exterior wall.

Steady-State Temperature Test Results

Thermal resistances of Walls L and S and thermal conductivity of Wall L were measured using a calibrated hot box test facility (ASTM: C 976) at CTL. Test specimens were 8-ft 7-in. (2.6 m) sq and 8-in. (200-mm) thick. Wall thermal resistances were measured at mean temperatures of approximately 37°F (3°C), 56°F (13°C), 86°F (30°C), and 104°F (40°C). Corresponding air-to-air temperature differentials across the walls were approximately 68°F (38°C), 32°F (18°C), 25°F (14°C), and 59°F (33°C). Total thermal resistances, R_T , for Walls L and S, respectively, were 5.2 and 4.7 hr·ft²·°F/Btu (0.92 and 0.83 m²·K/W). Resistances are for a wall mean temperature of 75°F (24°C) and were interpolated from steady-state calibrated hot box test results. Values include design surface film resistances.

A comparison of steady-state calibrated hot box test results for Walls L and S shows that the 6-in. (150-mm) thick normal weight concrete strip of Wall S decreased wall resistance by 11%. Normal weight concrete is 5.8% of Wall S's total surface area.

Thermal conductivity of Wall L concrete measured by the calibrated hot box (ASTM Designation: C 976) at a mean temperature of 75°F (24°C) was 1.86

Btu·in./hr·ft²·°F (0.27 W/m·K). This value was interpolated from steady-state test results.

Calibrated hot box air temperatures, wall surface temperatures, and concrete temperature at approximate wall mid-thickness were measured using 16 thermocouples in each of the five planes. Additional thermocouples were used to evaluate the effects of the normal weight concrete strip in Wall S. Wall temperature profiles are presented for steady-state tests.

A guarded hot plate was used to measure thermal resistances of the concrete used to construct Walls L and S. Thermal conductivities were determined at CTL in accordance with ASTM Designation: C 177 "Steady-State Thermal Transmission Properties by Means of the Guarded Hot Plate." Nominal specimen dimensions were 2x12x12 in. (50x300x300 mm). Specimens were oven-dried before testing. Thermal resistances were determined at specimen mean temperatures ranging from approximately 40 to 110°F (4 to 43°C). Concrete thermal resistances at a specimen mean temperature of 75°F (24°C) were interpolated from measured values. Thermal conductivities of Wall L, Wall S lightweight, and Wall S normal weight specimens were 1.43, 1.48, and 12.7 Btu·in./hr·ft²·°F (0.21, 0.21, and 1.82 W/m·K), respectively, at a specimen mean temperature of 75°F (24°C).

Based on guarded hot plate test results, average measured thermal conductivity of the lightweight concrete developed for this project is about 1/9th that for normal weight concrete.

Thermal resistances of Walls L and S were predicted using calculation procedures from the ASHRAE Handbook - 1985 Fundamentals, results from guarded hot plate tests on oven-dry specimens, and measured wall thicknesses. Predicted thermal resistance of Wall S was 17% less than that for Wall L.

This compares to an 11% decrease in measured thermal resistance for Wall S compared to Wall L.

Thermal conductivity of a lightweight concrete portion of Wall S was measured using heat flux transducers (ASTM Designation: C 1046). Thermal conductivity at a mean temperature of 75°F (24°C), interpolated from steady-state test results, was 1.75 Btu·in./hr·ft²·°F (0.25 W/m·K).

Thermal conductivities from calibrated hot box and heat flux transducer measurements are greater than those from guarded hot plate tests because guarded hot plate specimens were oven-dried to remove moisture, while wall specimens were air-dried. An increase in specimen moisture content increases thermal conductivity.

Dynamic Temperature Test Results

Dynamic calibrated hot box tests were performed on Wall L, the homogeneous lightweight concrete wall. Dynamic tests are a means of evaluating thermal response under controlled conditions that simulate temperature changes actually encountered by building envelopes. For these tests, the calibrated hot box indoor air temperatures were held constant while outdoor air temperatures were cycled over a pre-determined temperature versus time relationship.

Three 24-hour (diurnal) temperature cycles were applied to Wall L in this investigation. The cycles had mean temperatures of approximately 58, 68, and 78°F (14, 20, and 26°C) and temperature swings of about 60°F (33°C). Average indoor air temperature over the 24-hour period for each cycle was approximately 72°F (22°C).

Dynamic calibrated hot box tests were used to determine dynamic thermal properties of thermal lag, reduction in amplitude, and total heat flow ratio.

As indicated by thermal lag, heat storage capacity of the lightweight concrete wall delayed heat flow through the specimens. Average thermal lag values ranged from 5.5 to 6.5 hours for the three diurnal temperature cycles applied to Wall L.

As indicated by the damping effect, heat storage capacities of Wall L reduced peak heat flows through the specimen for dynamic temperature conditions when compared to predictions based on steady-state thermal resistances (R-values). Reduction in amplitude values ranged from 47 to 53% for the three diurnal temperature cycles applied to Wall L.

For the three diurnal temperature cycles applied to Wall L, total heat flow for a 24-hour period was less than would be predicted by steady-state R-values. Total measured heat flows for the 24-hour cycles ranged from 44 to 54% of those predicted using steady-state equations. These reductions in total heat flow are attributed to wall thermal storage capacity and reversals in heat flow.

A fourth dynamic cycle, composed of three sinusoidal temperature functions, was applied to Wall L to investigate an alternative analysis technique. The analysis technique uses calibrated hot box test data to determine a time constant and thermal diffusivity of the homogeneous lightweight structural concrete wall. The test approach was suggested by Mr. Mark P. Modera, Lawrence Berkeley Laboratory. Calibrated hot box tests and data reduction were performed at CTL. Mr. Modera performed the data analysis and presented results in a paper included in this report as Appendix C.

Transient test data were collected during calibrated hot box testing of Walls L and S. Results of a transient test are determined from data collected in the period of time between two steady-state tests. After a wall is in a steady-state condition, the outdoor chamber temperature setting is changed.

The transient test continues until the wall reaches equilibrium heat flow for the new outdoor chamber air temperature. The initial wall mean temperature for the tests was 72°F (22°C) for Wall L and 73°F (23°C) for Wall S. The final wall mean temperature was approximately 36°F (2°C) for Wall L and 37°F (3°C) for Wall S.

Transient test results indicated that heat storage capacities of the three insulated concrete sandwich panel walls delayed heat flow through the specimens. The amount of time required for both walls to reach 63% of a final heat flow were approximately six times greater than predicted by steady-state calculations based on measured surface temperatures.

Test results presented in this report are limited to the specimens and temperature cycles used in this investigation. Results may be different for alternative materials and temperature cycles. This report provides data on thermal response of two concrete walls subjected to steady-state and dynamic temperature cycles. A complete analysis of building energy requirements must include consideration of the entire building envelope, building orientation, building operation, and yearly weather conditions. Data developed in this experimental program provide a quantitative basis for modeling the building envelope, which is part of the overall energy analysis process.

The concrete heat transmission test results presented in this report show that the newly developed lightweight structural concrete meets the project objectives as a potential structural thermal break material for use in buildings. Test results for the wall constructed using the newly developed concrete are compared to test results for other concrete walls. The comparison shows the newly developed concrete exhibits beneficial thermal properties and adequate structural capacity for load-bearing walls.

STRUCTURAL THERMAL BREAK SYSTEMS FOR BUILDINGS -
HEAT TRANSFER CHARACTERISTICS OF LIGHTWEIGHT STRUCTURAL CONCRETE WALLS

by

Martha G. Van Geem*

INTRODUCTION

This report is the third of three for a project to investigate lightweight concrete systems for potential use as structural thermal breaks in buildings. This report presents results from tests conducted to evaluate heat transfer characteristics of two walls constructed of a newly developed lightweight concrete.

A thermal break is an exterior building element made of a material with a relatively high thermal resistance used in place of a material with a lower thermal resistance to reduce energy losses through a building envelope. A thermal break may range in size from a small plastic nail used in place of a metal nail, to a large sheet of insulation used to prevent energy losses through a building foundation. The term "structural" used as an adjective to "thermal break" implies the material has load bearing capabilities.

The overall project objective was to develop portland cement concrete with sufficient thermal resistance and strength properties to serve as an effective structural thermal break in building envelopes. A concrete was developed with an air-dry unit weight of 50 pcf (800 kg/m³), a compressive strength of approximately 2000 psi (13.8 MPa), and a thermal conductivity of about 1.6 Btu·in./hr·ft²·°F (0.23 W/m·K). Although it is envisioned that concrete with these properties could be used for many building components, project

*Senior Research Engineer, Fire/Thermal Technology Section, Construction Technology Laboratories, Inc., Skokie, Illinois 60077 (312) 965-7500

emphasis is to evaluate the concrete for use in exterior walls for low-rise buildings.

The portland cement concrete developed for this project combines the structural, thermal insulation, and heat storage capacity functions of exterior walls in one element. Based on BLAST analyses and ANSI/ASHRAE/ISE Standard 90A-1980 building standard requirements considered in Reference 1, an 8-in. (200-mm) thick wall of the newly developed concrete exceeds minimum thermal performance criteria for commercial and residential buildings in most regions of the continental United States.

OBJECTIVES AND SCOPE

The project was divided into five major tasks. This is the third of three project reports. The first report^{(1)*} summarized results of Task 1, which was a feasibility study to identify uses for the proposed lightweight portland cement concrete in buildings.

The second project report⁽²⁾ summarized results from Tasks 2 through 4. Task 2 included work to select materials and mix designs for the lightweight portland cement and lightweight polymer concretes. Physical and thermal properties of candidate concretes were determined in Task 3. Casting and surface finishing techniques for the most desirable mixes were developed in Task 4.

This report describes Task 5 work, which was heat transfer measurements of two full-size wall assemblies constructed of the developed portland cement concrete. Heat flow through the walls was measured in the calibrated hot box

*Superscript numbers in parentheses refer to references listed at the end of this report.

test facility (ASTM Designation: C 976)⁽³⁾ at Construction Technology Laboratories, Inc. (CTL). One test specimen, designated Wall L, was an 8-in. (200-mm) thick wall constructed entirely of the newly developed lightweight structural concrete. The second specimen, designated Wall S, was the same as the first except for a 6-in. (150-mm) high normal weight concrete strip running horizontally across the wall at mid-height, as shown in Fig. 1. The horizontal strip simulates a floor slab extending through an exterior wall.

Walls were tested for steady-state temperature conditions to obtain average heat transmission coefficients, including total thermal resistance (R_T) and thermal transmittance (U). A comparison of test results for the two walls shows the effect of the normal weight concrete strip.

Wall L, the homogeneous concrete wall, was also tested for dynamic temperature conditions. Dynamic tests provided a measure of thermal response for selected temperature ranges. Three simulated sol-air dynamic cycles were selected to permit comparison of results with those obtained in previous investigations.⁽⁴⁻¹²⁾ A fourth cycle, a combination of sinusoidal temperature functions, was used to investigate an alternative analysis technique.

The program was conducted at Construction Technology Laboratories, Inc. (CTL). The project is sponsored jointly by the U.S. Department of Energy (DOE) Office of Buildings and Community Systems, and the Portland Cement Association. It is part of the Building Thermal Envelope Systems and Materials Program (BTESM), Energy Division, at Oak Ridge National Laboratory (ORNL). Work was authorized by a contract signed September 25, 1984 by Walker K. Love. The DOE Project Manager is Dr. George E. Courville, ORNL.

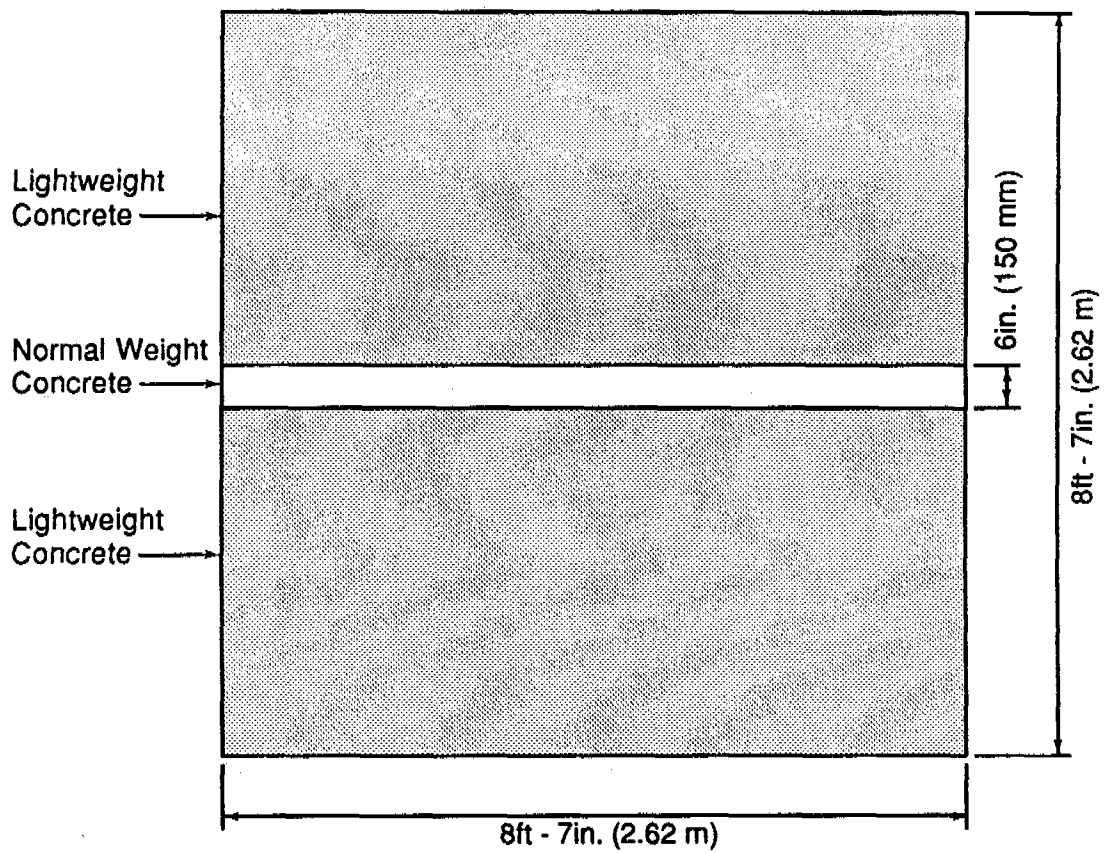


Fig. 1 Lightweight Concrete Wall with Normal Weight Concrete Strip

TEST SPECIMENS

Two lightweight structural concrete walls were constructed by CTL and subsequently tested in a calibrated hot box. Walls were cast horizontally and have overall nominal dimensions of 103x103 in. (2.62x2.62 m).

Wall Construction

Wall L is a lightweight structural concrete wall with an average thickness of 8.00 in. (203 mm). Wall S is similar to Wall L except for a 6-in. (150-mm) high normal weight concrete strip running horizontally across the wall at mid-height. Average thickness of Wall S is 8.13 in. (206 mm).

The concrete mix for Wall L and the lightweight portion of Wall S utilized a newly developed aggregate from 3M called MacroliteTM Ceramic Spheres. Reference 2 presents the concrete mix development. The mix design is repeated in Table 1 of this report for convenience.

Reinforcement representative of actual wall construction was placed within Walls L and S. Reinforcement consisted of a single layer of No. 4 (13 mm) bars spaced 12 in. (305 mm) center-to-center in each direction detailed as shown in Fig. 2. The reinforcement was located at the walls approximate mid-thickness.

Threaded concrete inserts were cast into the walls at mid-thickness to aid in transporting walls after concrete had attained the necessary strength.

Thermocouples were cast into the concrete walls at the same level as the reinforcing bars. A detailed discussion of thermocouple placement and instrumentation is included in the "Instrumentation" section.

Ten 5-1/2 cu ft (0.156 m³) batches were made for casting each of the two wall panels. Average fresh unit weight of the 10 batches for each of the two walls was 50.4 pcf (806 kg/m³). Unit weights ranged from 48.1 to 55.9 pcf (770 to 894 kg/m³) for Wall No. 1 and from 48.4 to 52.8 pcf (774 to 845 kg/m³) for Wall No. 2.

TABLE 1 - LIGHTWEIGHT STRUCTURAL CONCRETE MIX DESIGN

Material	Quantities per 1.0 cubic yard (Quantities per 1.0 m ³)		
	Absolute Volume, cu ft (m ³)	Weight, lb (kg)	
		Wall L	Wall S
Portland Cement	2.16 (0.080)	425 (252)	425 (252)
Silica Fume	0.33 (0.012)	43 (26.1)	43 (26.1)
Water	4.01 (0.149)	250 (149)	250 (149)
Air content	1.62 ⁺ (0.060)	--	--
3M Macrolite 1/2" to #4 (12.7 to 4.75 mm)	9.25 (0.342)	293 (174)	327 (195)
#4 to #50 (4.75 to 0.30 mm)	8.88 (0.329)	459 (273)	466 (277)
Fillite* 30 to 300 μm	0.76 (0.028)	33 (20)	33 (20)
Vinsol Resin,** 2% Solution	1275-1488 ml (1670-1950 ml)	2.81 (1.7)	3.28 (2.0)
WRDA,*** 7oz/100 lb cement (4.55 ml/kg cement)	888 ml (1160 ml)	1.96 (1.2)	1.96 (1.2)

+Air content estimated at 6%.

*Hollow alumina silica microspheres furnished by Fillite USA, Inc.,
Huntington, West Virginia.

**Air-entraining agent.

***Water-reducing admixture.

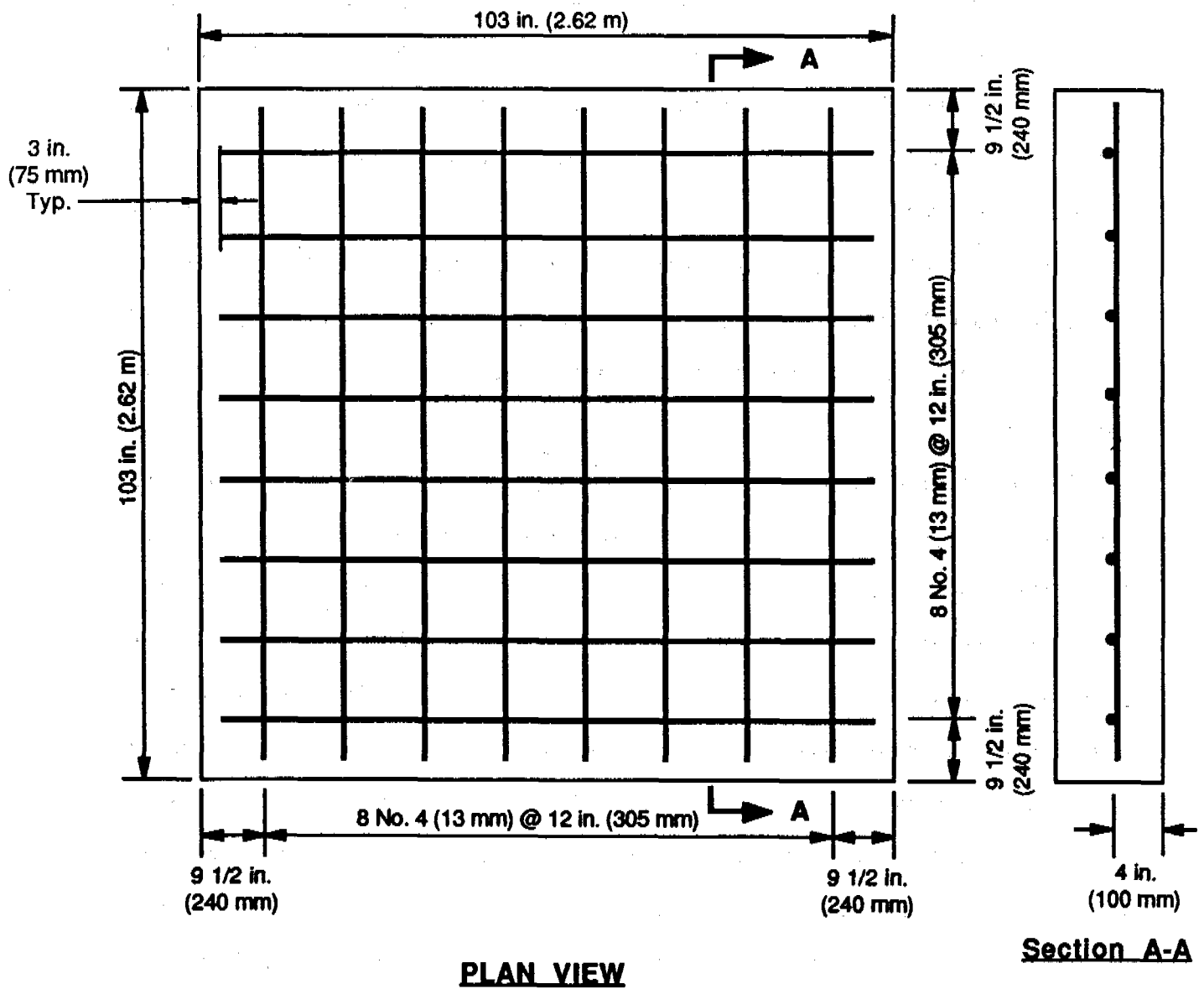


Fig. 2 Reinforcement Details for Lightweight Concrete Walls L and S

Concrete for each wall was mixed using a 6 cu ft (0.17m^3) mixer and was transported, as each batch was made, in a 6 cu ft (0.17m^3), plastic container to the form location. Shovels were used to place the concrete in the formwork. A 4 in. (100-mm) layer of concrete was placed in the formwork, working from one side of the formwork to the opposite side. The concrete was consolidated using a plate vibrator as shown in Fig. 3. Reinforcement and thermocouples were placed on top of the 4 in. (100-mm) layer before the next 4-in. (100-mm) of concrete were added. After the full concrete thickness was consolidated with a plate vibrator, the top surface was struck off, floated, and trowelled. Plastic sheets were used to cover the top surface of the walls for curing.

To construct Wall S a fill material was placed in the proposed location of the normal weight concrete while the lightweight concrete was cast. Figure 4 shows the expanded polystyrene fill material in the formwork before concrete was cast. Reinforcement placed on the first 4-in. (100-mm) layer of concrete is shown in Fig. 5. The fill material was removed after the lightweight concrete hardened as shown in Fig. 6. Normal weight concrete was placed in the strip, as shown in Fig. 7, one day after the lightweight concrete was cast.

Walls L and S were allowed to cure in the formwork for approximately 2 weeks. After removing from formwork, Wall L was allowed to air dry in the laboratory at a temperature of $65\pm 10^\circ\text{F}$ ($18\pm 6^\circ\text{C}$) for approximately 3 months. Wall S was air dried in the laboratory at a temperature of $70\pm 10^\circ\text{F}$ ($21\pm 6^\circ\text{C}$) for approximately 4 months.

Prior to testing, the faces of Walls L and S were coated with a cementitious waterproofing material to seal minor surface imperfections. A textured, noncementitious paint was subsequently used as a finish coat. These

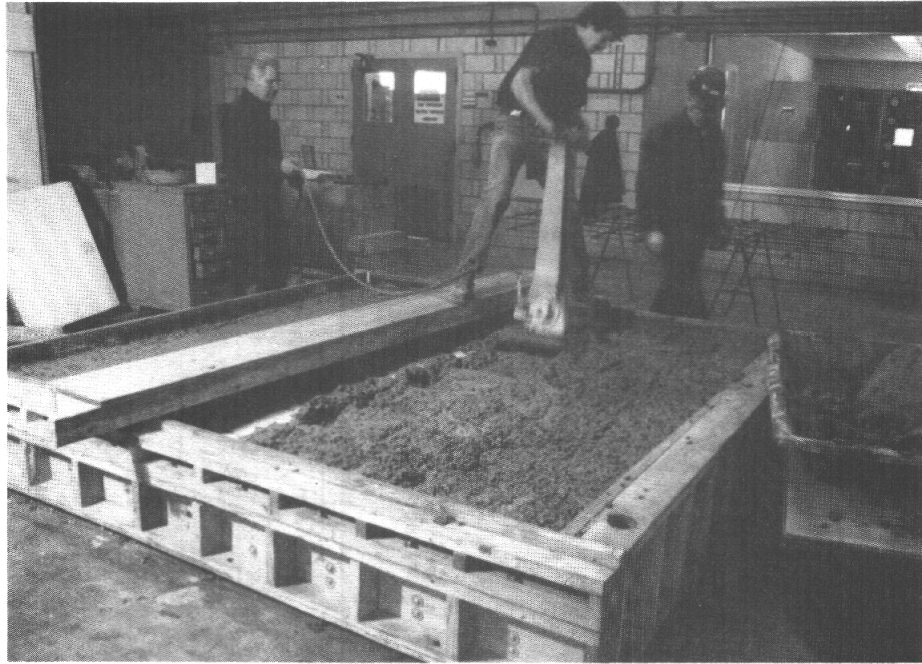


Fig. 3 Consolidation of Concrete in Wall Panel Using a Plate Vibrator

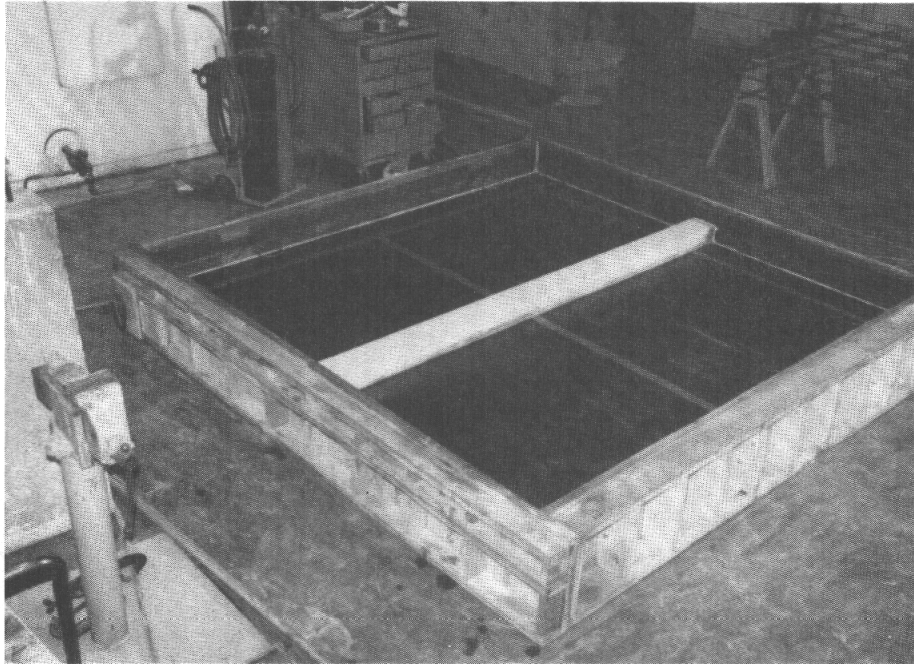


Fig. 4 Wall S Formwork with Fill Material in Place of Normal Weight Concrete Strip



Fig. 5 Reinforcement Placed over First Layer of Concrete for Wall S

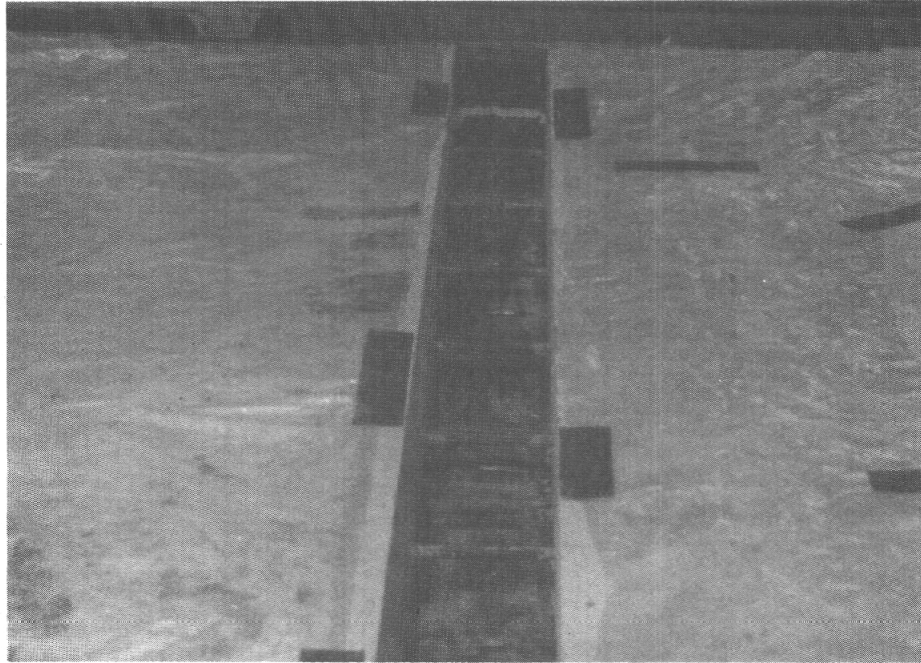


Fig. 6 Wall S after Lightweight Concrete Cast and Before Normal Weight Concrete Cast

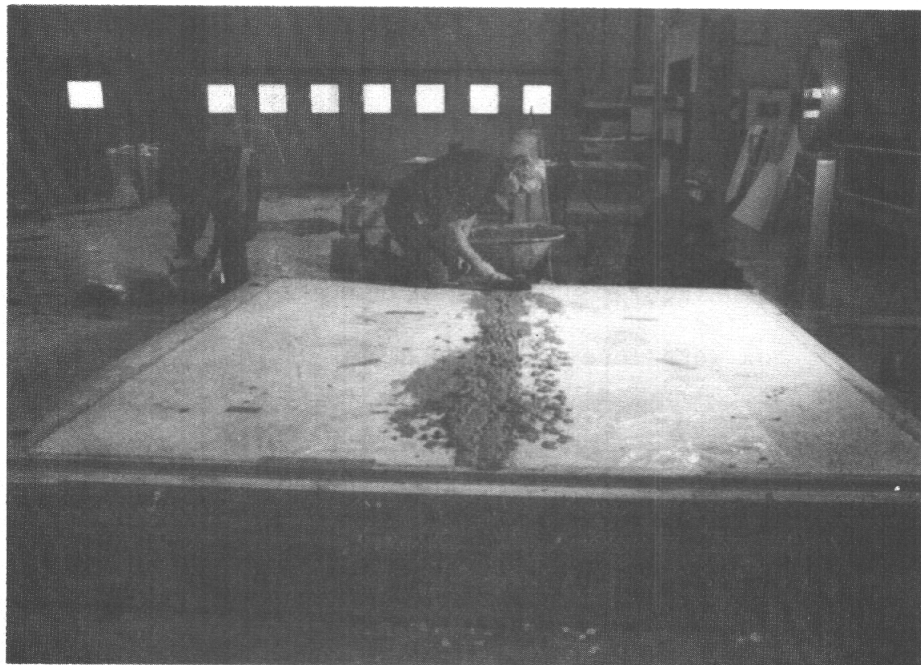


Fig. 7 Normal Weight Concrete Cast for Wall S

coatings provided a white, uniform surface for both faces of each wall. Wall edges were left uncoated.

Physical Properties of Walls

Measured weights, thicknesses, surface areas, and estimated moisture contents of Walls L and S are summarized in Table 2. Wall weights immediately before and after calibrated hot box tests are presented.

Instrumentation

Eighty, 20 gauge, Type T thermocouples, corresponding to ASTM Designation: E 230, "Standard Temperature-Electromotive Force (EMF) Tables for Thermocouples,"⁽³⁾ were used to measure temperatures during thermal testing. For each test wall, 16 thermocouples were located in the air space on each side of the test specimen, 16 on each face of the test wall, and 16 at the approximate concrete mid-thickness. The 16 thermocouples in each plane were spaced 20-3/5-in. (525-mm) apart in a 4x4 grid over the wall area, as shown in Figs. 8 and 9.

An additional four thermocouples were located on each wall surface and at concrete mid-thickness along the centerline of the normal weight concrete strip of Wall S, as shown in Fig. 9.

Thermocouples measuring temperatures in the air space of each chamber of the calibrated hot box were located approximately 3 in. (75 mm) from the face of the test wall.

Surface thermocouples were securely attached to the wall with duct tape for a length of approximately 4 in. (100 mm). The tape covering the sensors was painted the same color as the test wall surface. Thermocouples attached to indoor and outdoor surfaces of Walls L and S are shown in Figs. 10 through 13. Indoor and outdoor surfaces face the metering chamber and climatic chamber, respectively, during calibrated hot box tests.

TABLE 2 - SUMMARY OF PHYSICAL PROPERTIES FOR WALLS L and S

Property	Measured Value	
	Wall L	Wall S
Weight of Wall, lb (kg) Before testing	2760 (1250)	2910 (1320)
After testing	2720 (1240)	2890 (1310)
Unit Weight of Wall,* lb/ft ² (kg/m ²)	37.4 (182)	39.4*** (192)
Average Wall Thickness, in. (mm)	8.00 (203)	8.13 (207)
Wall Area, ft ² , (m ²)	73.88 (6.86)	73.92 (6.87)
Estimated Moisture Content**, % oven dry weight	2	2

*Before calibrated hot box tests.

**Estimated from air dry and oven dry weights of thermal conductivity specimens.

***Average unit weight of wall including normal weight concrete strip.

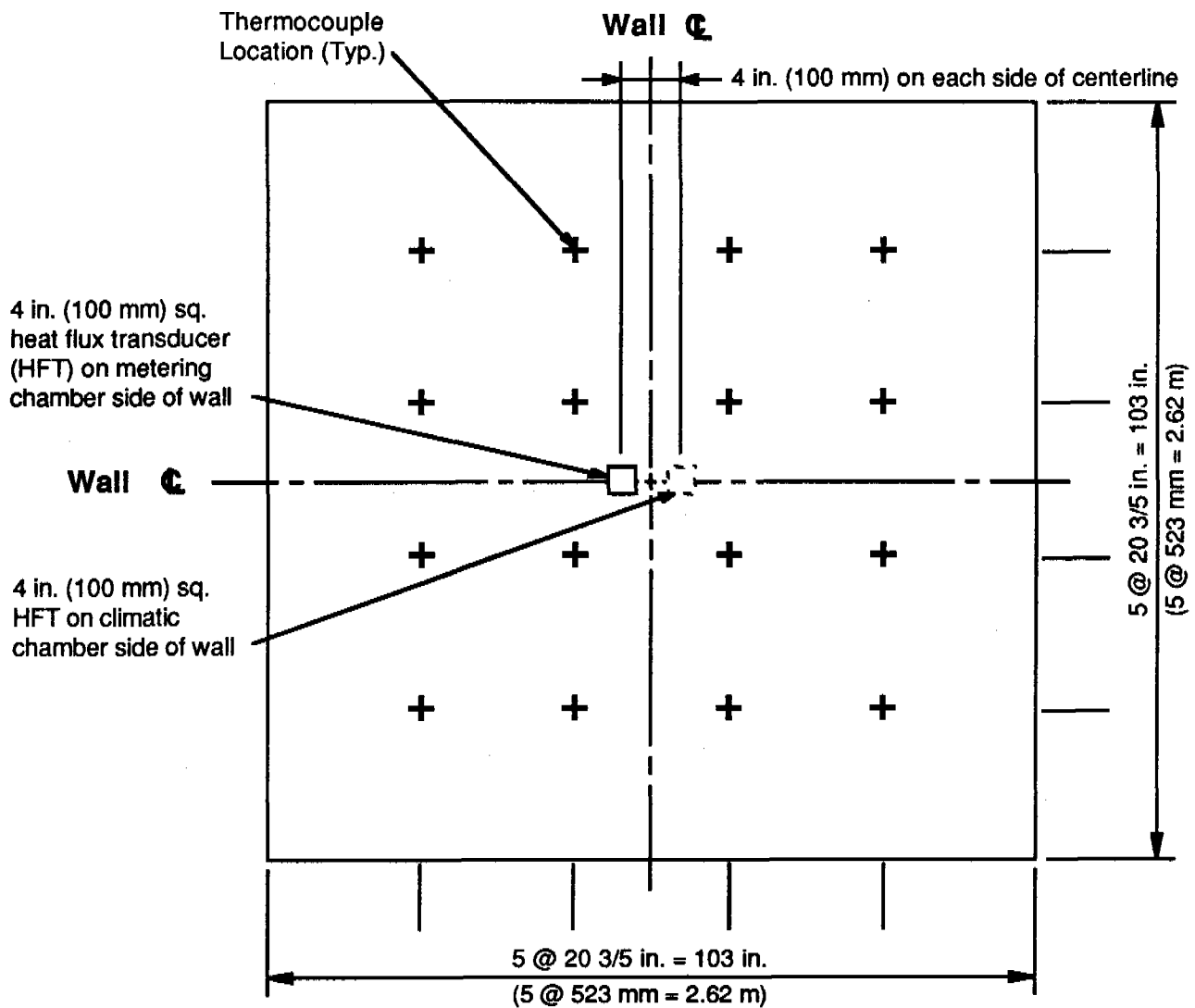


Fig. 8 Wall L Air, Surface, and Internal Thermocouple Locations

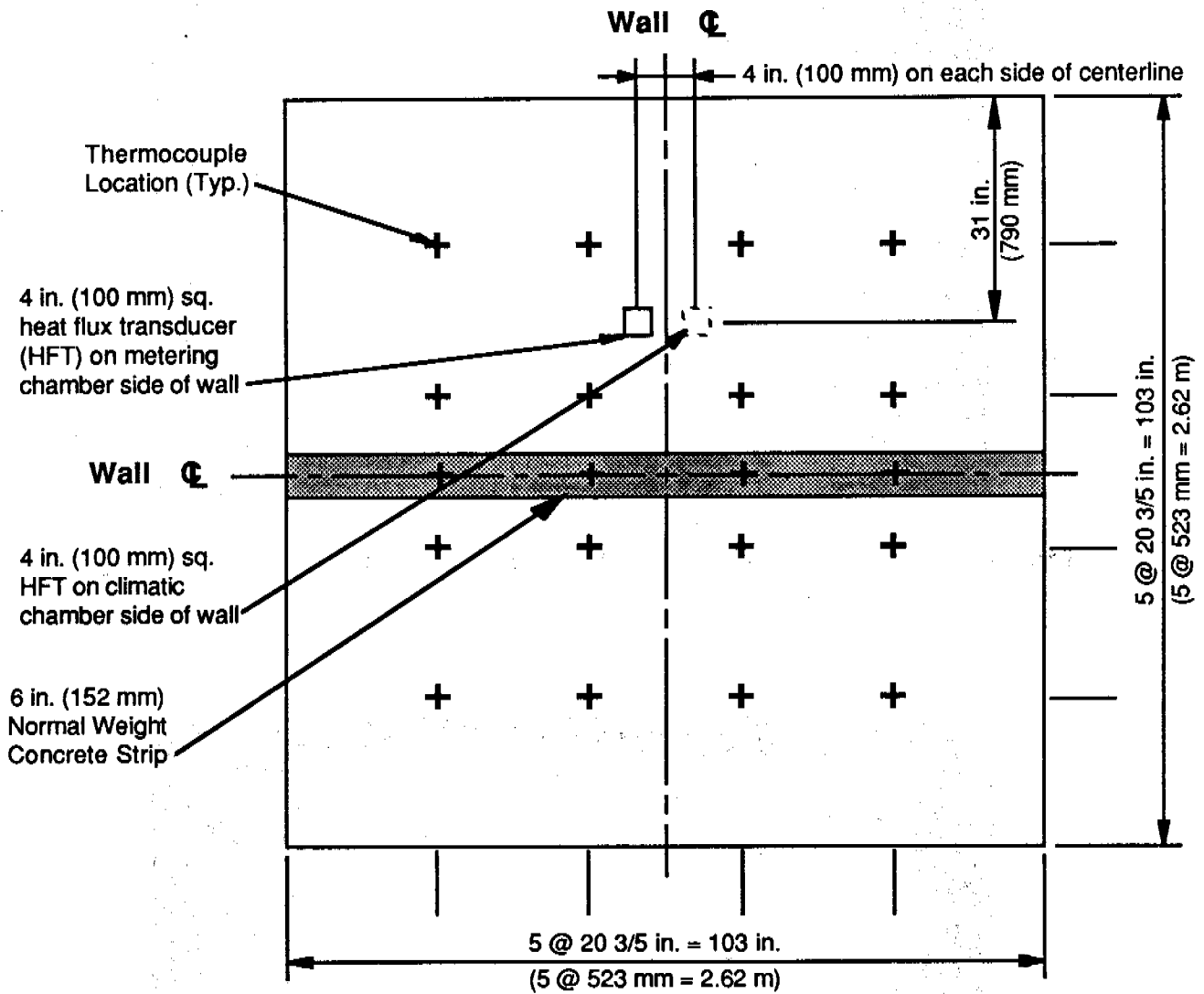


Fig. 9 Wall S Air, Surface, and Internal Thermocouple Locations

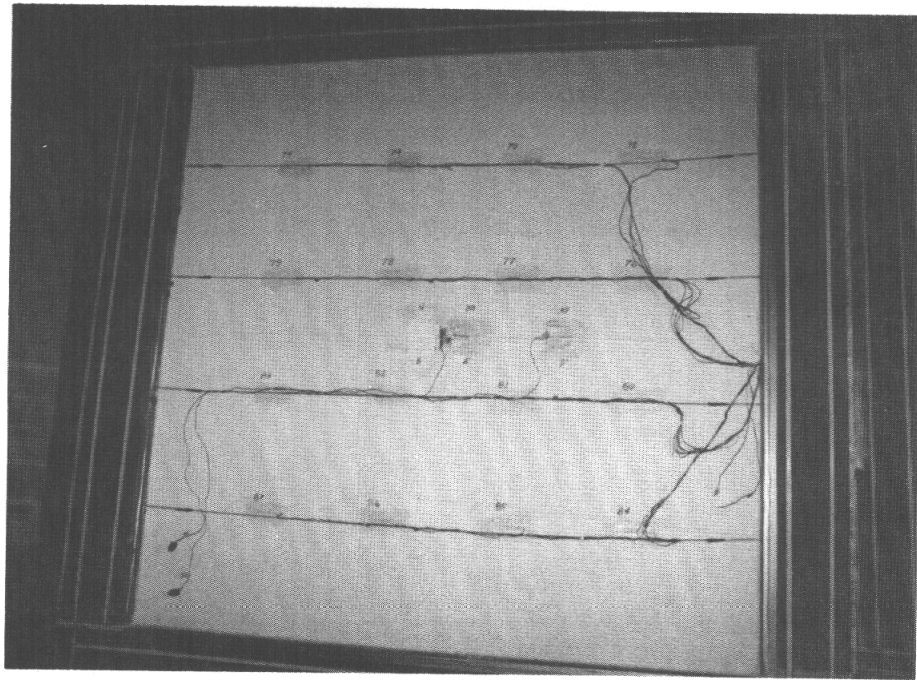


Fig. 10 Indoor Surface of Wall L Before Calibrated Hot Box Testing

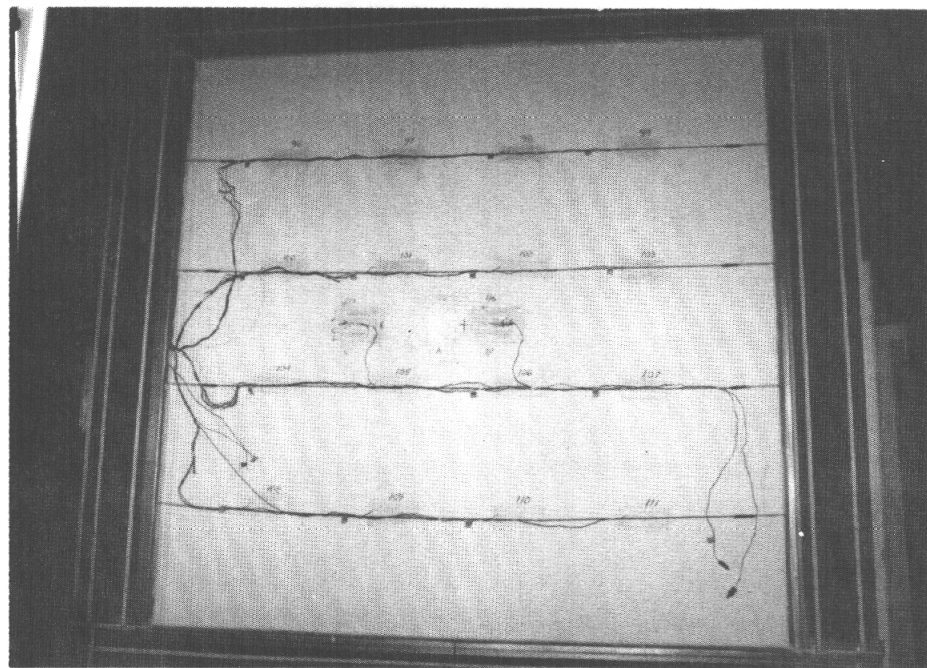


Fig. 11 Outdoor Surface of Wall L Before Calibrated Hot Box Testing

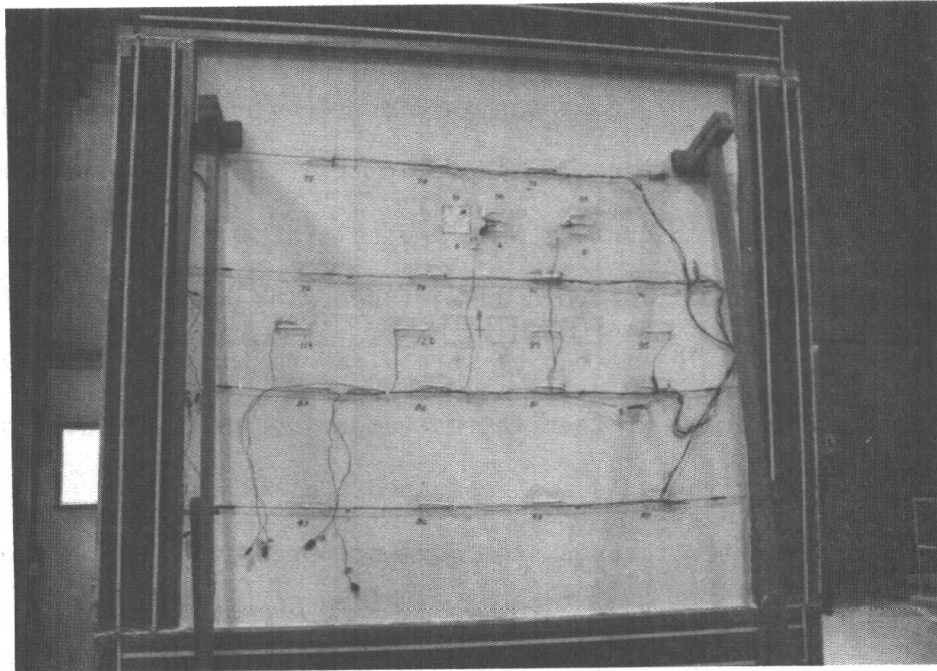


Fig. 12 Indoor Surface of Wall S Before Calibrated Hot Box Testing

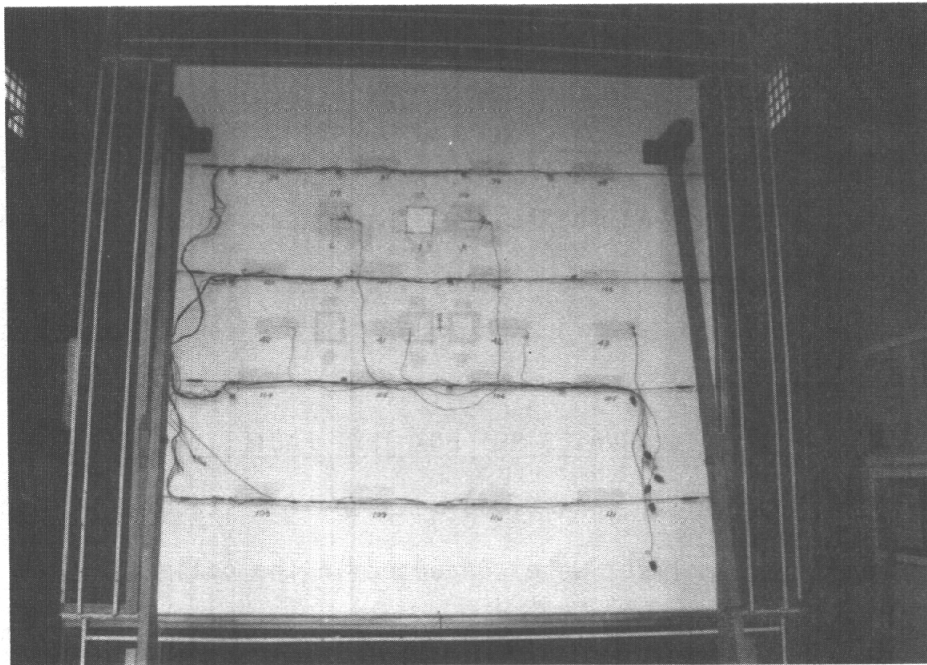


Fig. 13 Outdoor Surface of Wall S Before Calibrated Hot Box Testing

Internal thermocouples were placed at wall mid-thickness on top of the first 4-in. (100-mm) concrete layer. To secure their location, thermocouples were taped to reinforcement, as shown in Fig. 14, or suspended by wire between reinforcement, as shown in Fig. 15. Note in Fig. 14 that the thermocouple junction was not placed in contact with the reinforcement. This was done for all internal thermocouples to avoid any influence by internal heat flow through reinforcement. Thermocouples were wired to form a thermopile such that an electrical average of four thermocouple junctions, located along a horizontal line across the grid, was obtained. Wires for internal thermocouples were routed through side formwork prior to casting the second 4-in. (100-mm) concrete layer.

One heat flux transducer measuring 4x4-in. (100x100-mm) was mounted on each of the indoor and outdoor surfaces of the test walls. Sensors were located near the center of the walls as shown in Figs. 8 and 9. The surface of the heat flux transducer in contact with a wall surface was coated with a thin layer of high-conductivity silicon grease. The silicon grease provided uniform contact between the heat flux transducer and wall surface. Duct tape was used to secure heat flux transducers to the wall surfaces. The duct tape was painted the same color as the test wall surface. Heat flux transducers were calibrated using results from steady-state calibrated hot box tests on Wall L.

CALIBRATED HOT BOX TEST FACILITY

Heat flow through Walls L and S was measured for steady-state and dynamic temperature conditions. Tests were conducted in the calibrated hot box facility shown in Figs. 16 and 17. Tests were performed in accordance with ASTM Designation: C 976, "Thermal Performance of Building Assemblies by Means of a Calibrated Hot Box."⁽³⁾

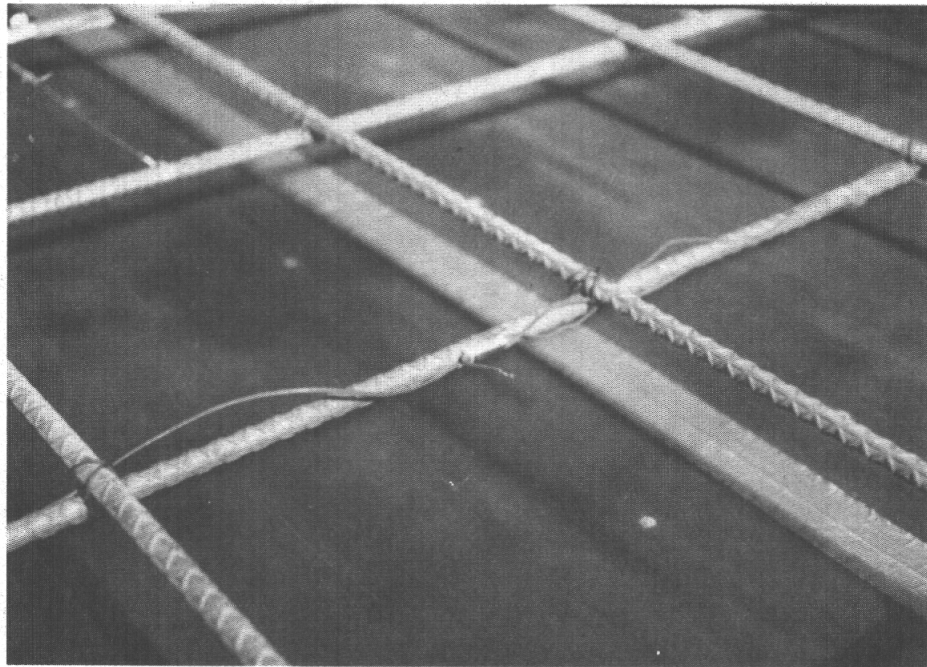


Fig. 14 Mounting of Internal Thermocouple Using Reinforcement as Support

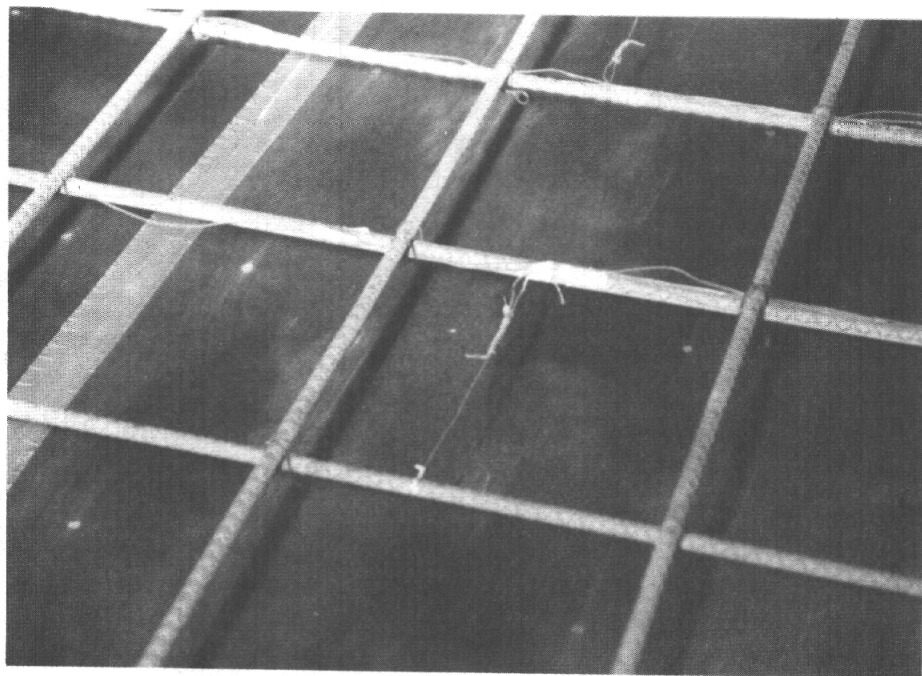


Fig. 15 Mounting of Internal Thermocouple Within Reinforcement Grid

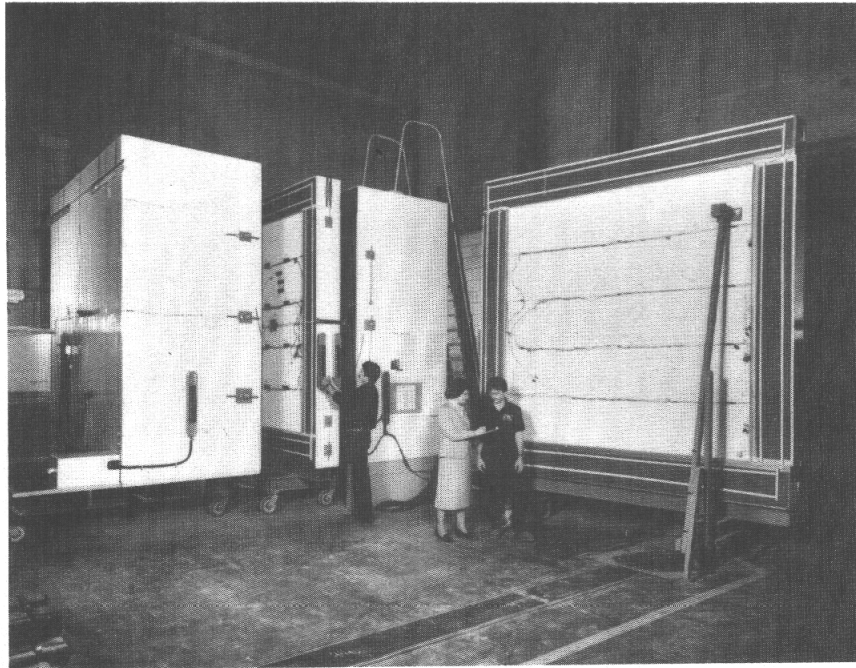


Fig. 16 Calibrated Hot Box Test Facility

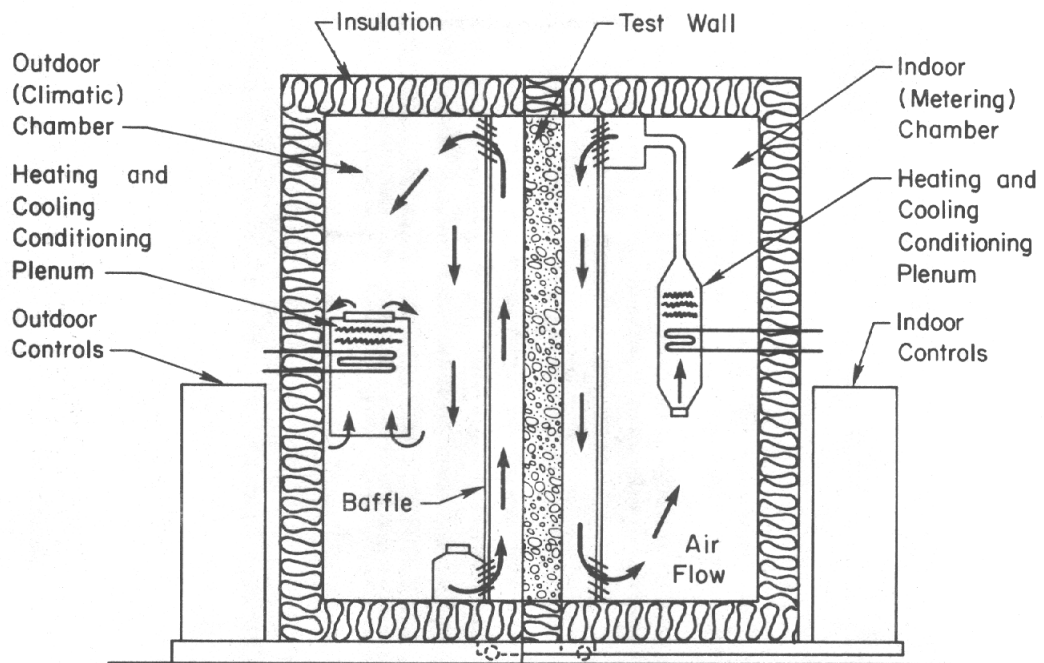


Fig. 17 Schematic of Calibrated Hot Box

The following is a brief description of the calibrated hot box. Instrumentation and calibration details are described in Appendix A and Reference 13.

The facility consists of two highly insulated chambers as shown in Fig. 17. Walls, ceiling, and floors of each chamber are insulated with foamed urethane sheets to obtain a nominal thickness of 12 in. (300 mm). During tests, the chambers are clamped tightly against an insulating frame that surrounds the test wall. Air in each chamber is conditioned by heating and cooling equipment to obtain desired temperatures on each side of the test wall.

The outdoor (climatic) chamber can be held at a constant temperature or cycled within the range -15 to 130°F (-26 to 54°C). Temperatures can be programmed for a 24-hour cycle to obtain the desired temperature-time relationship. The indoor (metering) chamber, which simulates an indoor environment, can be maintained at a constant room temperature between 65 and 80°F (18 and 27°C).

The specimen is oriented vertically in the CTL calibrated hot box. Therefore, heat flows horizontally through the wall. The facility was designed to accommodate walls with thermal resistance values ranging from 1.5 to 20 hr·ft²·°F/Btu (0.26 to 3.52 m²·K/W).

The pressure in both the metering and climatic chambers is atmospheric.

THERMAL PROPERTIES OF CONCRETE FOR STEADY-STATE TEMPERATURE CONDITIONS

Thermal resistances of Walls L and S were measured using the calibrated hot box. Thermal conductivity of the lightweight concrete portion of Wall S was measured using heat flux transducers. Thermal conductivities of specimens made from concrete mixes used to make Walls L and S were measured using a guarded hot plate.

Calibrated Hot Box Test Results

Four calibrated hot box tests for steady-state temperature conditions were performed on each wall. Heat flow and temperature measurements were used to determine average overall thermal resistance (R_T) and thermal conductivity (k).

Test Procedures

Steady-state calibrated hot box tests were conducted by maintaining constant metering and climatic chamber air temperatures. Results are calculated from data collected when specimen temperatures reach equilibrium and the rate of heat flow through the test wall is constant.

Hot box tests on Wall L were performed in April 1986. Tests on Wall S were performed in July and August 1986.

Thermal Resistance and Conductivity

Steady-state results from calibrated hot box tests on Walls L and S are summarized in Table 3. Data are averages for 16 consecutive hours of testing. Wall mean temperature, heat flow, and overall thermal resistance are listed for each steady-state test condition applied to the walls. Thermal conductivity is also listed for Wall L.

The first column of Table 3 lists the wall mean temperature during each steady-state test. Wall mean temperature is determined from the average of the metering and climatic wall surface temperatures. Average temperatures for Wall S, with the normal weight concrete strip, are the area-weighted averages of the lightweight and normal weight concrete temperatures.

Table 3 presents climatic and metering chamber air temperatures, and wall surface-to-surface temperature differentials. Additional measured temperatures are presented in the "Steady-State Temperatures Profiles" section of this report.

TABLE 3 - STEADY-STATE RESULTS FROM CALIBRATED HOT BOX TESTS

Wall Designation	Wall Mean Temp.,* °F (°C)	tc Climatic Chamber Temp., °F (°C)	tm Metering Chamber Temp., °F (°C)	Δt Surface-to-Surface Temp. Diff., °F (°C)	q** Heat Flow, Btu/hr·sq ft (W/sq m)	Rt*** Thermal Resistance, hr·sq ft·°F/Btu (sq m·K/W)	k Thermal Conductivity, Btu·in./hr·sq ft·°F (W/m·K)	Relative Humidity		Laboratory Air Temperature	
								Metering Chamber, %	Climatic Chamber, %	Max., °F (°C)	Min., °F (°C)
L	36.9 (2.7)	0.9 (-17.3)	70.4 (21.3)	58.2 (32.3)	12.2 (38.5)	5.6 (0.99)	1.68 (0.24)	35	20	75 (23.9)	74 (23.3)
L	55.7 (13.2)	38.6 (3.7)	71.4 (21.9)	27.1 (15.1)	5.5 (17.2)	5.8 (1.02)	1.61 (0.23)	34	17	75 (23.9)	72 (22.2)
L	85.6 (29.8)	97.2 (36.2)	72.8 (22.7)	22.2 (12.3)	5.5 (17.4)	4.9 (0.86)	1.99 (0.29)	33	11	74 (23.3)	72 (22.2)
L	103.7 (39.8)	132.5 (55.8)	73.7 (23.2)	51.6 (28.7)	12.7 (40.2)	4.9 (0.86)	1.97 (0.28)	33	10	75 (23.9)	73 (22.8)
S	37.9 (3.3)	3.3 (-15.9)	70.7 (21.5)	56.3 (31.3)	14.2 (44.9)	4.8 (0.85)	-	55	21	74 (23.3)	74 (23.3)
S	56.7 (13.7)	40.3 (4.6)	71.6 (22.0)	25.9 (14.4)	6.9 (21.6)	4.6 (0.81)	-	53	18	74 (23.3)	74 (23.3)
S	87.0 (30.6)	99.5 (37.5)	73.4 (23.0)	22.4 (12.4)	5.7 (18.1)	4.8 (0.85)	-	51	12	79 (26.1)	75 (23.9)
S	105.1 (40.6)	134.3 (56.8)	74.7 (23.7)	51.0 (28.3)	13.9 (43.8)	4.5 (0.79)	-	51	10	80 (26.7)	78 (25.6)

* Average of metering and climatic wall surface temperatures.

** Heat flow through wall measured by calibrated hot box (ASTM Designation: C976).

*** Overall thermal resistance calculated using design surface coefficients of 0.85 hr·sq ft·°F/Btu and measured values of heat flow.

Overall thermal resistances were calculated using heat flow measured by the calibrated hot box and design surface resistance coefficients of 0.68 $\text{hr}\cdot\text{ft}^2\cdot^\circ\text{F}/\text{Btu}$ ($0.12 \text{ m}^2\cdot\text{K}/\text{W}$) for still indoor air and 0.17 $\text{hr}\cdot\text{ft}^2\cdot^\circ\text{F}/\text{Btu}$ ($0.03 \text{ m}^2\cdot\text{K}/\text{W}$) for 15 mph (24 km/h) outdoor air.⁽¹⁴⁾

Thermal conductivity is listed only for the homogeneous specimen, Wall L. Measured relative humidity within the metering and climatic chambers of the CTL calibrated hot box is listed in Table 3.

Maximum and minimum laboratory air temperatures obtained during each steady-state test are also listed in Table 3. The laboratory acts as a guard for the metering chamber during tests conducted in CTL's calibrated hot box.

Wall thermal resistances from Table 3 are shown as a function of wall mean temperature in Fig. 18.

Thermal conductivity of Wall L and thermal resistances of Walls L and S at a specimen mean temperature of 75°F (24°C) were interpolated from measured values. Thermal conductivity of Wall L is 1.86 $\text{Btu}\cdot\text{in.}/\text{hr}\cdot\text{ft}^2\cdot^\circ\text{F}$ ($0.27 \text{ W}/\text{m}\cdot\text{K}$) at 75°F (24°C). Overall thermal resistances of Walls L and S are 5.2 and 4.7 $\text{hr}\cdot\text{ft}^2\cdot^\circ\text{F}/\text{Btu}$ (0.92 and $0.83 \text{ m}^2\cdot\text{K}/\text{W}$), respectively, at 75°F (24°C). Thermal resistance of Wall S is 11% less than that for Wall L at 75°F (24°C). Normal weight concrete comprises 5.8% of Wall S's total surface area.

Steady-State Temperature Profiles

Temperature profiles across Walls L and S for the steady-state tests are illustrated in Figures 19 and 20. The following notation is used to designate average measured temperatures:

- t_c = climatic chamber air temperature
- t_{cs} = wall surface temperature, climatic chamber side
- t_{md} = internal wall temperature at approximate mid-thickness of concrete
- t_{ms} = wall surface temperature, metering chamber side
- t_m = metering chamber air temperature

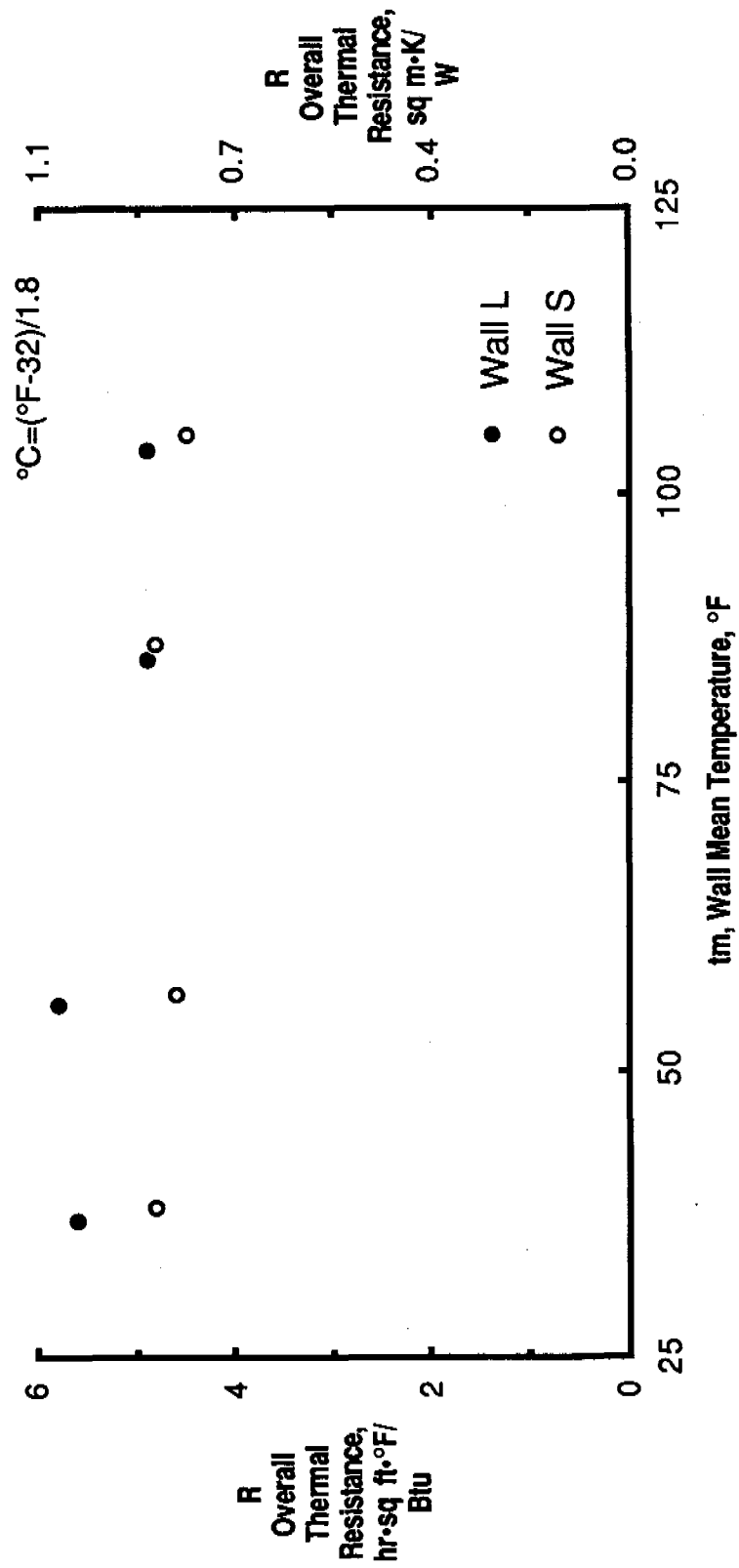
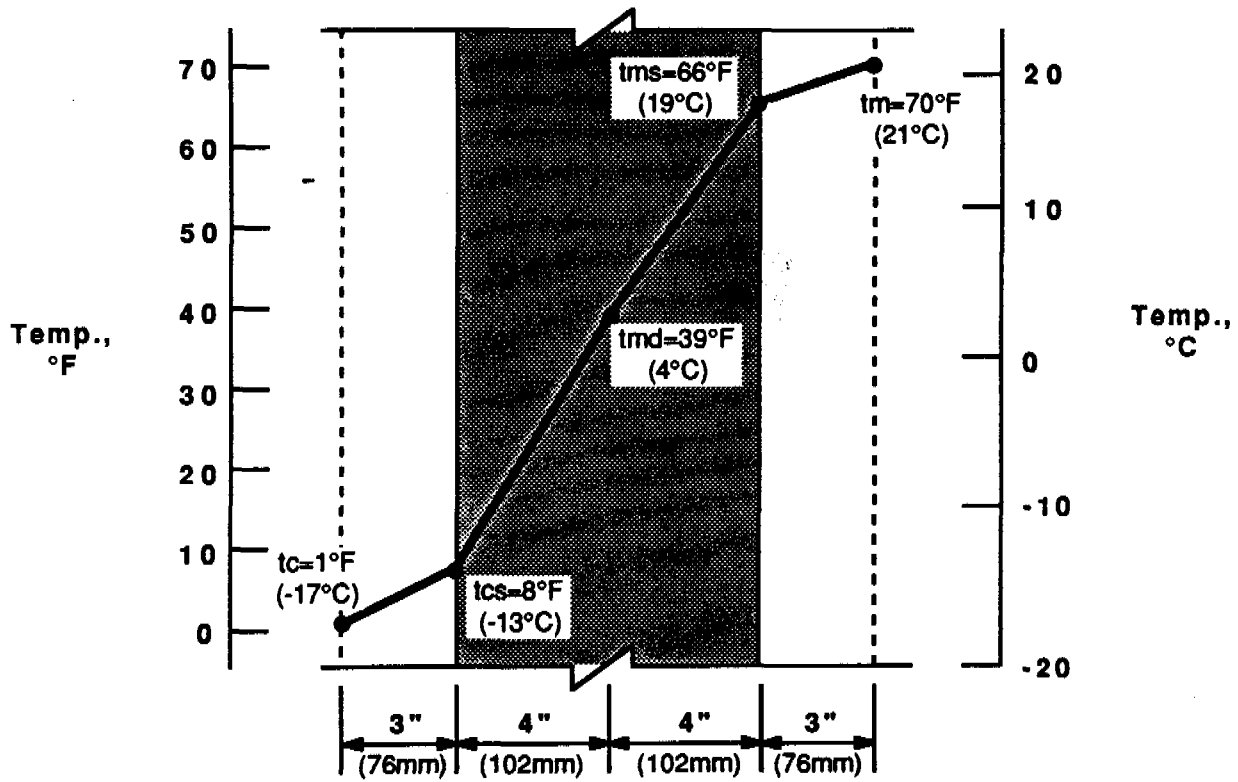
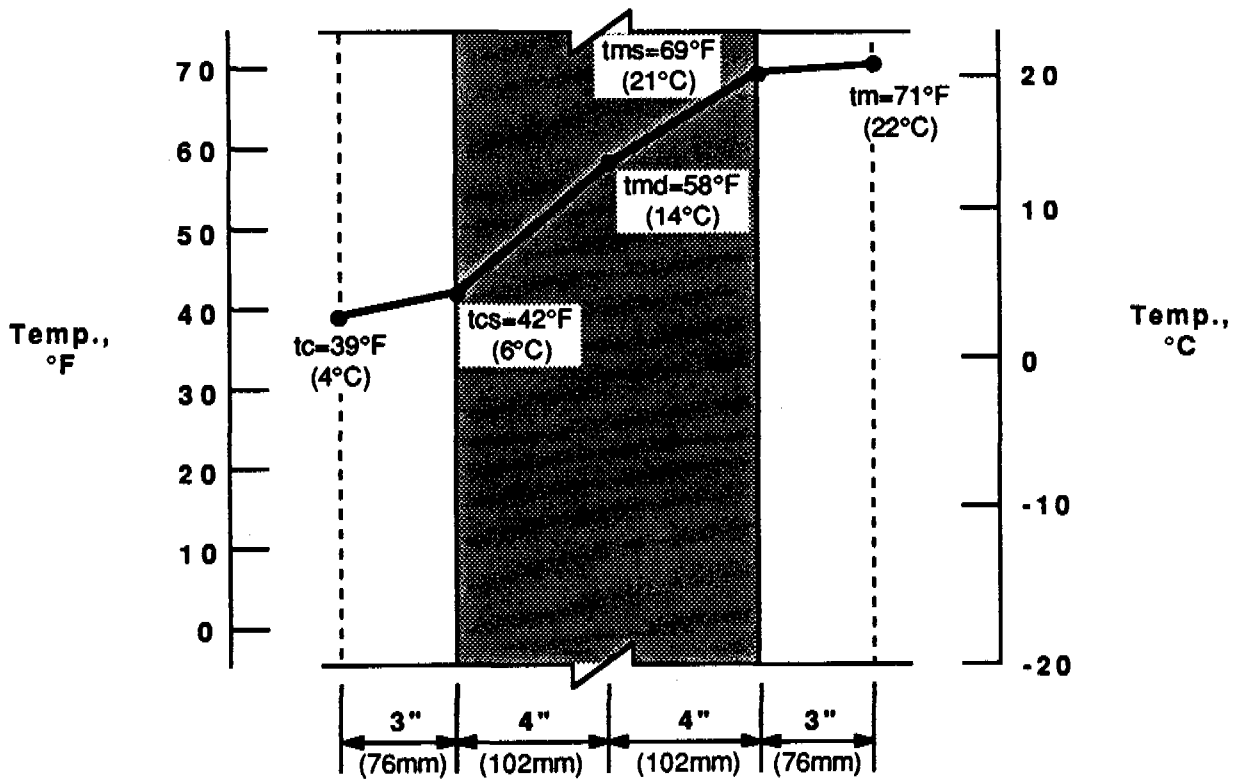


Fig. 18 Wall Thermal Resistances Measured by Calibrated Hot Box (ASTM: C976)

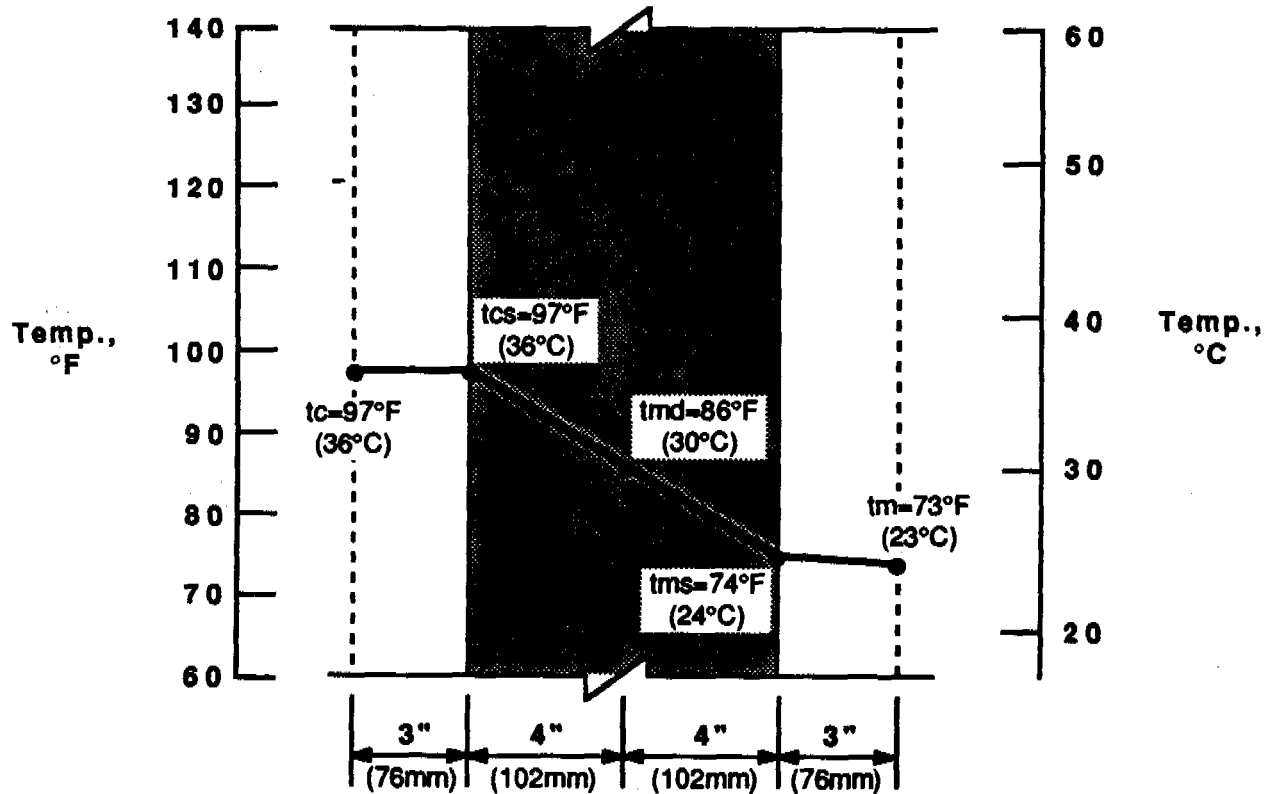


(a) Wall Mean Temperature = 37°F (3°C)

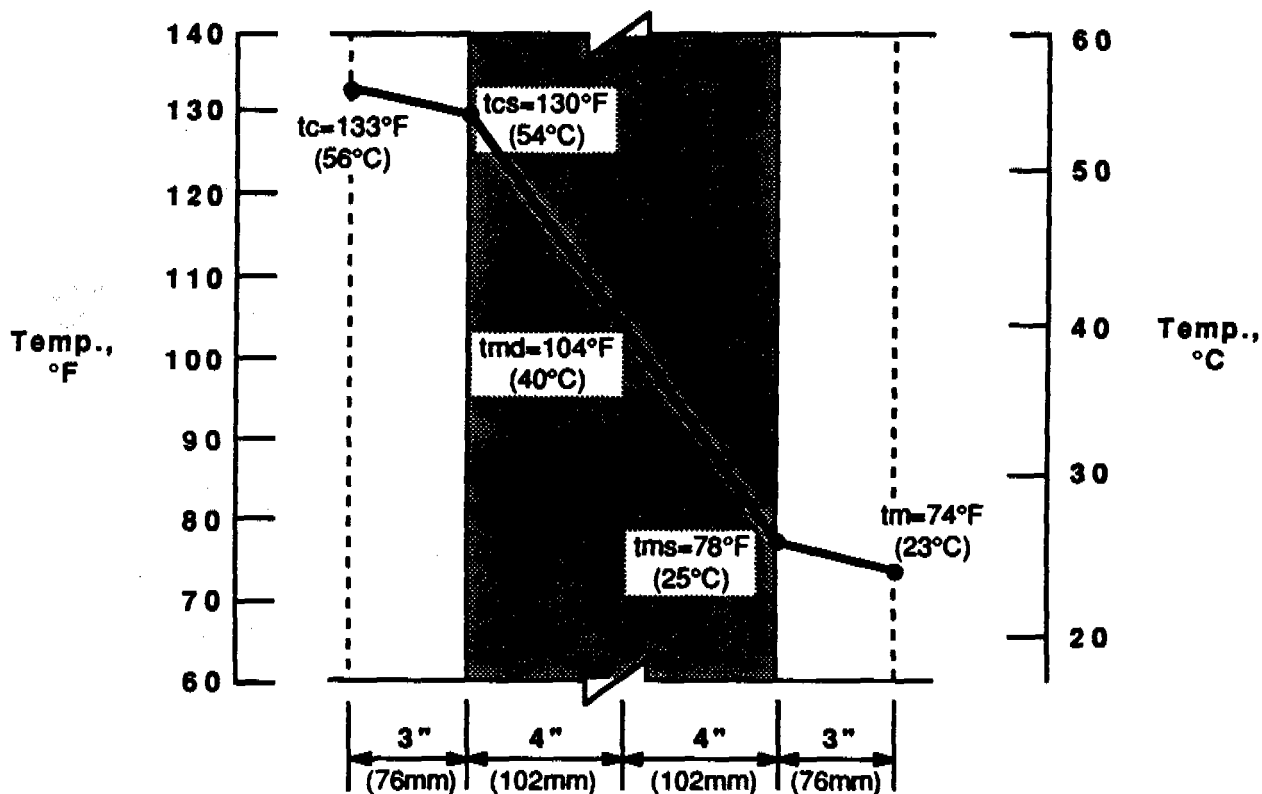


(b) Wall Mean Temperature = 56°F (13°C)

Fig. 19 Steady-State Temperature Profiles Across Wall L



(c) Wall Mean Temperature = 86°F (30°C)



(d) Wall Mean Temperature = 104°F (40°C)

Fig. 19 Steady-State Temperature Profiles Across Wall L (continued)

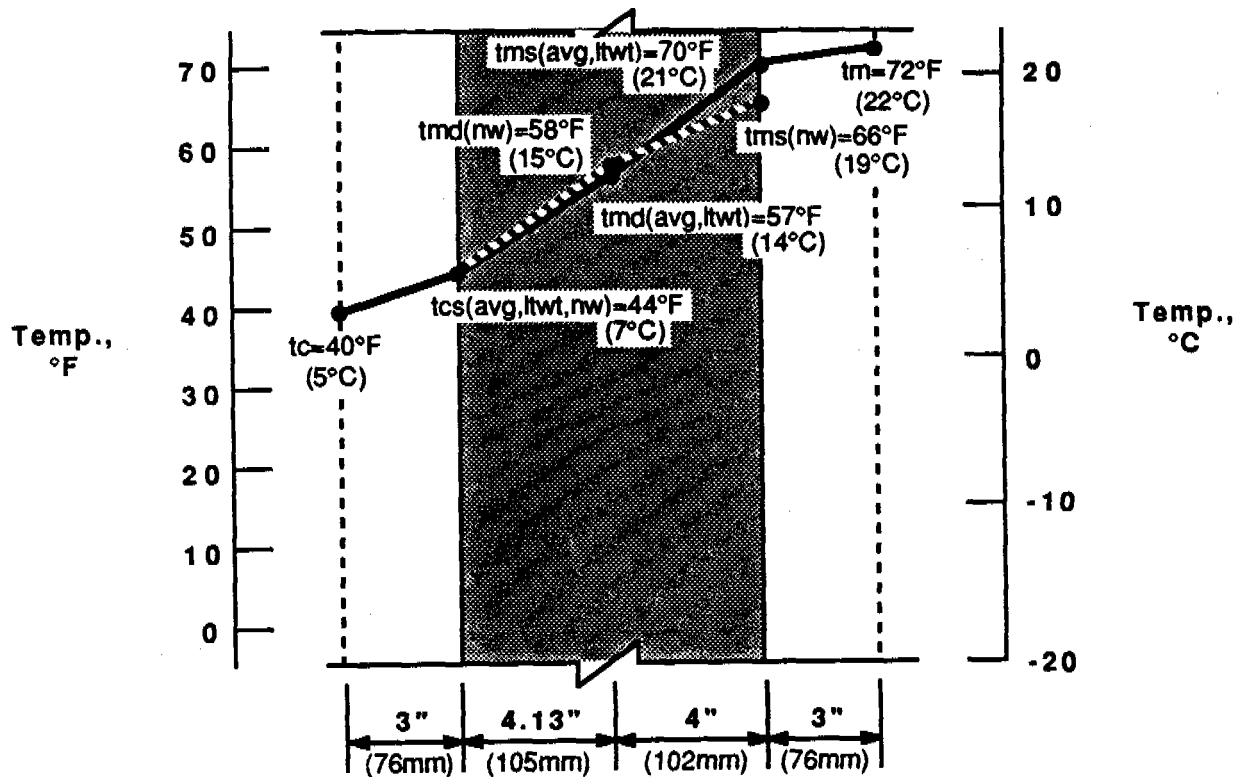
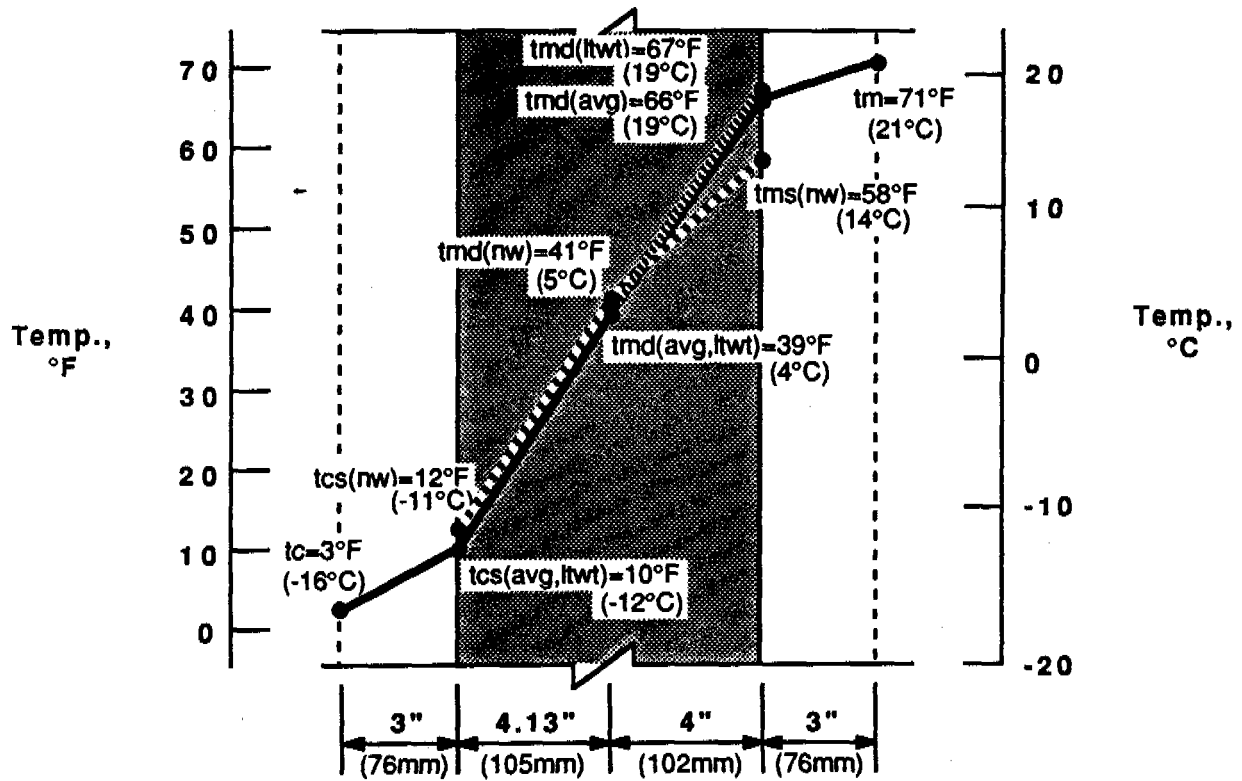
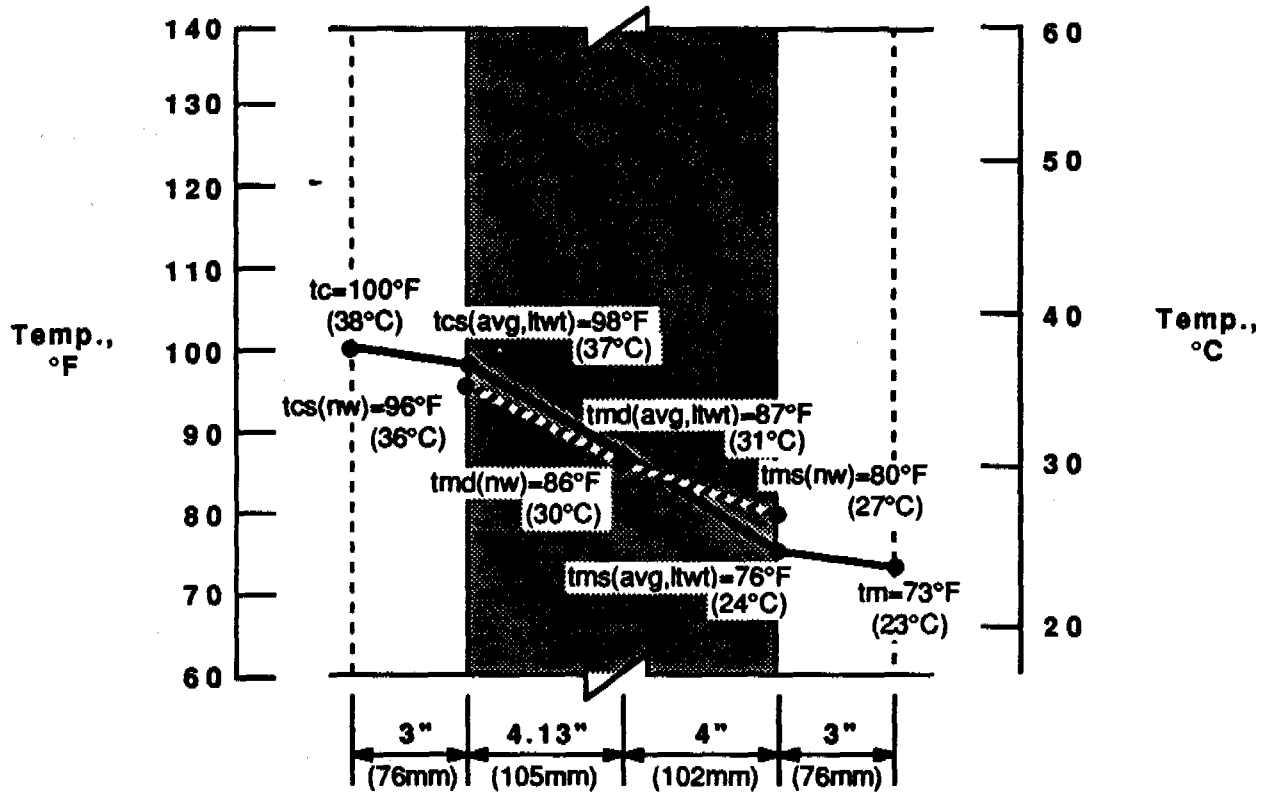
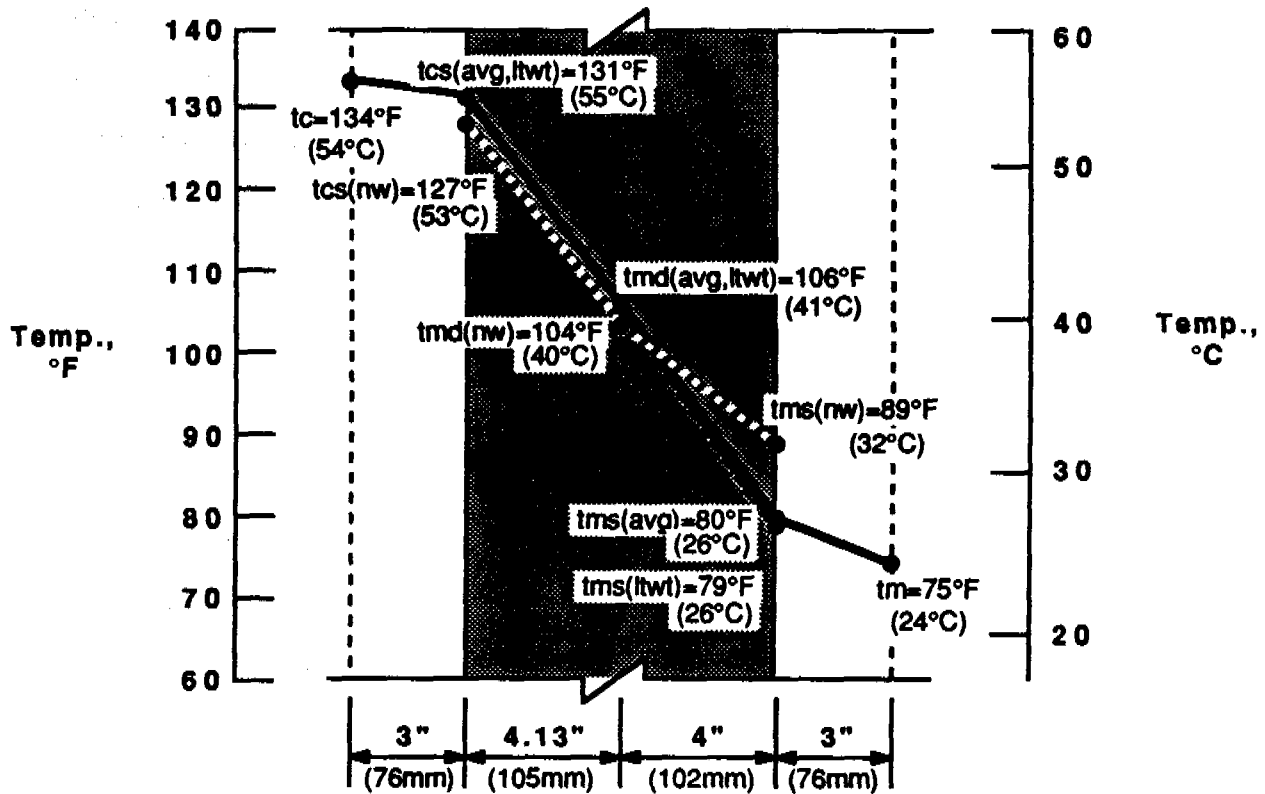


Fig. 20 Steady-State Temperature Profiles Across Wall S



(c) Wall Mean Temperature = 87°F (31°C)



(d) Wall Mean Temperature = 105°F (41°C)

Fig. 20 Steady-State Temperature Profiles Across Wall S (continued)

For Wall S air temperatures and all Wall L temperatures, values presented are averages from the 16 thermocouples located in each plane as previously described in the "Instrumentation" section of this report. Figure 20 shows Wall S surface and internal wall temperatures for:

- the lightweight concrete portion of the wall (average of 16 thermocouple readings), denoted (ltwt)
- the normal weight concrete portion of the wall (average of four thermocouple readings), denoted (nw)
- the area-weighted average of the lightweight and normal weight concrete temperatures, denoted (avg)

The normal weight concrete strip is 5.8% of the total wall area.

Guarded Hot Plate Test Results

Thermal conductivities of specimens made from concrete mixes used to make Walls L and S were measured using a guarded hot plate. Tests were conducted at CTL in accordance with ASTM Designation: C 177, "Steady-State Heat Flux Measurements and Thermal Transmission Properties by Means of the Guarded Hot Plate," and ASTM Designation: C 1045, "Calculating Thermal Transmission Properties from Steady-State Heat Flux Measurements."⁽³⁾

Test Specimens

Two specimens were tested from the lightweight concrete for Wall L, the lightweight concrete for Wall S, and the normal weight concrete for Wall S. Nominal specimen dimensions were 2x12x12 in. (50x300x300 mm). Specimens were moist-cured at $73.4 \pm 3^\circ\text{F}$ ($23 \pm 1.7^\circ\text{C}$) and 100% RH for seven days, and then air-dried at $73 \pm 5^\circ\text{F}$ ($23 \pm 3^\circ\text{F}$) and 45 \pm 15% RH. Specimens were oven-dried before testing to eliminate effects of moisture migration during testing. Measured specimen dimensions and unit weights are given in Table 4.

TABLE 4 - MEASURED PROPERTIES OF GUARDED HOT PLATE TEST SPECIMENS

Specimen		Overall Dimensions, in. (mm)	Average Thickness, in. (mm)	Ovendry Unit Weight, pcf (kg/cu m)
Wall C7 Lightweight Concrete	Top	12.2 x 12.1 (310 x 306)	1.98 (50)	48.1 (771)
	Bottom	12.1 x 12.1 (306 x 307)	2.03 (52)	46.8 (750)
Wall C8 Lightweight Concrete	Top	12.0 x 12.0 (305 x 305)	1.99 (51)	50.2 (805)
	Bottom	12.0 x 12.0 (305 x 305)	1.99 (50)	50.0 (801)
Wall C8 Normal Weight Concrete	Top	12.0 x 12.0 (305 x 305)	2.00 (51)	141 (2260)
	Bottom	12.0 x 12.0 (305 x 305)	2.02 (51)	142 (2270)

Test Procedures

Using a guarded hot plate, two identical samples of the material to be tested are placed on either side of a horizontal flat plate heater assembly consisting of a 5.88-in. (149-mm) square inner (main) heater surrounded by a separately controlled guard heater to form a 12-in. (305-mm) assembly. The function of the guard heater is to eliminate lateral heat flow to or from the main heater thereby forcing all heat generated in the main heater to flow in the direction of the two test samples. Liquid cooled heat sinks are also placed in contact with the samples producing a uniform and constant temperature on the outside of each sample. The apparatus is surrounded by a container filled with expanded perlite insulation. The perlite insulation serves as a secondary guard.

The guarded hot plate apparatus is located in a laboratory maintained at $73.4 \pm 3^\circ\text{F}$ ($23.0 \pm 1.7^\circ\text{C}$), and $50 \pm 5\%$ relative humidity.

The rate of heat flow through the specimens is determined by measuring

minutes.

Thermal conductivity was calculated using:

$$k = \frac{(Q/A)}{(\Delta T/\Delta x)} \quad (1)$$

where:

k = average thermal conductivity of 2 specimens

Q = power dissipation in the main heater

A = the metering surface area taken twice

Δx = total thickness of both test specimens

ΔT = the total temperature difference across both specimens

Test specimen temperatures are measured by chromel/alumel thermocouples embedded near the specimen surfaces. Thermocouples were placed in previously sawed grooves. A cement paste was used to fill the groove flush with the specimen surface and to secure thermocouples in place. A cement paste was also used to fill small holes in the specimen surface. The cement paste for lightweight concrete specimens had lightweight aggregate fines.

For each of the two surfaces of the two specimens, three thermocouples were located in the region of the main heater, and two were located in the region of the guard heater.

Embedded thermocouples reduce the effects of thermal contact resistance, which is due to the influence of any thin air gap between thermocouple wire and concrete. More information on embedding thermocouple wires and thermal contact resistance is given in Reference 15.

Test Results

Thermal conductivity was determined for each set of specimens at 3 or 4 mean temperatures. Thermal conductivity test results are given in Table 5. Results are averages for 3 consecutive data readings obtained after steady-state equilibrium was achieved. Test duration is the time lapsed from the first to the third reading. The average temperature gradient is the temperature gradient across each specimen, averaged for the two specimens. Other terms used in Table 5 are defined in ASTM Designation: C 1045, "Calculating Thermal Transmission Properties from Steady-State Heat Flux Measurements."⁽³⁾

Thermal conductivity as a function of mean specimen temperature is presented in Fig. 21 for Wall L and S lightweight concrete specimens and Fig. 22 for Wall S normal weight concrete specimens. Thermal conductivity

TABLE 5 - STEADY-STATE RESULTS FROM GUARDED HOT PLATE TESTS*

Specimen Description	Test Date	Test Duration, hrs:min	Specimen Mean Temp., °F (°C)	Hot Plate Temp., °F (°C)	Cold Plate Temp., °F (°C)	ΔT Temperature Differential, °F (°C)	q Heat Flux, Btu/hr·sq ft (W/sq m)	t Effective Thickness,** in. (mm)	k Thermal Conductivity, Btu·in./hr·sq ft·°F (W/m·K)
Wall L	6/19/86	2:40	38.7 (3.7)	48.6 (9.2)	28.8 (-1.8)	19.8 (11.0)	14.21 (44.8)	1.90 (48)	1.36 (0.20)
Wall L	6/23/86	1:50	80.8 (27.1)	90.1 (32.3)	71.4 (21.9)	18.7 (10.4)	14.14 (44.6)	1.90 (48)	1.44 (0.21)
Wall L	6/25/86	18:50	109.4 (43.0)	118.8 (48.2)	100.2 (37.9)	18.5 (10.3)	14.07 (44.4)	1.90 (48)	1.44 (0.21)
Wall S NW	11/4/86	3:35	51.4 (10.8)	54.8 (12.7)	48.0 (8.9)	6.8 (3.8)	45.4 (143.3)	1.91 (48)	12.82 (1.85)
Wall S NW	11/7/86	4:20	82.2 (27.9)	85.8 (29.9)	78.5 (25.9)	7.4 (4.1)	48.2 (152.2)	1.91 (48)	12.61 (1.82)
Wall S NW	11/12/86	2:35	112.8 (44.9)	119.4 (48.6)	106.2 (41.2)	13.3 (7.4)	86.4 (273.0)	1.91 (48)	12.45 (1.80)
Wall S Ltwt	12/18/86	2:00	40.7 (4.8)	50.3 (10.2)	31.1 (-0.5)	19.2 (10.7)	15.9 (50.2)	1.79 (45)	1.48 (0.21)
Wall S Ltwt	12/17/86	2:00	55.0 (12.8)	67.8 (19.9)	42.2 (5.7)	25.6 (14.2)	21.0 (66.4)	1.79 (45)	1.47 (0.21)
Wall S Ltwt	12/20/86	2:00	80.6 (27.0)	90.1 (32.3)	71.0 (21.7)	19.1 (10.6)	15.8 (49.9)	1.79 (45)	1.48 (0.21)
Wall S Ltwt	12/23/86	2:00	108.9 (42.7)	118.1 (47.8)	99.8 (37.7)	18.3 (10.2)	15.8 (49.7)	1.79 (45)	1.54 (0.22)

* Measured in accordance with ASTM Designation: C177 using a guarded hot plate

** Average effective thickness is the average distance between hot and cold surface thermocouples for the two specimens.

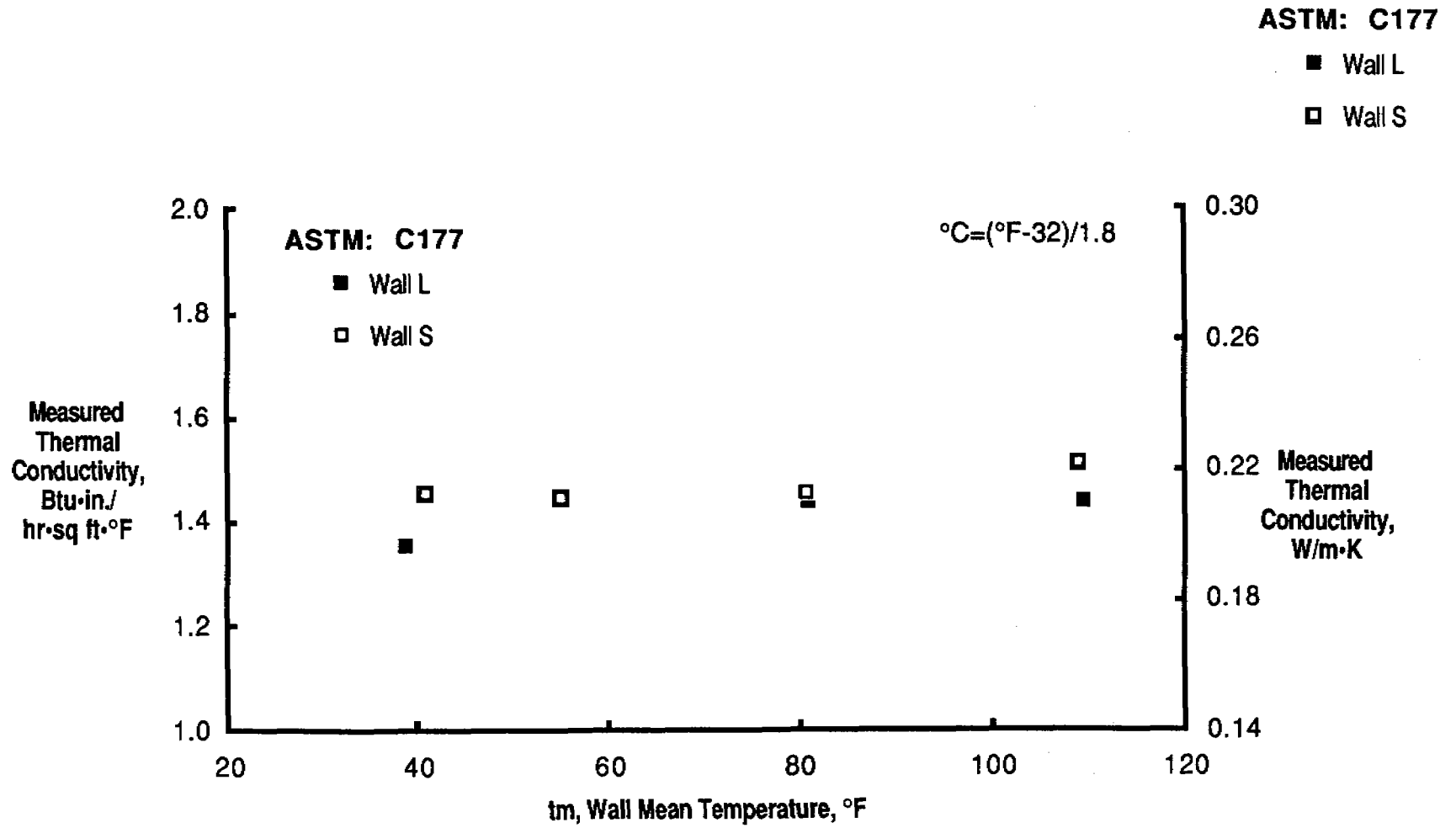


Fig. 21 Thermal Conductivity of Lightweight Concrete Specimens

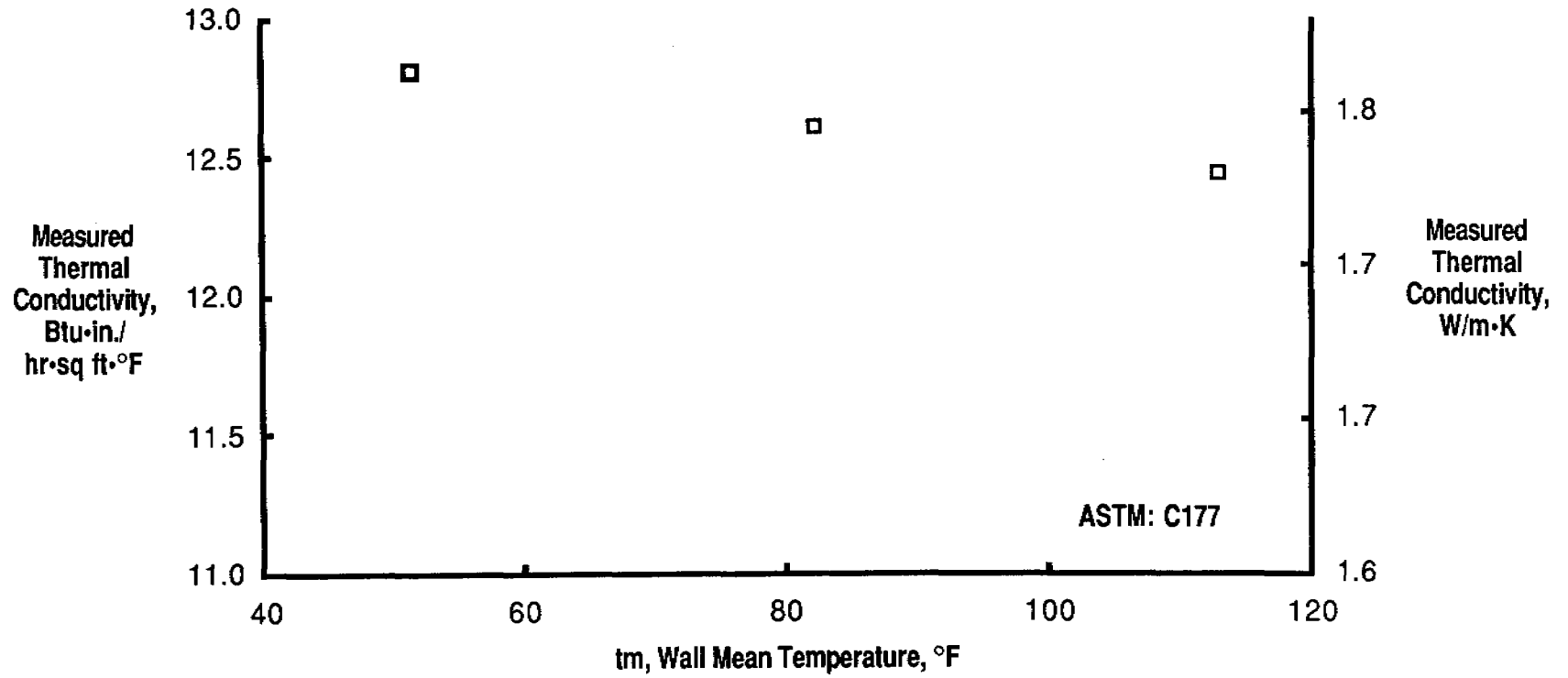


Fig. 22 Thermal Conductivity of Normal Weight Concrete Specimens

generally increases with increasing mean temperature for lightweight concrete and decreases with increasing mean temperature for normal weight concrete.⁽¹⁶⁾

Thermal conductivities at a specimen mean temperature of 75°F (24°C) were interpolated from measured values. Thermal conductivities for Wall L, Wall S lightweight, and Wall S normal weight specimens are 1.43, 1.48, and 12.7 Btu·in./hr·ft²·°F (0.21, 0.21, and 1.82 W/m·K), respectively, at a specimen mean temperature of 75°F (24°C).

Average measured thermal conductivity of the lightweight concrete developed for this project is about 1/9th that for normal weight concrete.

Heat Flux Transducer Test Results

Test Procedures

Two heat flux transducers (HFT's) were mounted on each wall specimen as shown in Figs. 8 and 9 and previously described in the "Instrumentation" section. Sensors were attached near the center of Wall L and on the lightweight concrete portion of Wall S.

Wall L calibrated hot box test results were used to calibrate the HFT's for Wall S. Heat flow through Wall S as measured by the HFT's was determined in accordance with ASTM Designation: C 1046, "Standard Practice for In-Situ Measurement of Heat Flux and Temperature on Building Envelope Components."⁽³⁾

Test Results

Heat flux and thermal conductivity of a lightweight concrete portion of Wall S are presented in Table 6. Results are averages for 16 consecutive hours of testing during steady-state temperature conditions. Data were collected during steady-state calibrated hot box tests.

Results are similar for the heat flux transducers mounted on the climatic chamber and metering chamber sides of the wall.

TABLE 6 - STEADY-STATE RESULTS FOR WALL S MEASURED USING HEAT FLUX TRANSDUCERS (ASTM: C1046)

Wall Mean Temp.,* °F (°C)	tcs Wall Surf. Temp.,* Climatic Side, °F (°C)	tms Wall Surf. Temp.,* Metering Side, °F (°C)	Δt Surface-to-Surface Temp. Diff.,* °F (°C)	q Heat Flux, Btu/hr·sq ft (W/sq m)		k Thermal Conductivity, Btu·in./hr·sq ft·°F (W/m·K)	
				HFT @ Climatic Side	HFT @ Metering Side	HFT @ Climatic Side	HFT @ Metering Side
39.5 (4.2)	12.8 (-10.7)	66.2 (19.0)	53.4 (29.7)	10.4 (33)	10.2 (32)	1.59 (0.23)	1.56 (0.22)
57.4 (14.1)	45.1 (7.3)	69.6 (20.9)	24.5 (13.6)	4.6 (15)	4.5 (14)	1.52 (0.22)	1.48 (0.21)
86.5 (30.3)	97.4 (36.3)	75.5 (24.2)	21.9 (12.2)	5.2 (16)	5.2 (16)	1.92 (0.28)	1.92 (0.28)
104.2 (40.1)	129.0 (53.9)	79.3 (26.3)	49.7 (27.6)	11.9 (33)	11.3 (32)	1.94 (0.28)	1.85 (0.27)

* Temperatures measured by HFT's on lightweight concrete portion of Wall S.

Thermal conductivity of Wall S lightweight concrete at a mean specimen temperature of 75°F (24°C), interpolated from measured values, is 1.75 Btu·in./hr·ft²·°F (0.25 W/m·K).

Discussion of Results

Figure 23 presents thermal conductivities of the lightweight concrete measured by the calibrated hot box (ASTM: C 976), the guarded hot plate (ASTM: C 177), and heat flux transducers (ASTM: C 1046). Thermal conductivities from calibrated hot box and HFT measurements are greater than those from guarded hot plate tests because guarded hot plate specimens were oven-dried to remove moisture, while the wall specimens were air-dried. An increase in specimen moisture content increases thermal conductivity. (7,8,9,16)

Predicted thermal resistances of Walls L and S are presented in Table 7. Values are calculated using results from guarded hot plate tests on oven-dry specimens and measured wall thicknesses. Calculation procedures are from the ASHRAE Handbook - 1985 Fundamentals. (14)

Predicted thermal resistance of Wall S is 17% less than that for Wall L. This compares to an 11% decrease in measured thermal resistance for Wall S compared to Wall L. A percent reduction comparison is used because predicted values are based on oven-dry specimens and measured values are based on air-dried specimens.

DYNAMIC (24-HR PERIODIC) CALIBRATED HOT BOX TESTS

Exterior building walls are seldom subjected to steady-state thermal conditions. Outdoor air temperatures and solar effects cause cyclic changes in outdoor surface temperatures. Generally, indoor surface temperatures are relatively constant compared to outdoor surface temperatures.

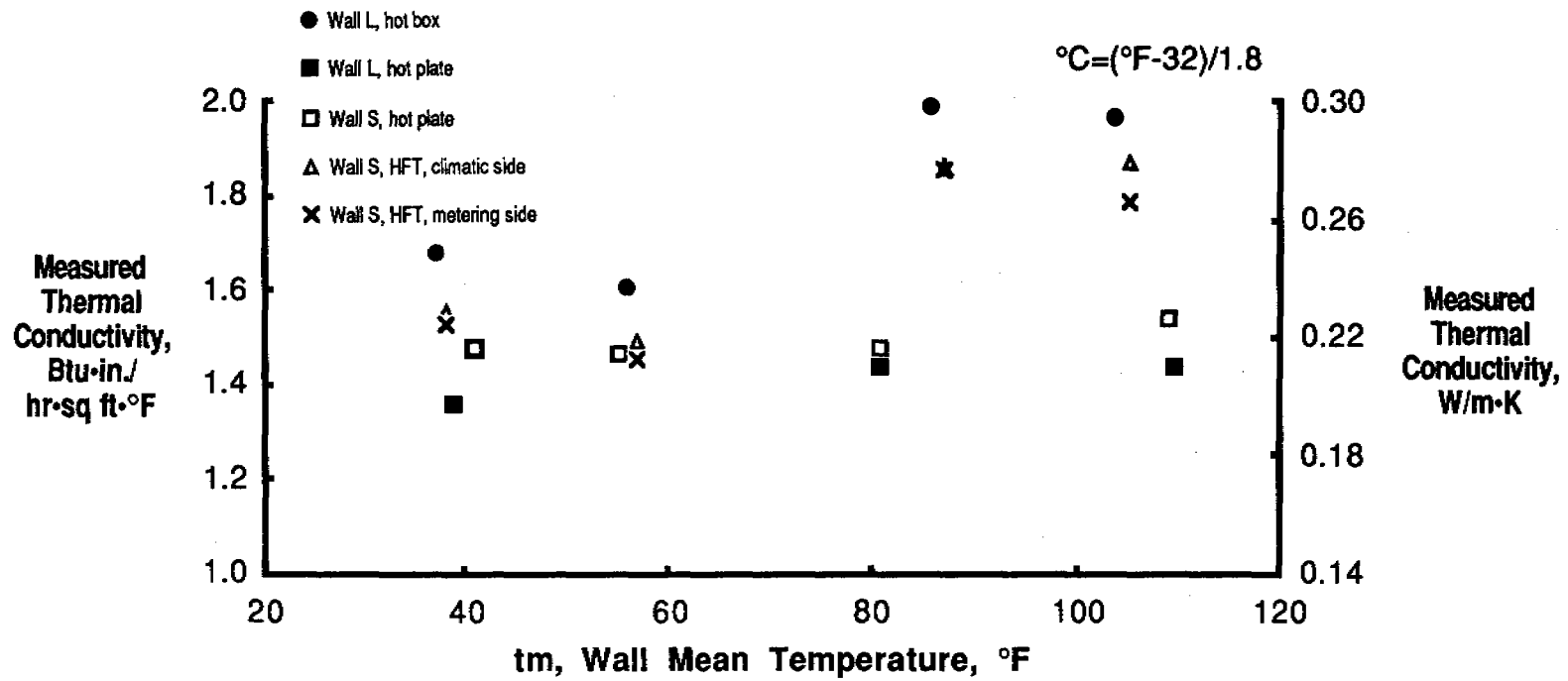


Fig. 23 Measured Thermal Conductivity of Lightweight Concrete

TABLE 7 - PREDICTED THERMAL RESISTANCE OF WALLS L AND S

Layer	R Thermal Resistance, hr•sq ft•°F/Btu (sq m•K/W)		
	Wall L	Wall S Lwt Concrete	Wall S NW Concrete
Outside Air Film	0.17 (0.03)	0.17 (0.03)	0.17 (0.03)
8-in. Thick Concrete Wall (200-mm)	5.59* (0.98)	5.49* (0.97)	0.64* (0.11)
Inside Air Film	0.68 (0.12)	0.68 (0.12)	0.68 (0.12)
Total R	6.44 (1.13)	6.34 (1.12)	1.49 (0.26)

* Calculated from guarded hot plate thermal conductivities of oven-dry specimens at 75°F (24°C) and measured wall thickness.

Wall S R-value calculated using ASHRAE parallel path method (Ref. 14):

$$U = (1/1.49) \cdot (6/103) + (1/6.34) \cdot (97/103)$$

$$= 0.188 \text{ Btu/hr} \cdot \text{sq ft} \cdot \text{°F}$$

$$(1.07 \text{ W/sq m} \cdot \text{K})$$

$$R = 1/U = 5.33 \text{ hr} \cdot \text{sq ft} \cdot \text{°F/Btu}$$

$$(0.94 \text{ sq m} \cdot \text{K/W})$$

Dynamic tests are a means of evaluating thermal response under controlled conditions that simulate temperature changes actually encountered in building envelopes. The heat flow through walls as a response to temperature changes is a function of both thermal resistance and thermal storage capacity.

Test Procedures

The lightweight concrete wall, designated Wall L, was subjected to four dynamic temperature cycles using the CTL calibrated hot box. For these tests, the calibrated hot box metering chamber air temperatures were held constant while climatic chamber air temperatures were cycled over a pre-determined time versus temperature relationship. The rate of heat flow through a test specimen was determined from hourly averages of data.

Three 24-hour (diurnal) temperature cycles were applied to Wall L in this investigation. The first cycle, denoted the NBS Test Cycle, has been used in previous CTL calibrated hot box studies.^(4-12,15,17,18) This periodic cycle is based on a simulated sol-air* cycle used by the National Bureau of Standards in their evaluation of dynamic thermal performance of an experimental masonry building.⁽¹⁹⁾ It represents a large variation in outdoor temperature over a 24-hour period. For the NBS Test Cycle, the mean air temperature of the climatic chamber is approximately equal to the mean air temperature of the metering chamber.

Two additional sol-air temperature cycles were run with climatic chamber mean air temperatures approximately 10°F (6°C) above and 10°F (6°C) below the

Sol-air temperature is that temperature of outdoor air that, in the absence of all radiation exchanges, would give the same rate of heat entry into the surface as would exist with the actual combination of incident solar radiation, radiant energy exchange, and convective heat exchange with outdoor air. (14)

metering chamber mean air temperature. The test cycle designated "NBS+10" was derived by increasing hourly climatic chamber air temperatures of the NBS Test Cycle by 10°F (6°C). The test cycle designated "NBS-10" was derived by decreasing hourly climatic chamber air temperatures by 10°F (6°C).

Climatic chamber air temperatures for the three sol-air test cycles applied to Wall L are illustrated in Fig. 24. Climatic chamber air temperatures represent the average from the 16 thermocouples located 3 in. (75 mm) from the test specimen surface in the climatic chamber. Average metering chamber air temperature over the 24-hour period for each cycle was approximately 72°F (22°C).

The fourth dynamic temperature cycle applied to Wall L was composed of 3 time-dependent temperature patterns. Test procedures and results for this test cycle, denoted the Sine Cycle, are presented in the "Dynamic (3-Frequency) Calibrated Hot Box Test" section of this report.

For all tests, dynamic cycles were repeated until conditions of equilibrium were obtained. Equilibrium conditions were evaluated by consistency of applied temperatures and measured heat flow. After equilibrium conditions were reached, each test was continued for a period of three days. Results are based on average readings for three consecutive 24-hour cycles. Each test required a total of approximately eight days for completion. Dynamic calibrated hot box tests were performed in May and June 1986.

Test Results

Measured temperatures, temperature differentials, and heat flow for dynamic temperature cycles applied to Wall L are presented in Appendix B. Brief descriptions of symbols used in test result figures and tables are listed in Table 8. Symbols are described in detail in the following paragraphs.

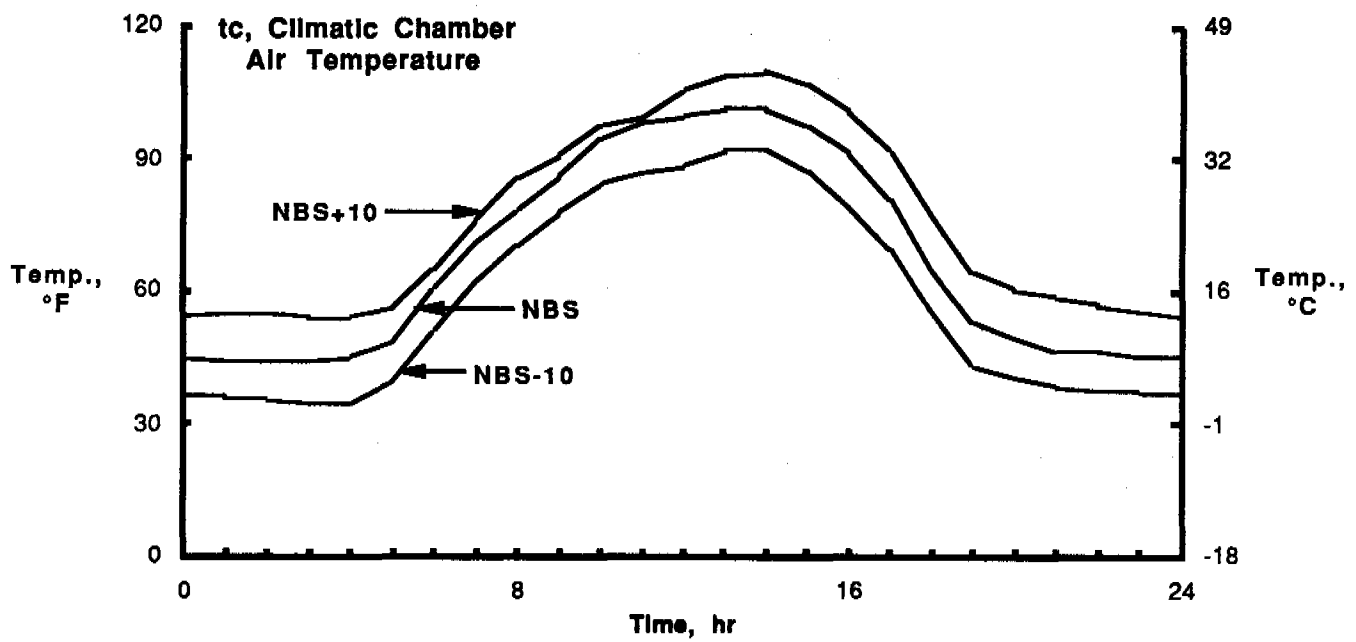


Fig. 24 Climatic Chamber Air Temperatures for Dynamic Sol-Air Temperature Cycles

TABLE 8 - ABBREVIATIONS FOR HEAT FLOW AND TEMPERATURE

qhft	=	heat flow measured by heat flux transducer mounted on metering chamber wall surface (ASTM: C 1046)
qhft	=	heat flow measured by heat flux transducer mounted on climatic chamber wall surface (ASTM: C 1046)
qss	=	heat flow predicted using steady-state equations and measured surface temperatures
qw	=	heat flow measured by calibrated hot box (ASTM: C 976)
tm	=	metering chamber air temperature
tms	=	wall surface temperature, metering chamber side
tmd	=	concrete temperature at wall mid-thickness
tcs	=	wall surface temperature, climatic chamber side
tc	=	climatic chamber air temperature
tavg	=	average of wall surface temperatures on metering and climatic chamber sides

Measured Temperatures and Temperature Differentials

Climatic chamber air (tc), metering chamber air (tm), climatic surface (tcs), metering surface (tms), and internal wall (tmd) temperatures are average readings of the 16 thermocouples placed as described in the "Instrumentation" section of this report, and are presented in Appendix B.

Air-to-air (tc-tm), surface-to-surface (tcs-tms), and surface-to-air (tc-tcs, tms-tm) temperature differentials are also presented in Appendix B.

Heat Flow

Heat flow is designated positive when heat flows from the calibrated hot box climatic chamber to the metering chamber. Heat flow determined from calibrated hot box tests (ASTM: C 976) is denoted qw.

Heat flow measurements from heat flux transducers (ASTM: C 1046) located on the metering and climatic chamber sides of the test specimen surface are denoted qhft and qhft, respectively. Heat flux transducer data were calibrated using results from steady-state calibrated hot box tests on Wall L.

Heat flow predicted using steady-state equations is denoted qss. Values were calculated on an hourly basis from wall surface temperatures using the following equation:

$$q_{ss} = (t_{ms} - t_{cs}) / R \quad (2)$$

where

qss = heat flow through wall predicted using steady-state equations,
Btu/hr·ft² (W/m²)

R = average thermal resistance of wall, hr·ft²·°F/Btu
(m²·K/W)

tcs = average temperature of wall surface, climatic chamber side, °F (°C)

tms = average temperature of wall surface, metering chamber side, °F (°C)

Thermal resistances are dependent on wall mean temperature and were derived from steady-state calibrated hot box test results.

Appendix B tables also footnotes calibrated hot box metering and climatic chamber relative humidities, and maximum and minimum laboratory air temperatures measured during tests.

Discussion of Test Results

Heat Flow Comparisons

Figure 25 shows measured and calculated heat flows through Wall L for the NBS, NBS+10, and NBS-10 Temperature Cycles. Heat flows measured by the calibrated hot box, q_w , and calculated from steady-state resistances using Eq. 2, q_{ss} , are shown.

Measured heat flow curves, q_w , show significantly reduced and delayed peaks compared to calculated heat flows, q_{ss} , for all three temperature cycles. Differences between the measured and calculated heat flows are due to the thermal storage capacity of the concrete wall.

Thermal Lag

One measure of dynamic thermal performance is thermal lag. Thermal lag is a measure of the response of indoor surface temperatures and heat flow to fluctuations in outdoor air temperatures. Lag is dependent on thermal resistance and heat storage capacity of the test specimen, since both of these factors influence the rate of heat flow.

For each sol-air test cycle, Table 9 lists thermal lags determined from calibrated hot box test results and measured heat flux transducer readings. Calibrated hot box thermal lag is quantified by two methods. In one measure, denoted " t_c vs t_{ms} ," lag is calculated as the time required for the maximum or minimum specimen surface temperature on the metering chamber side to be reached after the maximum or minimum climatic chamber air temperature is

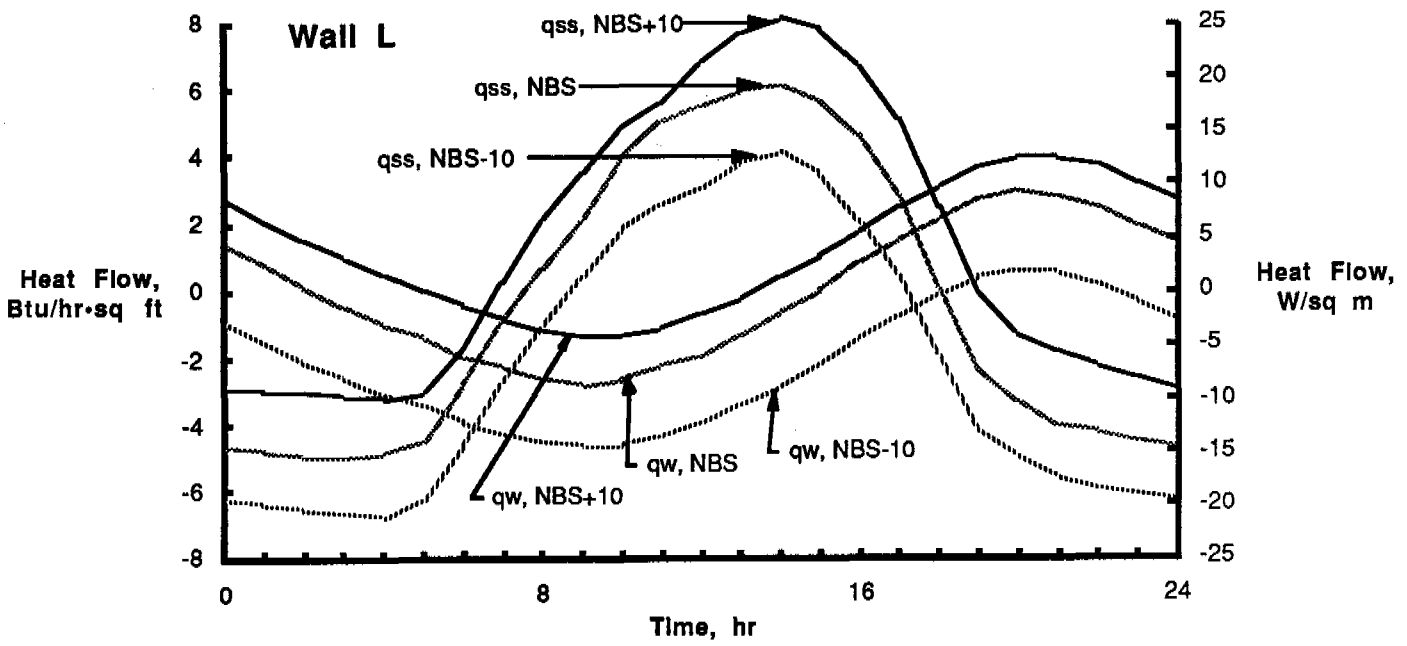


Fig. 25 Heat Flow for NBS, NBS+10, and NBS-10 Test Cycles

TABLE 9 - MEASURED THERMAL LAG FOR WALL L

Test Cycle	Measured Thermal Lag, hrs							
	Calibrated Hot Box					Heat Flux Transducer		
	tc vs trns		qss vs qw		Avg.	qss vs qhft		Avg.
	@ Max.	@ Min.	@ Max.	@ Min.		@ Max.	@ Min.	
NBS	6.5	6.5	6	6	6.5	6.5	6	6.5
NBS+10	6.5	5.5	6.5	6	6	7	6	6.5
NBS-10	5.5	4.5	6	5	5.5	6.5	5	6

attained. In the second measure, denoted "qss vs qw," lag is calculated as the time required for the maximum or minimum heat flow rate, q_w , to be reached after the maximum or minimum heat flow rate based on steady-state predictions, q_{ss} , is attained. The second measure is illustrated in Figure 26 for the NBS Test Cycle applied to Wall L. Both measures give similar results. The second measure was used to determine thermal lag for heat flux transducer data.

Average thermal lag values range from 5.5 to 6.5 hours. Thermal lag values are relatively constant regardless of the temperature cycle applied to the wall. Values determined using heat flux transducer data are similar to those determined from calibrated hot box test results.

Lag times of 3 to 15 hours are generally beneficial for exterior walls. Walls with these lag times delay peak afternoon heat loads until cooler night hours. Thermal lags as low as 3 hours are beneficial in delaying peak afternoon loads until cooler evening hours. These lower lag times are especially beneficial in commercial and industrial buildings that are vacated in the evening hours. The "lag effect" is also beneficial for passive solar applications.

Reduction in Amplitude

Reduction in amplitude is a second measure of dynamic thermal performance. Reduction in amplitude, as well as thermal lag, is influenced by both wall thermal resistance and heat storage capacity. Reduction in amplitude is dependent on the temperature cycle applied to the test specimen.

Reduction in amplitude is defined as the percent reduction in peak heat flow when compared to peak heat flow calculated using steady-state equations. Reduction in amplitude is also illustrated in Fig. 26. Values for reduction in amplitude were calculated using the following equation:

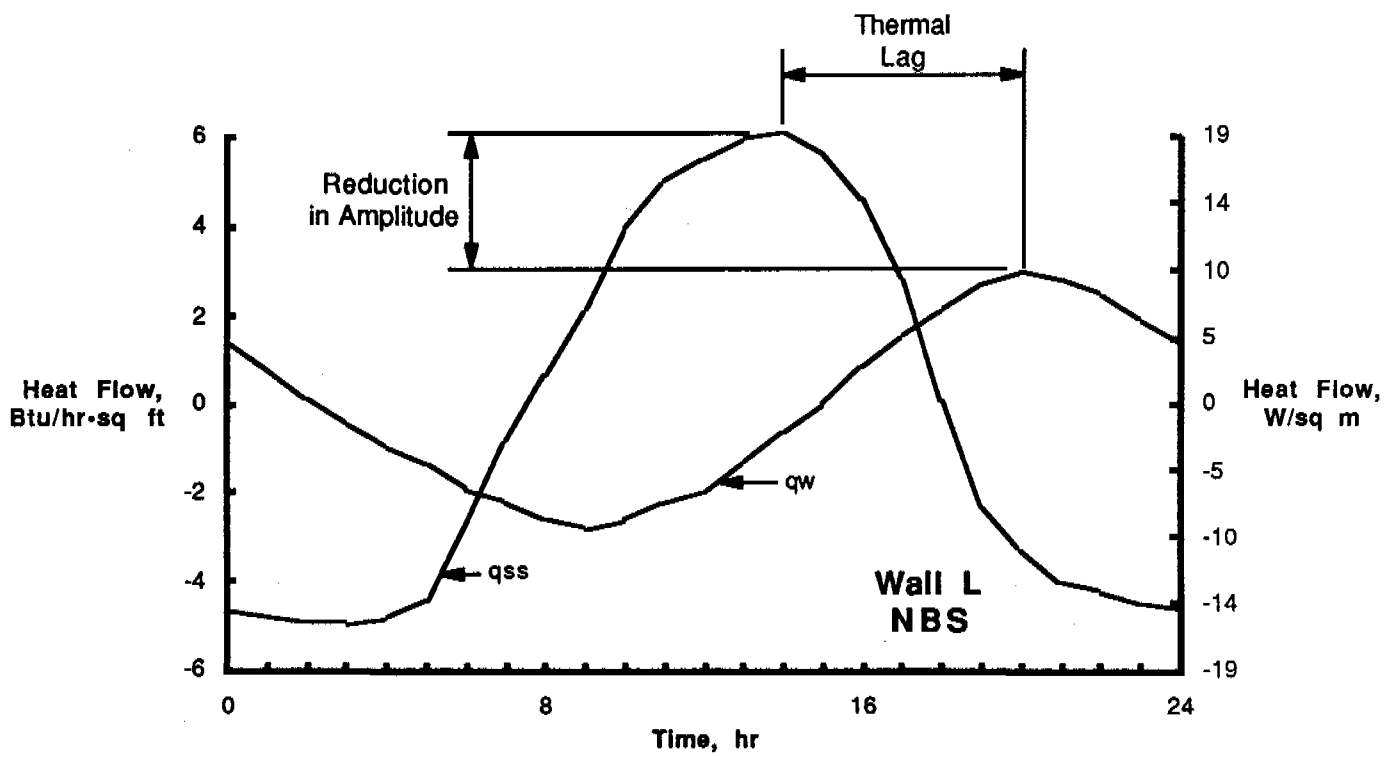


Fig. 26 Definition of Thermal Lag and Reduction in Amplitude

$$A = [1 - (q' - \bar{q}) / (q'_{ss} - \bar{q}_{ss})] \cdot 100 \quad (3)$$

where

A = reduction in amplitude, %

q' = maximum or minimum measured heat flow through wall

\bar{q} = mean measured heat flow through wall

q'_{ss} = maximum or minimum heat flow through wall predicted using steady-state equations (Eq. 2)

\bar{q}_{ss} = mean heat flow through wall predicted using steady-state equations (Eq. 2)

Table 10 lists reduction in amplitude values for each sol-air temperature cycle applied to Wall L. Average reduction in amplitude values for heat flow measured by the calibrated hot box, q_w, range from 47 to 53% for the three temperature cycles. Average reduction in amplitude values from heat flux transducer measurements range from 58 to 60% for the three walls.

Amplitudes for heat flux transducer data, q_{hft}, are generally more reduced or "dampened" compared to calibrated hot box measurements, q_w. Heat flow amplitudes differ because of the physical presence of the instrument mounted on a wall. A wall's thermal properties are locally altered by the heat flux transducer. The heat flux transducer adds mass and therefore "dampens" heat flows. In addition, heat flux transducer calibration using steady-state results may not fully correct for dynamic effects of the instrument location.

Actual maximum heat flow through a wall is important in determining the peak energy load for a building envelope. Data in Table 10 and Appendix B show anticipated peak energy demands based on actual heat flow will be less than those based on steady-state predictions for walls with thermal storage capacity. Calculations based on steady-state equations overestimate peak heat flow for the three sol-air temperature cycles applied to Wall L.

TABLE 10 - MEASURED REDUCTION IN AMPLITUDE FOR WALL L

Test Cycle	Measured, %					
	Calibrated Hot Box			Heat Flux Transducer		
	@ Max. Heat Flow	@ Min. Heat Flow	Avg.	@ Max. Heat Flow	@ Min. Heat Flow	Avg.
NBS	53	41	47	63	53	58
NBS+10	59	46	53	66	54	60
NBS-10	56	46	51	63	52	58

Total Heat Flow

Results of dynamic tests are also compared using measures of total heat flow through a specimen for a 24-hr temperature cycle. Total measured heat flow is illustrated in Fig. 27 for the NBS Test Cycle applied to Wall L. The curve marked "qw" is heat flow through the test wall measured by the calibrated hot box. Areas enclosed by the measured heat flow curve and the line for zero heat flow are total heat flow through a wall. The sum of the areas above and below the horizontal axis is total measured heat flow for a 24-hour period, denoted as q_w^T .

A similar procedure is used to calculate total heat flow for a 24-hour period from measured heat flux transducer data, q_{hft} , and predictions based on steady-state equations, q_{ss} .

Table 11 lists total heat flow values for the NBS, NBS+10, and NBS-10 Test Cycles applied to Wall L. Values measured by the calibrated hot box, measured by heat flux transducers, and calculated using steady-state thermal resistances are denoted q_w^T , q_{hft}^T , and q_{ss}^T , respectively. "Total Heat Flow Comparisons" listed in Table 11 show measured total heat flow as a percentage of predicted heat flow based on steady-state equations (Eq. 2).

As shown in the "Total Heat Flow Comparisons" column of Table 11, total heat flow measured by the calibrated hot box ranges from 44 to 54% of total heat flow calculated using steady-state analysis. The ratio of total measured heat flow to steady-state predictions depends on the climatic chamber air temperature cycle applied to the wall. Particularly for massive walls, greater reductions in actual heat flow, compared to steady-state predictions, occur for temperature cycles which produce heat flow reversals through a wall.

It should be noted that comparison of total measured heat flow values are limited to the specimen and dynamic cycles evaluated in this program. Results

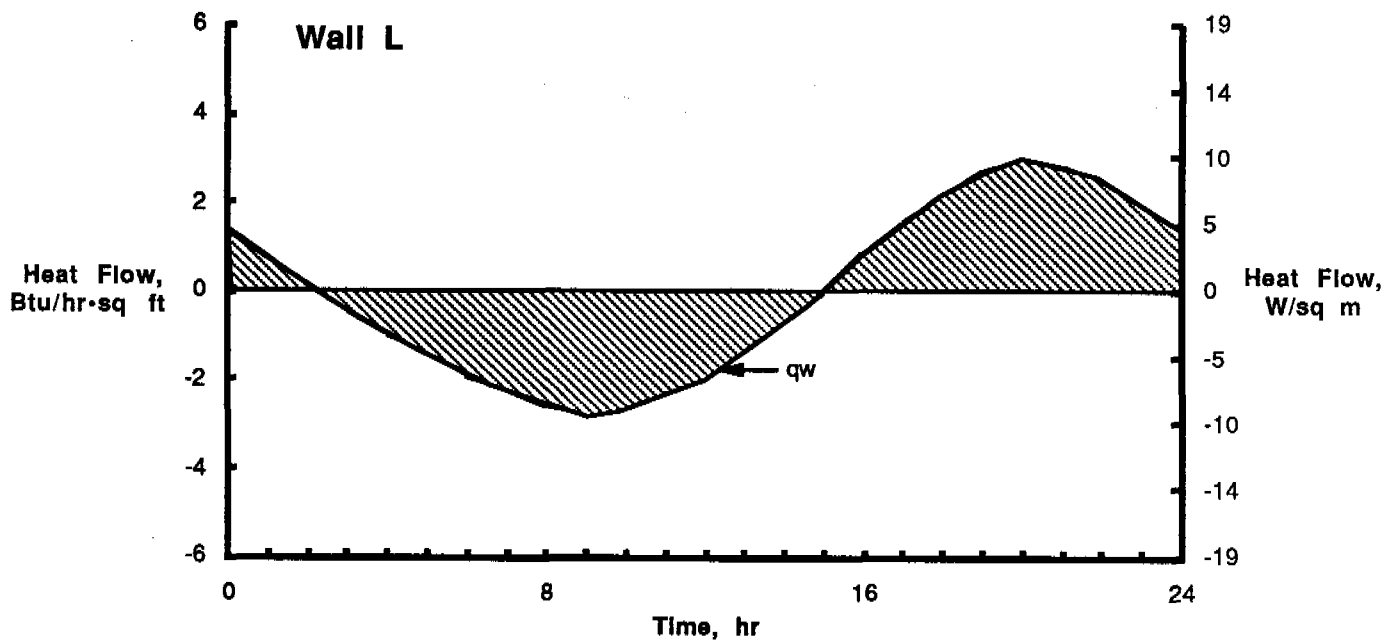


Fig. 27 Definition of Total Measured Heat Flow

TABLE 11 - TOTAL HEAT FLOW FOR WALL L

Test Cycle	Total Heat Flow, Btu/sq ft (W·hr/sq m)			Total Heat Flow Comparisons, %	
	Measured		Calculated	$\frac{T}{q_w} / \frac{T}{q_{ss}}$	$\frac{T}{q_{hft}} / \frac{T}{q_{ss}}$
	$\frac{T}{q_w}$	$\frac{T}{q_{hft}}$	$\frac{T}{q_{ss}}$		
NBS	40.9 (129)	33.8 (107)	93.3 (294)	44	36
NBS+10	42.0 (132)	42.0 (132)	88.5 (279)	47	47
NBS-10	56.5 (178)	45.9 (145)	97.8 (308)	54	47

are for three particular diurnal test cycles and should not be extrapolated to represent annual heating and cooling loads. In additions, results are for individual opaque wall assemblies. As such, they are representative of only one component of the building envelope.

Comparisons with Other Concrete Walls

Dynamic heat transmission coefficients of thermal lag, reduction in amplitude, and total heat flow ratio are used to compare dynamic thermal response of alternative wall systems.

Thermal lag and reduction in amplitude are dependent on both thermal resistance, R , and heat storage capacity,

$$\rho c L$$

where

ρ = wall density, pcf (kg/m^3)

c = wall specific heat, Btu/lb·F ($\text{J/kg}\cdot\text{K}$)

L = wall thickness, ft (m)

Mass per unit area, ρL , is the predominant factor in determining heat storage capacity of most building materials.

For homogeneous walls, thermal lag and reduction in amplitude increase with an increase in M .⁽²⁰⁾

$$M = \frac{L^2/\alpha}{p}^{1/2} = \frac{(R)\cdot(\rho c L)}{p}^{1/2} \quad (4)$$

where

L = wall thickness, ft (m)

α = thermal diffusivity, $\text{k}/\rho c$, ft^2/hr (m^2/s)

k = thermal conductivity of wall, Btu/hr·ft·°F ($\text{W/m}\cdot\text{K}$)

ρ = wall density, pcf (kg/m^3)

c = wall specific heat, Btu/lb·°F ($\text{J/kg}\cdot\text{K}$)

R = wall resistance, $\text{hr}\cdot\text{ft}^2\cdot^\circ\text{F}/\text{Btu}$ ($\text{m}^2\cdot\text{K}/\text{W}$)

P = period of dynamic cycle, hr

Table 12 presents values of M and dynamic heat transmission coefficients for Wall L and three other homogeneous concrete walls. Thermal lag, reduction in amplitude, and total heat flow ratio are for the NBS Temperature Cycle applied to each wall using a calibrated hot box. Thermal resistances used in Eq. 4 to calculate M are for a wall mean temperature of 75°F (24°C) and are from measurements using CTL's calibrated hot box. Surface film resistances are not included in resistances used in Eq. 4. The dynamic cycle period, P , is 24 hrs.

Specific heat values were measured using U.S. Army Corps of Engineers Method CRD-C124-73, "Method of Test for Specific Heat of Aggregates, Concrete, and Other Materials (Method of Mixtures)." (21) Table 12 specific heat values are for air-dried concrete. Values for Wall L are from Reference 2.

Figures 28 and 29, respectively, show that thermal lag and reduction in amplitude generally increase as M increases. Figure 30 shows that total heat flow ratio generally decreases with an increase in M .

Wall C3, low density concrete, has the greatest lag time, equal to 8.5 hours. Concretes in Walls L and C3 have less mass but much higher resistances than most concrete and masonry materials. Equation 4 shows that M varies with the square root of both mass and resistance.

The newly developed Wall L concrete exhibits beneficial thermal and structural properties. Compared to the low density concrete of Wall C3, the newly developed Wall L concrete has 80% of the resistance, 80% of the thermal lag, 120% of the mass, but 230% of the compressive strength. Twenty-eight day compressive strengths for Wall C3 and Wall L concretes, respectively, are 880 psi (6.1 MPa)⁽⁹⁾ and 2000 psi (13.8 MPa).⁽²⁾ The concrete for Wall L can be used as a load-bearing wall whereas the concrete for Wall C3 cannot.

TABLE 12 - CONCRETE WALL COMPARISONS

Wall Designation	Wall Type	Reference	Measured Properties								Calculated M
			L Thickness, in. (mm)	ρ Unit Weight, pcf (kg/cu m)	Estimated Moisture Content, % oven-dry wt.	R* Thermal Resistance, hr·sq ft·°F/Btu (sq m·K/W)	c** Specific Heat, Btu/lb·°F (J/kg·K)	Thermal Lag,*** hr	Amplitude Reduction,*** %	Thermal Heat Flow Ratio,*** %	
C1	Normal weight structural concrete with sand and gravel aggregate	7	8.31 (211)	144 (2310)	2	0.71 (0.12)	0.19 (810)	4.0	45	53	0.75
C2	Lightweight structural concrete with expanded shale aggregate	8	8.28 (210)	102 (1630)	9	1.75 (0.31)	0.23 (960)	5.5	54	48	1.09
L	Lightweight structural concrete with Macrolite™ aggregate	-	8.00 (203)	56 (900)	2	4.4 (0.77)	0.11 (460)	6.5	47	44	0.87
C3	Low density concrete with expanded perlite aggregate	9	8.52 (216)	46 (740)	10	5.9 (1.00)	0.18 (750)	8.5	61	39	1.20

* From calibrated hot box (ASTM: C976) test results at a wall mean temperature of 75°F (24°C). Values do not include surface film resistances.

** For air dry concrete, measured using U.S. Army Corps of Engineers Method CRD-C124-73. See Ref. 2.

*** Measured using the NBS Dynamic Temperature Cycle.

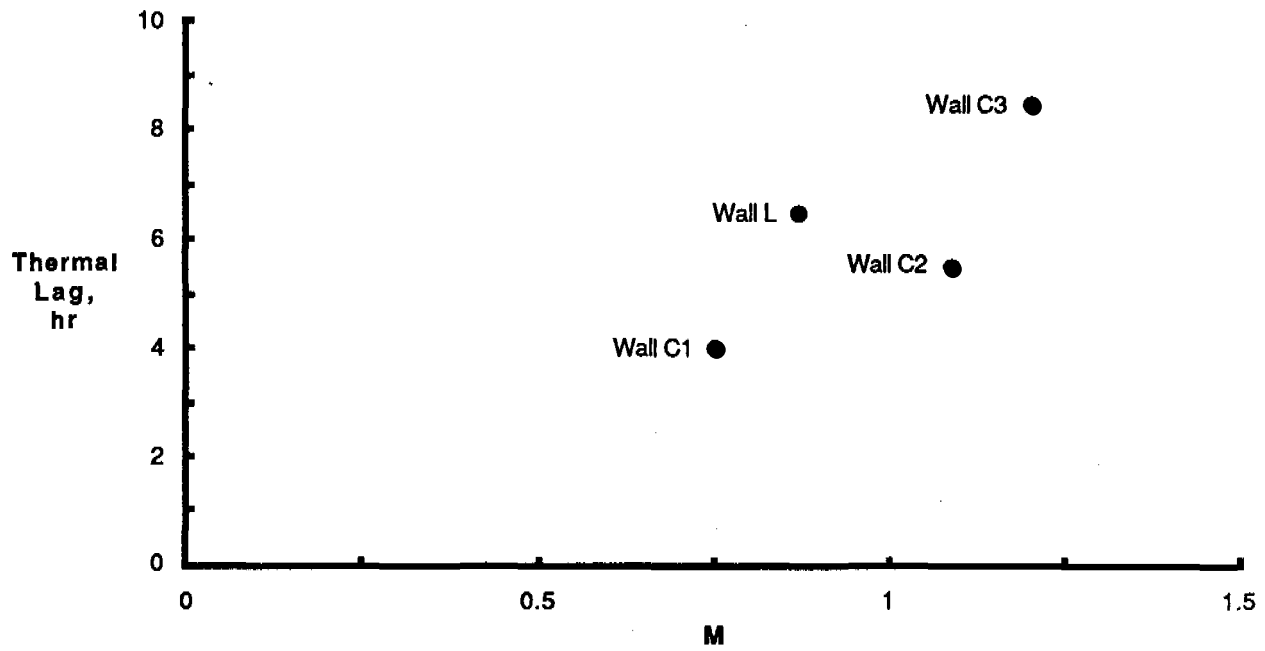


Fig. 28 Thermal Lag and M Values for the NBS Test Cycle Applied to Concrete Walls

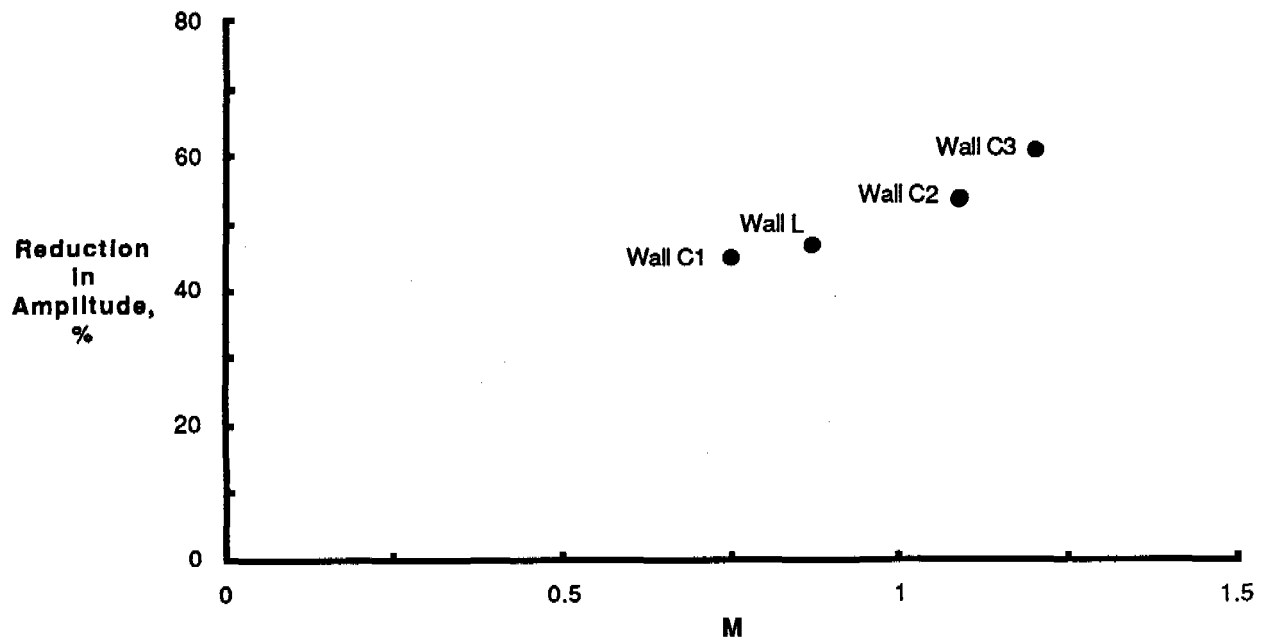


Fig. 29 Reduction in Amplitude and M Values for the NBS Test Cycle Applied to Concrete Walls

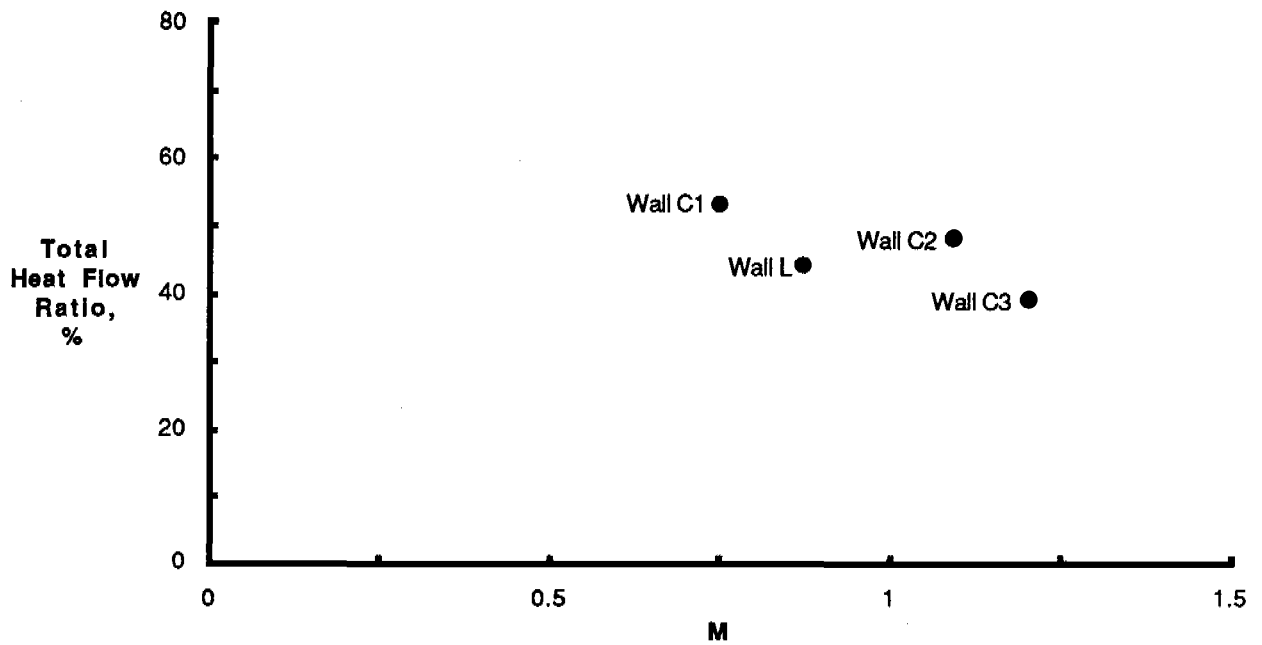


Fig. 30 Total Heat Flow Ratio and M Values for the NBS Test Cycle Applied to Concrete Walls

DYNAMIC (3-FREQUENCY) CALIBRATED HOT BOX TEST

A fourth dynamic cycle composed of three sinusoidal temperature functions was applied to Wall L to investigate an alternative analysis technique. The analysis technique uses calibrated hot box test data to determine a time constant and thermal diffusivity of the homogeneous lightweight structural concrete wall. The test approach was suggested by Mr. Mark P. Modera,* Lawrence Berkeley Laboratory. Calibrated hot box tests and data reduction were performed at CTL. Mr. Modera performed the data analysis and presented results in a paper⁽²²⁾ included in this report as Appendix C.

Test Cycle

The sinusoidal temperature cycle applied to Wall L is denoted the Sine Cycle and is the sum of three sine functions with differing periods. Three functions were chosen so that a thermal diffusivity and time constant could be determined from data for each function. The resulting diffusivities and time constants are theoretically equal. If they are not experimentally equal, their trends are a means of evaluating the accuracy of the dynamic technique.

The Sine Cycle is composed of sine functions with 6, 12, and 24-hr periods and 15°F (8.33°C) amplitudes, as shown in Fig. 31.

The Sine Cycle can be expressed as:

$$F = 30 + 15\sin\frac{\pi}{3}t + 15\sin\frac{\pi}{6}t + 15\sin\frac{\pi}{12}t \quad (\text{IP}) \quad (5)$$

$$F = -1.11 + 8.33\sin\frac{\pi}{3}t + 8.33\sin\frac{\pi}{6}t + 8.33\sin\frac{\pi}{12}t \quad (\text{SI})$$

where

F = temperature, °F (°C)

t = time, hr

*Energy Performance of Buildings Group, Applied Science Division, Lawrence Berkeley Laboratory, Berkeley, CA 94720

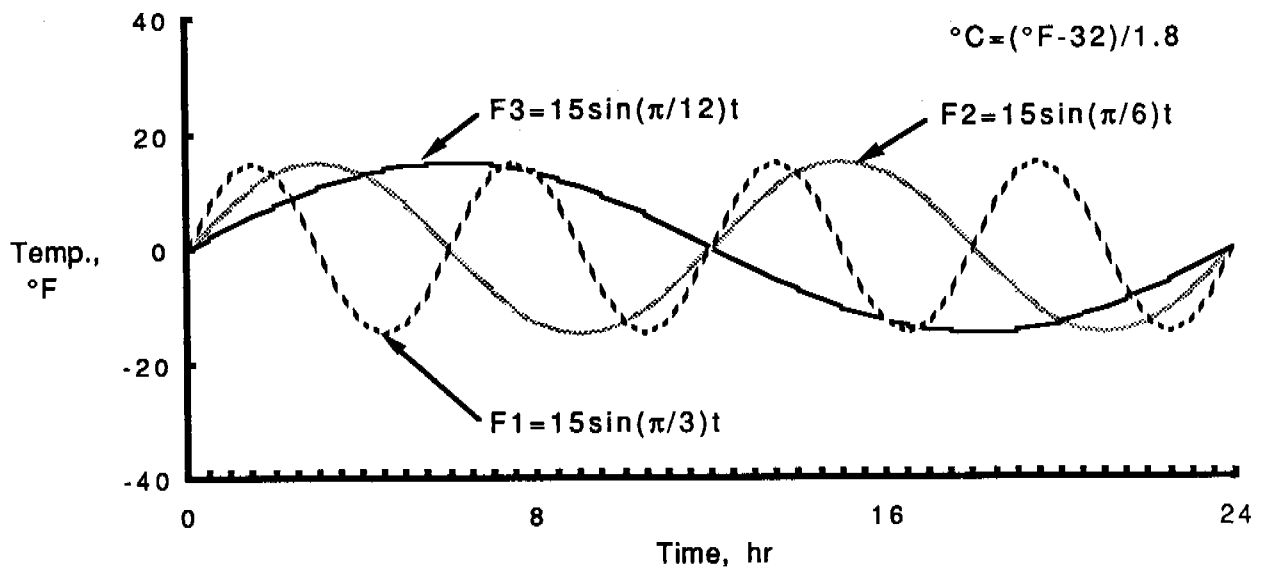


Fig. 31 Sine Functions with 6, 12, and 24-hr Periods

The Sine Cycle has a 24-hr period and an amplitude of 67°F (37.2°C). The amplitude was determined based on climatic chamber temperature limitations and a desire to have no reversals in heat flow through the wall. The climatic chamber air temperature is currently limited to a minimum of -15°F (-26°C). To provide no reversal in the heat flow through Wall L, the maximum cycle temperature had to be less than 71°C (22°C), the metering chamber air temperature.

The climatic chamber air temperature followed the Sine Cycle. The metering chamber air temperature was maintained at 71° (22°C). The cycle was repeated until conditions of equilibrium were obtained. Equilibrium conditions were evaluated by consistency of applied temperatures and measured heat flow.

Figure 32 presents the theoretical Sine Cycle from Eq. 5 and the actual climatic chamber air temperature for the 24-hr period selected for data analysis.

Data Collection

For the Sine Cycle, test data channels were scanned every two minutes. Average temperature and supplementary data were obtained from average readings for 12 minutes. The cumulative watt-hour transducer output was scanned every 12 minutes.

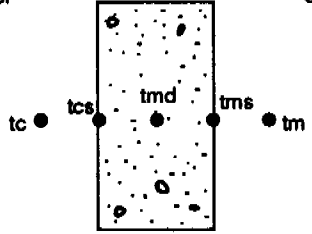
Test Results

Measured temperatures and heat flow for the Sine Cycle applied to Wall L are presented in Figs. 33 and 34, respectively. Brief descriptions of symbols used in test results figures and tables are listed in Table 8. Symbols are described in detail in the "Test Results" portion of the "Dynamic (24-hr Periodic) Calibrated Hot Box Tests" section of this report.

Heat flow measured by the calibrated hot box is denoted q_w in Fig. 34 and has been smoothed by averaging five 12-min. increments for each data point.

Climatic
(Outdoor)
Chamber

Metering
(Indoor)
Chamber



Legend

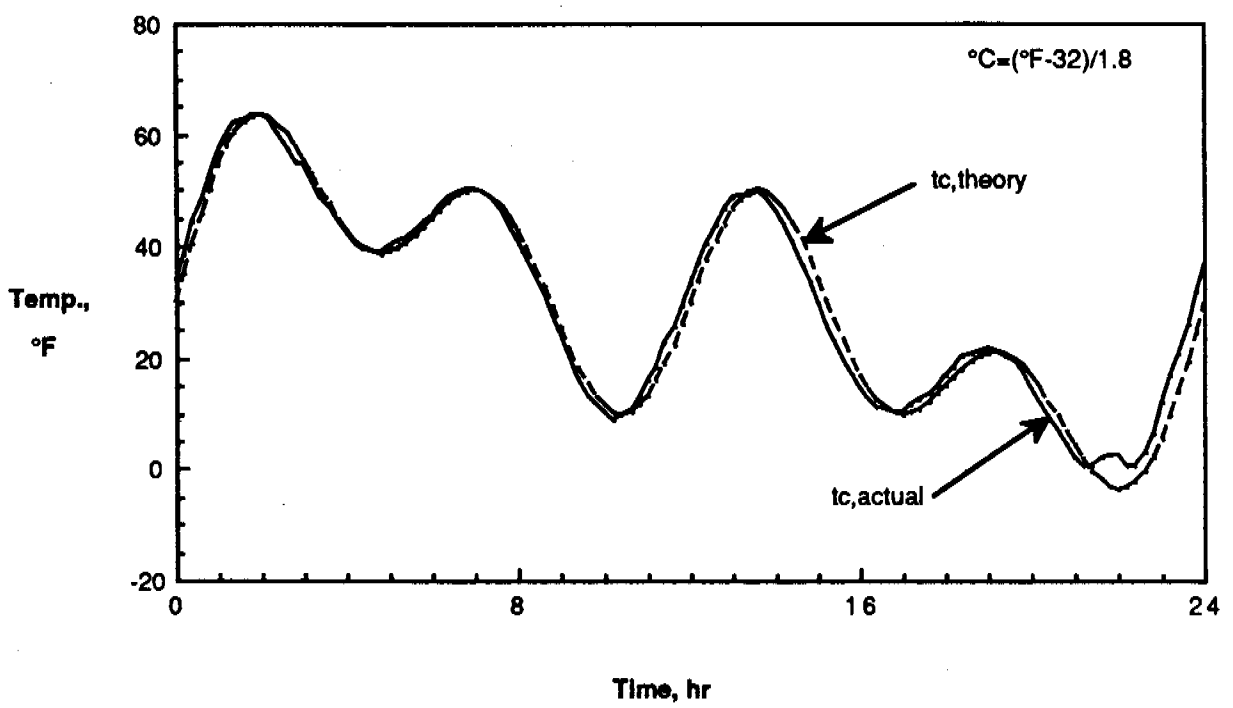
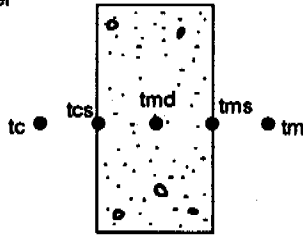


Fig. 32 Climatic Chamber Air Temperature for Sine Temperature Cycle

Climatic
(Outdoor)
Chamber

Metering
(Indoor)
Chamber



Legend

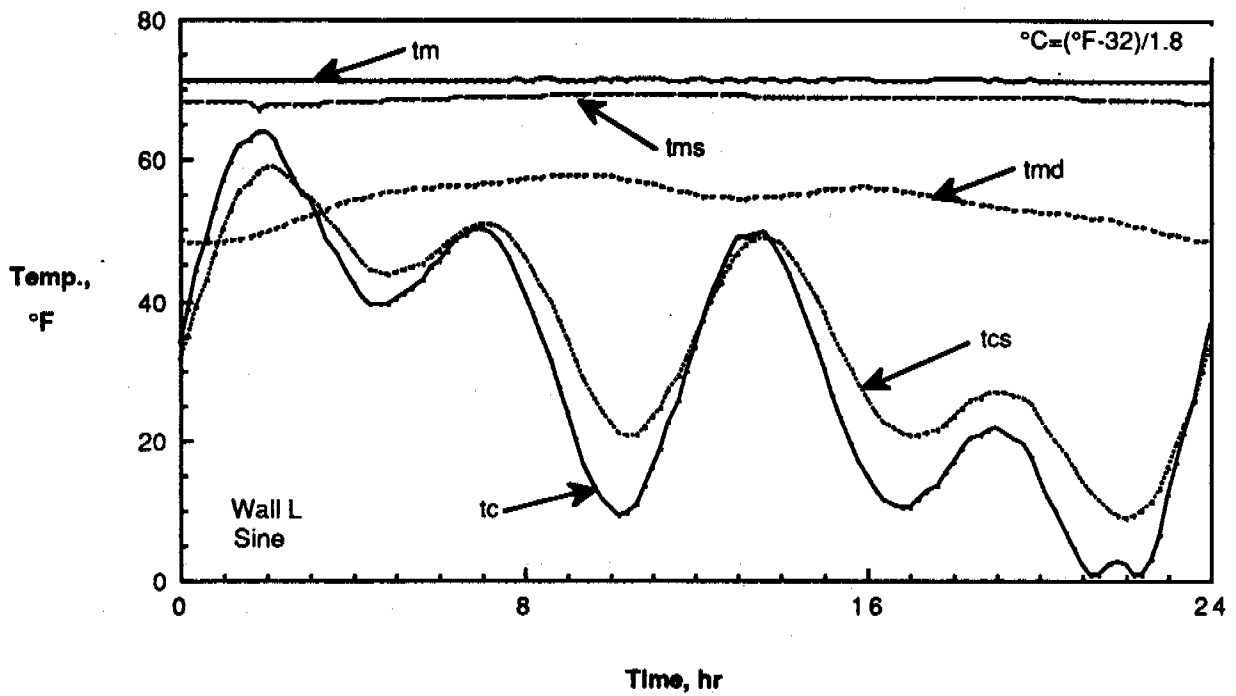


Fig. 33 Measured Temperatures for Sine Test Cycle

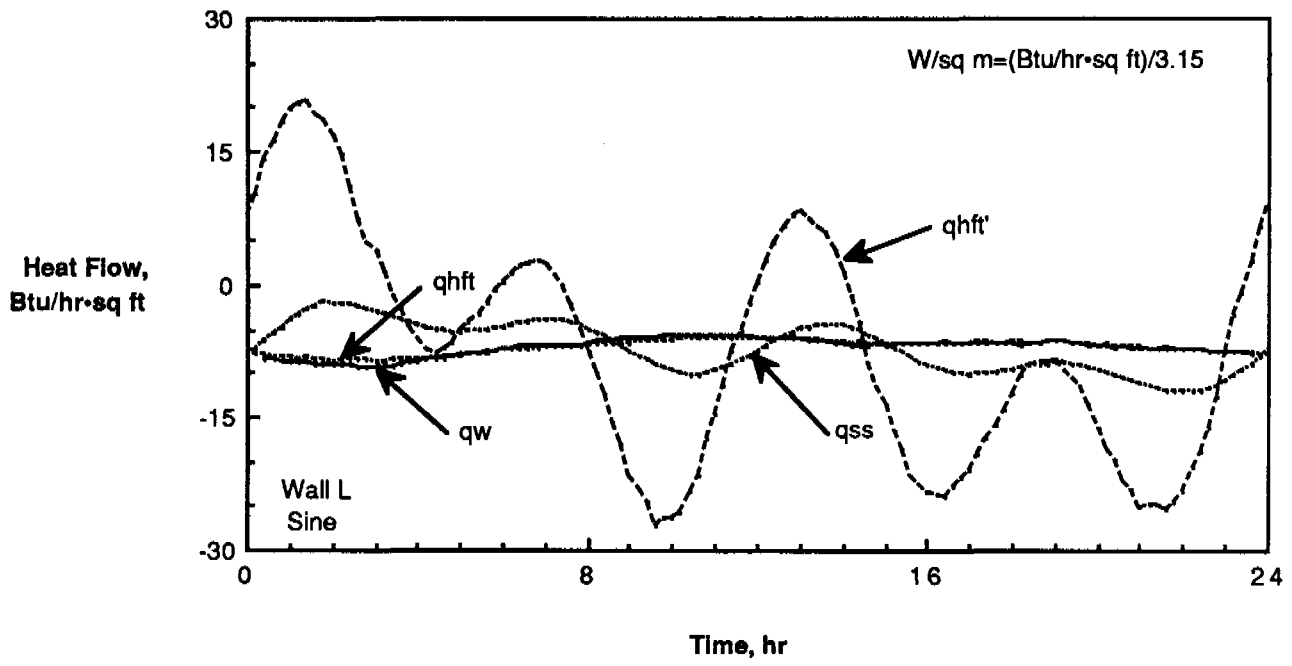


Fig. 34 Heat Flow for Sine Cycle

The calibrated hot box metering and climatic chambers had average relative humidities of 19 and 48%, respectively, during the time of reported Sine Cycle data. The maximum and minimum laboratory air temperatures for the same time period were 73°F (23°C) and 72°F (22°F), respectively.

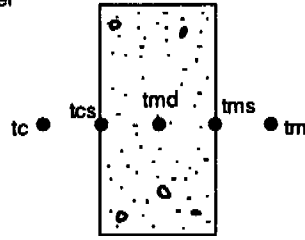
Data analysis was performed using wall surface temperatures and heat flow data from heat flux transducers mounted on each side of the wall. Surface temperatures used for data analysis were averages from a cluster of five thermocouples located along the horizontal centerline of the wall at point 20 in. (0.50 m) from the vertical centerline of the wall. Each cluster had five thermocouples within a 4 in. (100 mm) sq area. Heat flux transducer locations are shown in Fig. 8. It was anticipated that thermocouple cluster and heat flux transducer data would contain less noise than the average surface temperature data and heat flow data measured by the calibrated hot box.

Figure 35 presents comparisons of wall surface temperature measurements from thermocouple clusters and overall averages from 16 thermocouples. Measurements using the two methods were similar. The average temperature from the thermocouple cluster on the climatic chamber side of the wall, denoted $tcs(5)$, was 0.7°F (0.4°C) greater than the overall average, denoted $tcs(16)$. The average temperature from the thermocouple cluster on the metering chamber side of the wall, denoted $tms(5)$ was 0.8°F (0.5°C) less than the overall average, denoted $tms(16)$.

Figure 36 presents comparisons of heat flow through Wall L measured using an energy balance of the hot box metering chamber, denoted q_w , and a heat flux transducer on the wall surface, metering chamber side, denoted q_{hft} . The figure also presents actual and smoothed hot box data, denoted $q_{w,raw}$, and $q_{w,smoothed}$. Average heat flow measured by the hot box was 0.09 Btu/hr·ft² (0.3 W/m²) less than that from the heat flux transducer. Measurements using the two methods were similar.

Climatic
(Outdoor)
Chamber

Metering
(Indoor)
Chamber



Legend

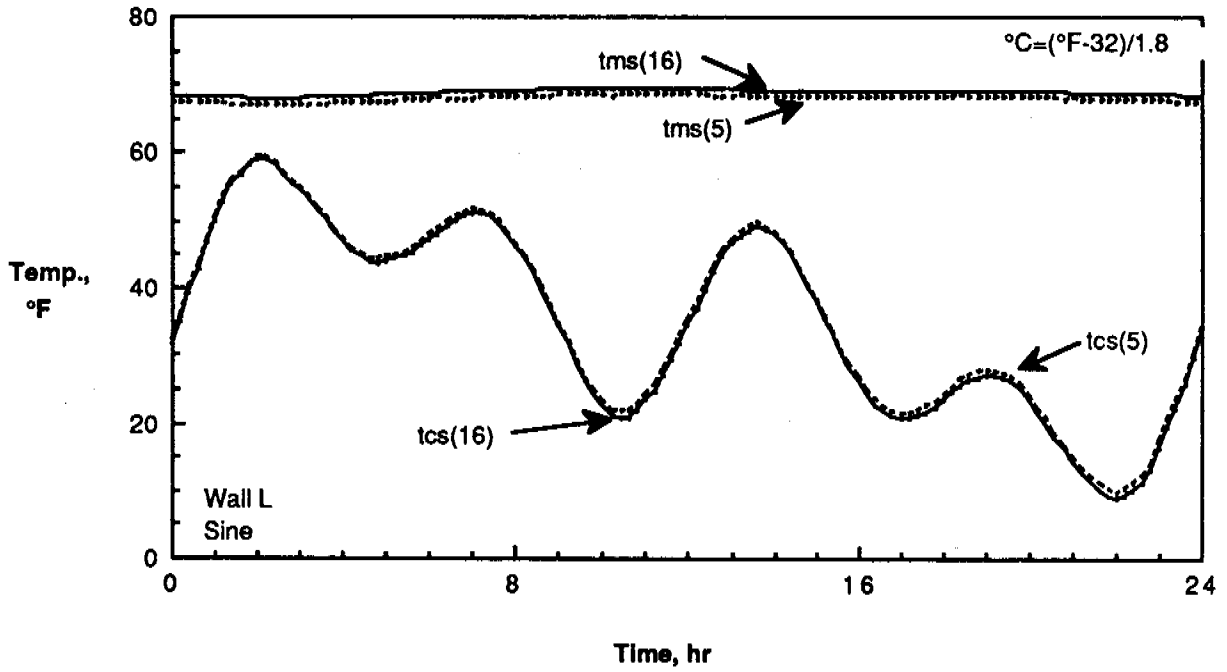


Fig. 35 Comparison of Wall Surface Temperature Measurement Methods

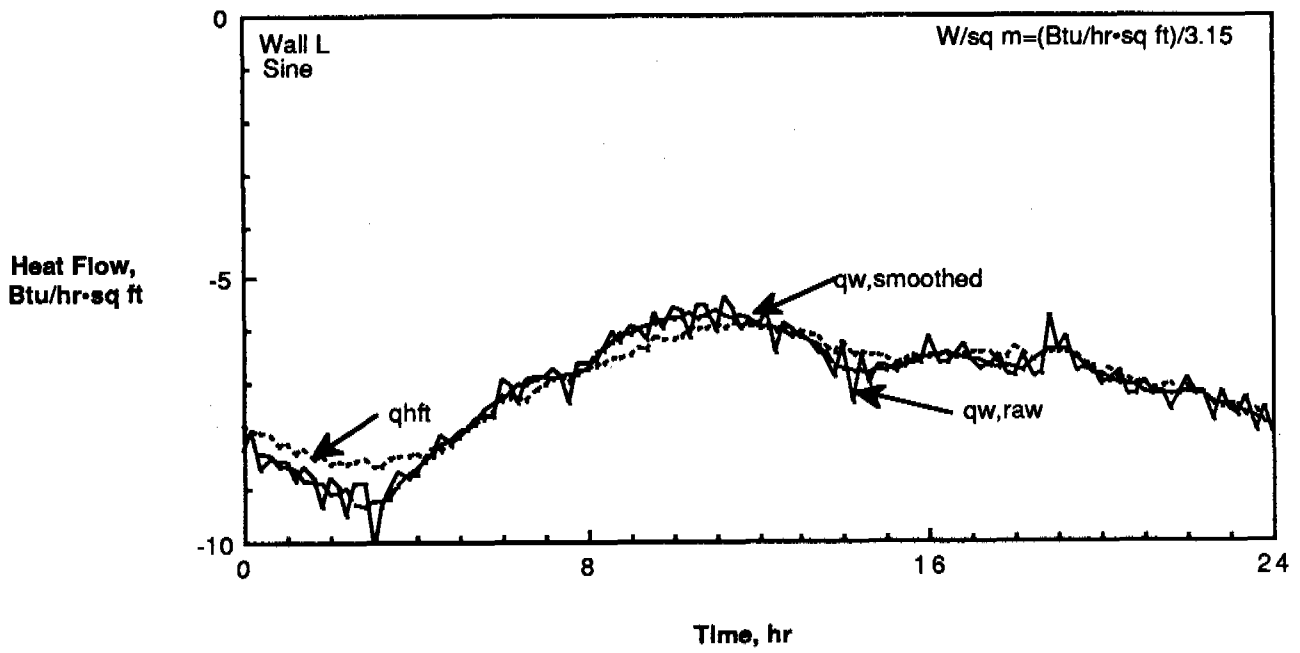


Fig. 36 Comparison of Wall Heat Flow Measurement Methods

Analysis

Wall surface temperature and heat flow digitized data were reduced to Fourier coefficient form using the HP9825 math subroutine "Four". This routine produces fourier series coefficients for equally spaced data points. Results were obtained for wall surface temperatures measured using a five-thermocouple cluster and heat flow measured on the metering chamber side of the wall surface using a heat flux transducer. Data from the Sine Cycle test was accumulated at and analyzed for 12-min. intervals.

Fourier transformations are presented in Table 13. These results were used by Mr. Modera to perform further data analysis. The wall's time constant and thermal diffusivity were calculated. Mr. Modera's results are presented in Reference 22 and included in this report as Appendix C.

TRANSIENT TEMPERATURE TESTS

Time required for a wall to reach a steady-state condition can be determined from transient tests. This time is affected by both thermal resistance and thermal storage capacity of the test wall.

Test Procedures

Results of a transient test are determined from data collected in the period of time between two steady-state tests. After a wall is in a steady-state condition, denoted time 0, the outdoor chamber temperature setting is changed. The transient test continues until the wall reaches equilibrium heat flow for the new outdoor chamber air temperature. The rate of heat flow through a test specimen is determined from hourly averages of data.

Transient test data were collected during calibrated hot box testing of Walls L and S. The initial wall mean temperature for the tests was 72°F

TABLE 13 - FOURIER TRANSFORMATIONS FOR SINE CYCLE DATA

$$F = a + b_1 \sin\left(\frac{2\pi t}{120} + c_1\right) + b_2 \sin\left(\frac{4\pi t}{120} + c_2\right) + b_3 \sin\left(\frac{8\pi t}{120} + c_3\right) + b_4 \sin\left(\frac{10\pi t}{120} + c_4\right)$$

where

F = temperature or heat flow function

t = time, in 12-min. increments, for a 24-hr period

Units	Designation	Description	a	b ₁	b ₂	b ₃	b ₄	c ₁	c ₂	c ₃	c ₄
°F	tcs(cluster)	Wall surface temperature, climatic chamber side, measured by thermocouple cluster	35.58	12.25	11.07	10.214	0.48	-0.0785	-0.0886	-0.0294	0
°F	tms(cluster)	Wall surface temperature, metering chamber side, measured by thermocouple cluster	67.89	0.5686	0.273	0.0671	0	4.260	3.306	4.248	0
W/m ²	qhft	Heat flow through wall measured by heat flux transducer mounted on metering chamber side of wall	-22.12	3.360	1.330	0.3512	0	4.196	3.027	1.542	0

(22°C) for Wall L and 73°F (23°C) for Wall S. The final wall mean temperature was 36°F (2°C) for Wall L and 37°F (3°F) for Wall S.

Test Results

Results from transient tests are presented in Appendix D. Values are shown as a function of time. Table 8 in the "Test Results" portion of the "Dynamic Calibrated Hot Box Tests" section lists brief descriptions of symbols used in test data figures and tables.

Heat flows through Walls L and S for the transient tests are illustrated in Appendix D Figs. D3 and D6, respectively. Heat flows measured by the calibrated hot box, denoted q_w , are delayed compared to heat flows calculated from steady-state resistances, q_{ss} . Calculated heat flows, q_{ss} , were determined using Eq. (2). Values of q_{ss} change dramatically during the first portion of a transient test because of changes in outdoor surface temperatures.

Table 14 lists time required to reach 99.5, 95, 90, and 63% of the final steady-state heat flow achieved during the transient tests for Walls L and S. Table 14(a) lists values measured by the calibrated hot box. Table 14(b) lists values predicted using steady-state equations.

Steady-state analysis predicted that 63% of the final heat flow would be reached after 2 hours. Calibrated hot box test results show that 63% of the final heat flow is reached after 12 hours for Walls L and S. The time required for Walls L and S to reach 63% of the final heat flow were 6 times greater than steady-state predictions. Similarly, the times required for Walls L and S to reach 90% of the final heat flow were 8.6 and 7.0 times, respectively, greater than steady-state predictions.

As shown by the data, massive walls, such as Walls L and S, "damp out" effects of a sudden change in temperature.

TABLE 14 - SUMMARY OF TRANSIENT TEST RESULTS FOR WALLS L AND S

(a) Results Measured by the Calibrated Hot Box

Heat Flow	Wall L		Wall S	
	qw, Btu/hr·ft ² (W/m ²)	Time to Reach qw, hr	qw, Btu/hr·ft ² (W/m ²)	Time to Reach qw, hr
99.5% of Final Heat Flow	-12.14 (-38.3)	32	-14.24 (-44.9)	42
95% of Final Heat Flow	-11.59 (-36.6)	29	-13.59 (-42.9)	27
90% of Final Heat Flow	-10.98 (-34.6)	26	-12.88 (-40.6)	21
63% of Final Heat Flow	-7.69 (-24.3)	12	-9.02 (-28.5)	12

(b) Results Calculated Using Steady-State Equations

Heat Flow	Wall L		Wall S	
	qss, Btu/hr·ft ² (W/m ²)	Time to Reach qss, hr	qss, Btu/hr·ft ² (W/m ²)	Time to Reach qss, hr
99.5% of Final Heat Flow	-11.70 (-36.9)	6	-14.29 (-45.08)	7
95% of Final Heat Flow	-11.17 (-35.2)	4	-13.64 (-43.04)	4
90% of Final Heat Flow	-10.58 (-33.4)	3	-12.92 (-40.76)	3
63% of Final Heat Flow	-7.41 (-23.4)	2	-9.05 (-28.54)	2

SUMMARY AND CONCLUSIONS

This report presents results of an experimental investigation of heat transmission characteristics of two concrete walls. One test specimen, designated Wall L, was an 8-in. (200-mm) thick wall constructed entirely of a newly developed lightweight structural concrete. The second specimen, designated Wall S, was the same as the first except for a 6-in. (150-mm) high normal weight concrete strip running horizontally across the wall at mid-height.

The following conclusions are based on results obtained in this investigation.

Steady-State Temperature Conditions

1. Thermal conductivity of Wall L concrete measured by the calibrated hot box (ASTM Designation: C 976) at a mean temperature of 75°F (24°C) was 1.86 Btu·in./hr·ft²·°F (0.27 W/m·K). This value was interpolated from steady-state test results.
2. Total thermal resistances, R_T , for Walls L and S were 5.2 and 4.7 hr·ft²·°F/Btu (0.92 and 0.83 m²·K/W), respectively. Resistances are for a wall mean temperature of 75°F (24°C) and were interpolated from steady-state calibrated hot box test results. Values include standard surface film resistances.
3. A comparison of steady-state calibrated hot box test results from Walls L and S shows that the 6-in. (150-mm) thick normal weight concrete strip of Wall S decreased wall resistance by 11%. Normal weight concrete is 5.8% of Wall S's total surface area.
4. Thermal conductivities of Wall L, Wall S lightweight, and Wall S normal weight specimens measured using a guarded hot plate (ASTM Designation:

C 177), were 1.43, 1.48, and 12.7 Btu·in./hr·ft²·°F (0.21, 0.21, and 1.82 W/m·K), respectively, at a specimen mean temperature of 75°F (24°C). Values were interpolated from steady-state test results. Guarded hot plate specimens were oven-dried before testing.

5. Based on guarded hot plate test results, average measured thermal conductivity of the lightweight concrete developed for this project is about 1/9th that for normal weight concrete.
6. Thermal conductivity of Wall S lightweight concrete measured using heat flux transducers (ASTM Designation: C 1046) was 1.75 Btu·in./hr·ft²·°F (0.25 W/m·K) at a specimen mean temperature of 75°F (24°C). This value was interpolated from steady-state test results.
7. Predicted thermal resistance of Wall S was 17% less than that for Wall L. This compares to an 11% decrease in measured thermal resistance for Wall S compared to Wall L. Predicted values were based on results from guarded hot plate tests on oven-dry specimens and measured wall thicknesses. Calculation procedures are from the ASHRAE Handbook - 1985 Fundamentals.
8. Thermal conductivities from calibrated hot box and heat flux transducer measurements are greater than those from guarded hot plate tests because guarded hot plate specimens were oven-dried to remove moisture, while wall specimens were air-dried. An increase in specimen moisture content increases thermal conductivity.

Dynamic Temperature Conditions

1. As indicated by thermal lag, thermal storage capacity of the newly developed lightweight concrete delayed heat flow through a specimen. Average thermal lag values ranged from 5.5 to 6.5 hours for three diurnal temperature cycles applied to Wall L.

2. As indicated by the damping effect, thermal storage capacity of Wall L reduced peak heat flows through the specimen for dynamic temperature conditions when compared to steady-state predictions. Reduction in amplitude values ranged from 47 to 53% for the three diurnal temperature cycles applied to Wall L.
3. For the three diurnal temperature cycles applied to Wall L, total heat flow for a 24-hr period were less than would be predicted by steady-state equations. Total measured heat flows for the 24-hour cycles ranged from 44 to 54% of those predicted by steady-state equations. These reductions in total heat flow are attributed to wall thermal storage capacity and reversals in heat flow.
4. A dynamic cycle composed of three sinusoidal temperature functions was applied to Wall L to investigate an alternative analysis technique. The analysis technique uses hot box test data to determine a time constant and thermal diffusivity of the homogeneous lightweight structural concrete wall.
5. Transient test results indicated that thermal storage capacity of Walls L and S delay heat flow through the specimens. The amount of time required for Walls L and S to reach 63% of a final heat flow were approximately six times greater than predicted by steady-state equations using measured surface temperatures.
6. The newly developed concrete exhibits beneficial thermal properties and adequate structural capacity for load-bearing walls.

Limitations

Test results presented in this report are limited to the test specimens and temperature cycles used in this investigation. Results may be different for alternative materials and temperature cycles. This report provides data

on thermal response of two concrete walls subjected to steady-state and dynamic temperature cycles. A complete analysis of building energy requirements must include consideration of the entire building envelope, building orientation, building operation, and yearly weather conditions. Data developed in this experimental program provide a quantitative basis for modeling the building envelope, which is part of the overall energy analysis process.

ACKNOWLEDGMENTS

The work was performed in the Engineering and Planning Division of the Construction Technology Laboratories, Inc. (CTL), under the direction of Dr. W. G. Corley, Vice-President. Dr. Bruce J. Morgan, Principal Engineer, Structural Engineering Department, assisted with data reduction of the Sine Cycle. Mr. Mark P. Modera, Lawrence Berkeley Laboratory, helped develop the Sine Cycle and performed an analysis of test results.

REFERENCES

1. Larson, S. C. and Van Geem, M. G., "Structural Thermal Break Systems for Buildings - Feasibility Study," Oak Ridge National Laboratory Report No. ORNL/Sub/84-21006/1, Construction Technology Laboratories, Inc., Skokie, 1987, 88 pages.
2. Litvin, A. and Van Geem, M. G., "Structural Thermal Break Systems for Buildings - Development and Properties of Lightweight Concrete Systems," Oak Ridge National Laboratory Report No. ORNL/Sub/84-21006/2, Construction Technology Laboratories, Inc., Skokie, 1988, 91 pages.
3. 1987 Annual Book of ASTM Standards, American Society for Testing and Materials, Philadelphia, 1987.
4. Fiorato, A. E. and Cruz, C. R., "Thermal Performance of Masonry Walls," Research and Development Bulletin RD071, Portland Cement Association, Skokie, 1980, 17 pages.
5. Fiorato, A. E., "Heat Transfer Characteristics of Walls Under Dynamic Temperature Conditions," Research and Development Bulletin RD075, Portland Cement Association, Skokie, 1981, 20 pages.
6. Fiorato, A. E. and Bravinsky, E., "Heat Transfer Characteristics of Walls Under Arizona Temperature Conditions," Construction Technology Laboratories, Portland Cement Association, Skokie, 1981, 61 pages.
7. Van Geem, M. G., Fiorato, A. E., and Julien, J. T., "Heat Transfer Characteristics of a Normal Weight Concrete Wall," Oak Ridge National Laboratory Report No. ORNL/Sub/79-42539/1, Construction Technology Laboratories, Portland Cement Association, Skokie, 1983, 89 pages.
8. Van Geem, M. G. and Fiorato, A. E., "Heat Transfer Characteristics of a Structural Lightweight Concrete Wall," Oak Ridge National Laboratory Report No. ORNL/Sub/79-42539/2, Construction Technology Laboratories, Portland Cement Association, Skokie, 1983, 88 pages.
9. Van Geem, M. G. and Fiorato, A. E., "Heat Transfer Characteristics of a Low Density Concrete Wall," Oak Ridge National Laboratory Report No. ORNL/Sub/79-42539/3, Construction Technology Laboratories, Portland Cement Association, Skokie 1983, 89 pages.
10. Van Geem, M. G. and Larson, S. C., "Heat Transfer Characteristics of a Masonry Cavity Wall With and Without Expanded Perlite Insulation," Construction Technology Laboratories, Portland Cement Association, Skokie, 1985, 135 pages.
11. Van Geem, M. G. and Larson, S. C., "Heat Transfer Characteristics of Walls with Similar Thermal Resistance Values," Oak Ridge National Laboratory Report No. ORNL/Sub/79-42539/6, Construction Technology Laboratories, Portland Cement Association, Skokie, 1986, 94 pages.

12. Van Geem, M. G., and Shirley, S. T., "Heat Transfer Characteristics of Insulated Concrete Sandwich Panel Walls," Oak Ridge National Laboratory Report No. ORNL/Sub/79-42539/8, Construction Technology Laboratories, Inc., Skokie, 1987, 217 pages.
13. Fiorato, A. E., "Laboratory Tests of Thermal Performance of Exterior Walls," Proceedings of the ASHRAE/DOE-ORNL Conference on Thermal Performance of the Exterior Envelopes of Building, Orlando, Florida, December 1979, ASHRAE SP28, Atlanta, 1981, pp. 221-236.
14. ASHRAE Handbook-1985 Fundamentals, American Society of Heating, Refrigerating, and Air Conditioning Engineers, Inc., Atlanta, 1985, Chapter 23.
15. Larson, S. C. and Van Geem, M. G., "Surface Temperature Measurement Techniques for a Calibrated Hot Box Test Specimen," Report No. ORNL/Sub/79-42539/7 prepared for Oak Ridge National Laboratory, Construction Technology Laboratories, Portland Cement Association, Skokie, IL, 1986, 78 pages.
16. Van Geem, M. G. and Fiorato, A. E., "Thermal Properties of Masonry Materials for Passive Solar Design - A State-of-the-Art Review," Construction Technology Laboratories, Portland Cement Association, Skokie, 1983, 93 pages.
17. Van Geem, M. G., "Calibrated Hot Box Test Results Data Manual - Volume I," Oak Ridge National Laboratory Report No. ORNL/Sub/79-42539/4, Construction Technology Laboratories, Portland Cement Association, Skokie, Illinois, 1984, 336 pages.
18. Van Geem, M. G. and Larson, S. C., "Calibrated Hot Box Test Results Data Manual - Volume II," Oak Ridge National Laboratory Report No. ORNL/Sub/79-42539/5, Construction Technology Laboratories, Portland Cement Association, Skokie, Illinois, 1985, 164 pages.
19. Peavy, B. A., Powell, F. J., and Burch, D. M., "Dynamic Thermal Performance of an Experimental Masonry Building," Building Science Series 45, U.S. Department of Commerce, National Bureau of Standards, Washington, D.C., 1973, 98 pages.
20. Childs, K. W., Courville, G. E., and Bales, E. L., "Thermal Mass Assessment," Oak Ridge National Laboratory for the U.S. Department of Energy, Oak Ridge, Tennessee, 1983, 86 pages.
21. Handbook for Concrete and Cement, U.S. Army Waterways Experimental Station, Vicksburg.
22. Modera, Mark P. "Characterizing the Dynamic Thermal Performance of a Wall Using Periodic Excitation," Report No. LBL-24113, Lawrence Berkeley Laboratory, Berkeley, CA, 1987, 14 pages.
23. Bales, E., "ASTM/DOE Hot Box Round Robin," Buildings Engineering and Architectural Research Center, New Jersey Institute of Technology, Newark, 1988, 80 pages.

APPENDIX A - CALIBRATED HOT BOX INSTRUMENTATION AND CALIBRATION

Calibrated hot box tests were performed according to ASTM Designation: C 976, "Thermal Performance of Building Assemblies by Means of a Calibrated Hot Box."⁽³⁾

Instrumentation

Instrumentation was designed to monitor temperatures inside and outside the metering chamber, air and surface temperatures on both sides of the test wall, internal wall temperatures, and heating energy input to the metering chamber. Additional measurements monitor metering chamber cooling system performance. Basically, the instrumentation provides a means of monitoring the energy required to maintain constant temperature in the metering chamber while temperatures in the climatic chamber are held constant or are varied. This energy, when corrected for thermal losses, provides a measure of heat flow through the test wall.

Thermocouples used to measure air and test specimen temperatures are described in the "Instrumentation" portion of the "Test Specimens" section of this report.

Laboratory and interior surface temperatures of the metering chamber sides were measured. These temperatures provided data for evaluating heat transfer between the chamber and the laboratory. Temperature data were supplemented with heat flux transducer measurements on chamber surfaces.

A digital humidity and temperature measurement system was used to measure relative humidity and temperature in air streams on each side of the test wall. Probes were located in the air streams approximately at the specimen mid-point.

A watt-hour transducer was used to measure cumulative electrical energy input to the metering chamber.

Measurements were monitored with a programmable digital data acquisition system capable of sampling and recording up to 124 independent channels of data at preselected time intervals. The data acquisition system is interfaced with a microcomputer that is programmed to reduce and store data. Channels were scanned every two minutes. Average temperature and supplementary data were obtained from average readings for one hour. The cumulative watt-hour transducer output was scanned every hour.

Air flow rates in each chamber were measured with air flow meters located approximately at the wall geometric center. Each flow rate meter was mounted perpendicular to the air flow. Air flow is vertical on both sides of the specimen. Air velocity is uniform and averages 20 ft/min. (0.10 m/s). Data for air flow meters were monitored periodically and were not part of the automated data acquisition apparatus. Reference 13 gives more information on instrumentation of CTL's calibrated hot box.

Calibration Procedure

Heat flow through a test wall is determined from measurements of the amount of energy input to the metering chamber to maintain a constant temperature. The measured energy input must be adjusted for heat losses.

Figure A1 shows sources of heat losses and gains by the metering chamber where:

- Q_w = heat transfer through test wall
- Q_c = heat removed by metering chamber cooling
- Q_h = heat supplied by metering chamber electrical resistance heaters
- Q_{fan} = heat supplied by metering chamber circulation fan
- Q_l = heat loss/gain from laboratory
- Q_f = heat loss/gain from flanking path around specimen

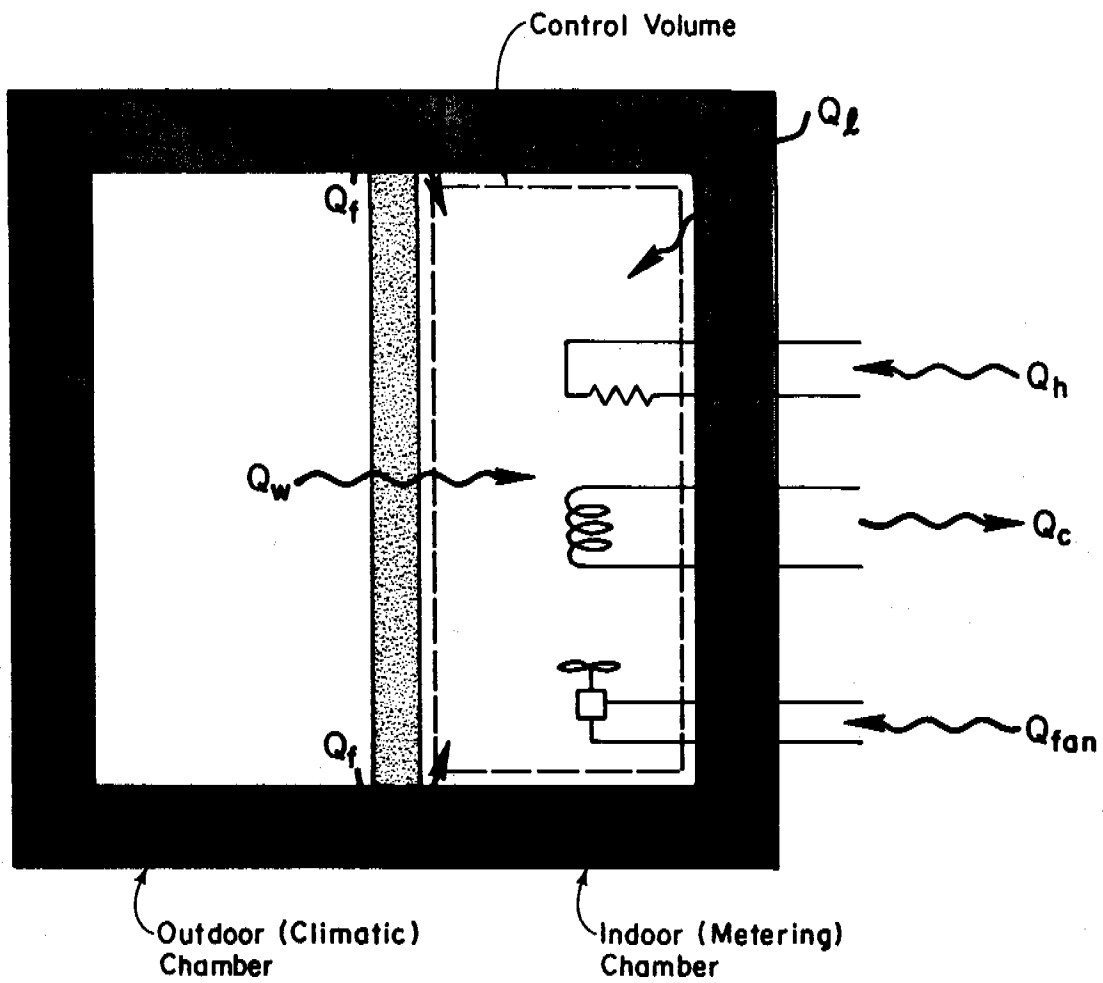


Fig. A1 Indoor (Metering) Chamber Energy Balance

The directions of arrows in Fig. A1 indicate positive heat flow.

Since net energy into the control volume of the metering chamber equals zero, heat transfer through the test wall can be expressed by the following energy balance equation:

$$Q_w = Q_c - Q_h - Q_{fan} - Q_l - Q_f \quad (A1)$$

The need for cooling in the metering chamber results from requirements for dynamic tests. In cases where outdoor temperatures exceed indoor temperatures, cooling capacity is required to maintain indoor temperature control.

Metering chamber cooling equipment operates continuously and is designed to remove heat at a constant rate. Control of metering chamber temperature is obtained by varying the amount of input heat required to balance the amount of heat removed by the refrigeration system, the amount of heat that flows through the test specimen, and the amount of heat lost to laboratory space.

Steady-state calibrated hot box tests on two "standard" calibration specimens were used to refine calculations of heat removed by metering chamber cooling, Q_c , and flanking losses, Q_f . The first calibration specimen, S1, has a relatively low thermal resistance of $6.8 \text{ hr}\cdot\text{ft}^2\cdot^\circ\text{F}/\text{Btu}$ ($1.2 \text{ m}^2\cdot\text{K}/\text{W}$). It consists of 1-3/8-in. (35-mm) thick fiberglass and was specially fabricated to insure uniformity.

The second calibration wall, S2, has a relatively high thermal resistance of $16.8 \text{ hr}\cdot\text{ft}^2\cdot^\circ\text{F}/\text{Btu}$ ($3.0 \text{ m}^2\cdot\text{K}/\text{W}$). Material for specimen S2 was selected as part of the ASTM Committee C16 Hot Box Round Robin program.⁽²³⁾ It consists of expanded polystyrene board that is specially produced and cut to insure uniformity. Board faces are coated to provide surfaces suitable for attachment of instrumentation.

Heat removed by metering chamber cooling, Q_c , was calculated from refrigerant enthalpy and mass flow rate, assuming an ideal basic vapor compression refrigeration cycle. Results from steady-state calibrated hot box tests on the two "standard" calibration specimens were used to adjust for inefficiencies in the actual refrigeration cycle.

Losses from the metering chamber to the laboratory, Q_l , were calculated from thermal properties of component materials making up walls and ceilings of the metering chamber and temperature conditions on the inner and outer surfaces of the metering chamber. Heat flux transducers mounted on the inside surface of the metering chamber were used to check calculations. Metering chamber air and laboratory air temperatures were generally maintained at the same nominal value, 72°F (22°C), to minimize laboratory losses. Thus, the value of Q_l is small relative to other terms of the energy balance equation.

A watt-hour transducer was used to measure heat supplied to the metering chamber by heaters and a fan, $Q_h + Q_{fan}$.

Heat loss or gain from flanking around the test specimen, Q_f , was determined from steady-state tests of the "standard" calibration walls. Since thermal conductance of each standard calibration wall is known, Q_w for a given steady-state test can be calculated using the following equation:

$$Q_w = A \cdot C \cdot (t_2 - t_1) \quad (A2)$$

where

- Q_w = heat transfer through test wall, Btu/hr (W·hr/hr)
- A = area of wall surface normal to heat flow, ft² (m²)
- C = average thermal conductance, Btu/hr·ft²·°F (W/m²·K)
- t_2 = average temperature of wall surface, climatic chamber side, °F (°C)
- t_1 = average temperature of wall surface, metering chamber side, °F (°C)

Thus, Q_f was determined from Eq. (A1) using calculated values of Q_w , Q_c , and Q_g , and measured values of Q_h and Q_{fan} .

For both standard calibration walls, values of Q_f were observed to follow the empirical relationship:

$$\begin{aligned} Q_f &= 0.802 (t_{cs} - t_{ms}) && \text{U.S. units} && (A3) \\ Q_f &= 0.131 (t_{cs} - t_{ms}) && \text{(SI units)} \end{aligned}$$

where

- Q_f = heat loss or gain from flanking around test specimen, Btu/hr (W·hr/hr)
- t_{cs} = average temperature of wall surface, climatic chamber side, °F (°C)
- t_{ms} = average temperature of wall surface, metering chamber side, °F (°C)

Since Q_f is the residual from Eq. (A1), it may include other undetermined losses from the metering chamber.

A round robin including six calibrated (ASTM Designation: C 976) and 15 guarded (ASTM Designation: C 236) hot boxes was conducted under the jurisdiction of ASTM Subcommittee C16.30. Reference 23, which contains results of the round robin, provides additional information on the precision of the calibrated hot box test method.

APPENDIX B - (24-HR PERIODIC) DYNAMIC TEMPERATURE TEST RESULTS FOR WALL L

Measured temperatures, temperature differentials, and heat flow for dynamic temperature cycles applied to Wall L are presented in Figs. B1 through B9 and listed in Tables B1 through B3. Data for the NBS Test Cycle are presented first, followed by results for the NBS+10 Test Cycle and the NBS-10 Test Cycle.

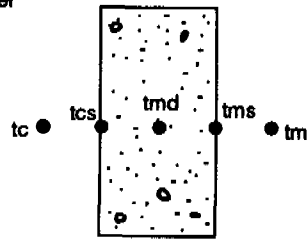
Tables B1 through B3 denoted (a) and (b), respectively, list hourly test data in IP and SI units.

Symbols used in these figures and tables are described in detail in the "Test Results" portion of the "Dynamic (24-Hr Periodic) Calibrated Hot Box Tests" section of this report.

Measured temperatures are listed in Tables B1, B2, and B3 and shown as a function of time in Figs. B1, B4, and B7. Air-to-air (t_c-t_m), surface-to-surface ($t_{cs}-t_{ms}$), and surface-to-air (t_c-t_{cs} , $t_{ms}-t_m$) temperature differentials are illustrated in Figs. B2, B5, and B8. Measured and calculated heat flows are listed in Tables B1, B2, and B3, and shown as a function of time in Figs. B3, B6, and B9.

Climatic
(Outdoor)
Chamber

Metering
(Indoor)
Chamber



Legend

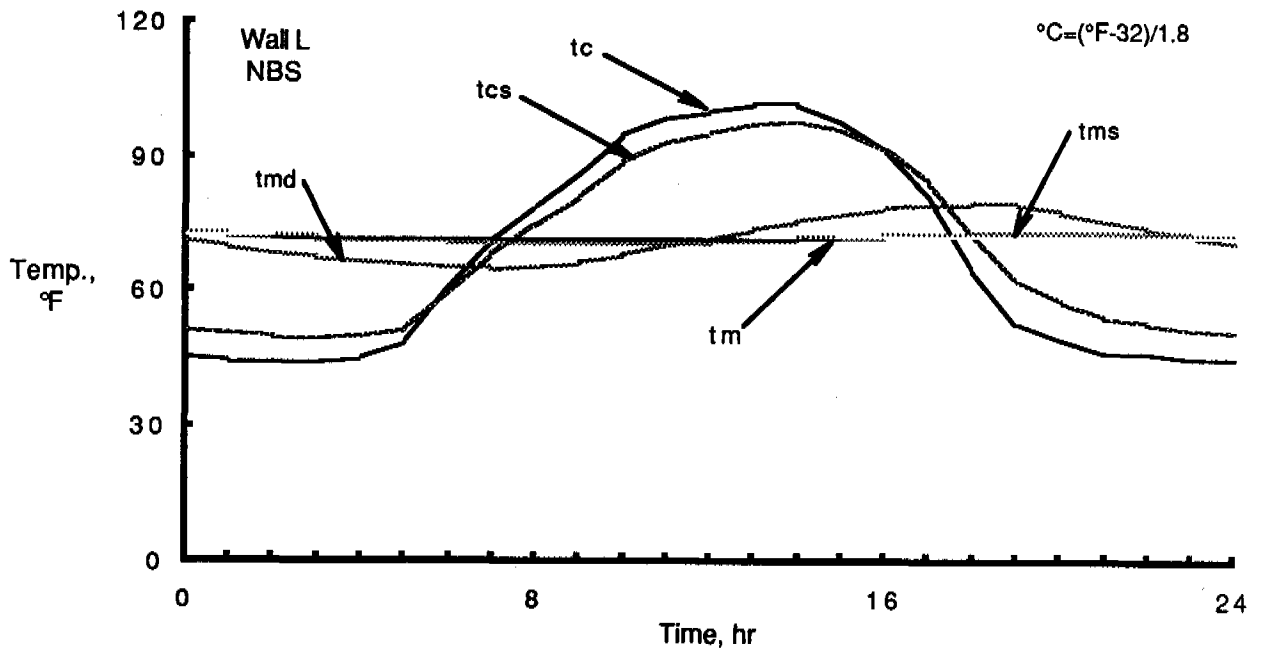
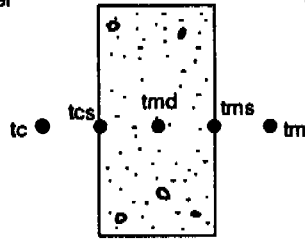


Fig. B1 Measured Temperatures for NBS Test Cycle

Climatic
(Outdoor)
Chamber

Metering
(Indoor)
Chamber



Legend

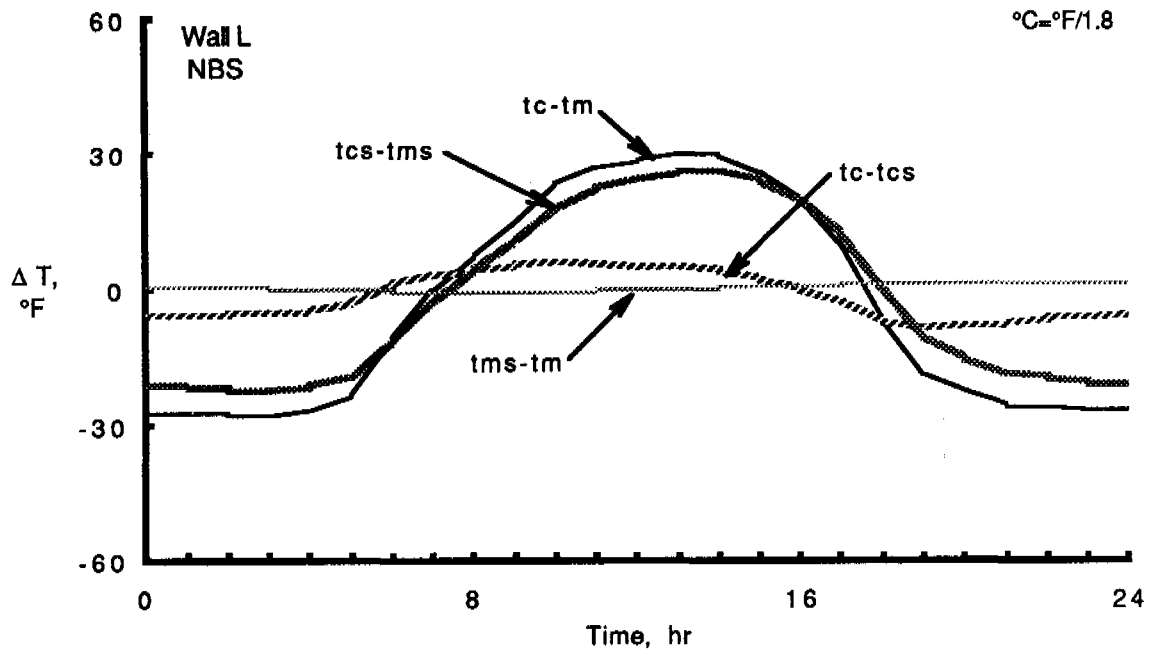


Fig. B2 Temperature Differentials for NBS Test Cycle

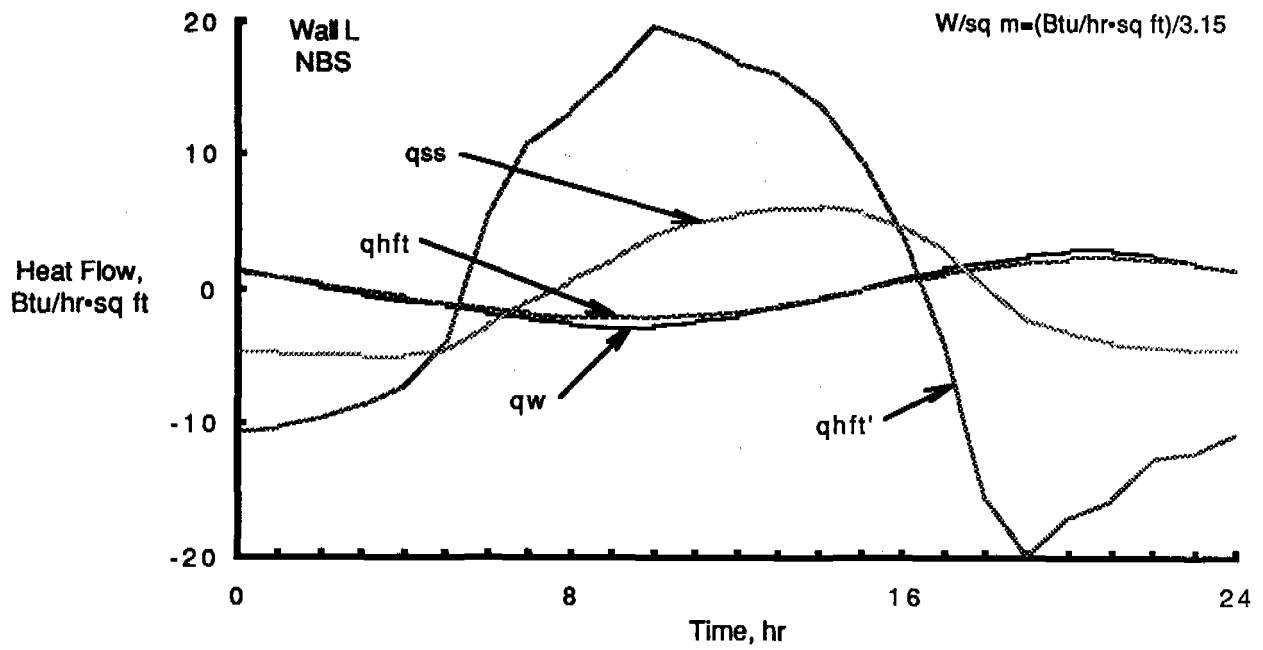


Fig. B3 Heat Flow for NBS Test Cycle

TABLE B1(a) - DYNAMIC (PERIODIC) TEST RESULTS FOR NBS TEMPERATURE CYCLE

Time, hr	Measured Temperatures, °F					Measured Heat Flow, Btu/hr-sq ft			Calculated Heat Flow Btu/hr-sq ft
	tc Climatic Chamber Air	tcs Climatic Surface	tmd Internal Therm.	tms Metering Surface	tm Metering Chamber Air	qw Calib. Hot Box	qhft HFT @ Metering Surface	qhft' HFT @ Climatic Surface	qss Steady- State
1	44.3	50.2	69.7	72.2	72.1	0.79	0.83	-10.28	-4.80
2	43.9	49.5	68.4	72.0	72.0	0.12	0.34	-9.64	-4.94
3	44.1	49.2	67.4	71.7	71.9	-0.48	-0.17	-8.62	-4.98
4	45.2	49.8	66.4	71.5	71.9	-0.99	-0.64	-7.16	-4.84
5	48.5	51.5	65.6	71.3	71.8	-1.37	-1.07	-3.94	-4.46
6	60.6	59.8	65.0	71.1	71.8	-1.95	-1.47	5.42	-2.72
7	71.2	68.1	65.0	70.9	71.8	-2.24	-1.82	11.06	-0.83
8	78.7	74.7	65.6	70.8	71.7	-2.60	-2.05	13.39	0.69
9	86.2	81.1	66.7	70.8	71.7	-2.82	-2.19	16.35	2.17
10	94.7	88.7	68.2	70.9	71.8	-2.62	-2.14	19.76	3.95
11	98.6	93.1	70.0	71.1	71.8	-2.23	-1.92	18.66	5.01
12	100.2	95.4	72.0	71.3	71.9	-1.99	-1.62	16.91	5.54
13	101.7	97.2	74.0	71.7	72.0	-1.29	-1.12	16.01	5.97
14	101.4	98.0	75.7	72.0	72.1	-0.63	-0.57	13.70	6.14
15	97.8	96.1	77.3	72.3	72.2	0.00	0.03	9.43	5.65
16	91.4	91.8	78.7	72.6	72.3	0.86	0.63	3.85	4.59
17	81.1	84.5	79.6	72.9	72.4	1.56	1.20	-4.11	2.81
18	65.0	72.7	79.8	73.2	72.5	2.15	1.71	-15.74	0.06
19	53.0	62.1	79.2	73.4	72.5	2.72	2.13	-19.92	-2.33
20	49.4	57.6	77.8	73.4	72.5	2.97	2.38	-16.87	-3.32
21	46.4	54.2	76.0	73.3	72.5	2.79	2.39	-15.55	-4.04
22	46.3	53.1	74.3	73.1	72.4	2.45	2.18	-12.60	-4.26
23	45.1	51.8	72.6	72.9	72.3	1.89	1.81	-12.16	-4.52
24	44.9	50.9	71.1	72.5	72.2	1.40	1.34	-10.68	-4.68
Mean	68.3	70.0	71.9	72.0	72.1	-0.06	0.01	-0.11	-0.34

Calibrated Hot Box Relative Humidity:
 Metering Chamber - 41%
 Climatic Chamber - 15%

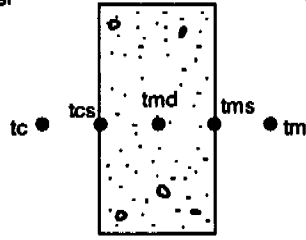
Laboratory Air Temperature:
 Max. - 73 °F
 Min. - 70 °F

TABLE B1(b) - DYNAMIC (PERIODIC) TEST RESULTS FOR NBS TEST CYCLE, SI UNITS

Time, hr	Measured Temperatures °C					Measured Heat Flow, W/sq m			Calculated Heat Flow W/sq m
	tc Climatic Chamber Air	tcs Climatic Surface	tmd Internal Therm.	tms Metering Surface	tm Metering Chamber Air	qw Calib. Hot Box	qhft HFT @ Metering Surface	qhft' HFT @ Climatic Surface	
1	6.9	10.1	20.9	22.4	22.3	2.48	2.61	-32.43	-15.16
2	6.6	9.7	20.2	22.2	22.2	0.37	1.07	-30.42	-15.57
3	6.7	9.6	19.6	22.1	22.2	-1.50	-0.53	-27.19	-15.71
4	7.4	9.9	19.1	21.9	22.2	-3.12	-2.03	-22.58	-15.27
5	9.2	10.8	18.7	21.8	22.1	-4.32	-3.36	-12.43	-14.09
6	15.9	15.3	18.4	21.7	22.1	-6.16	-4.64	17.10	-8.59
7	21.8	20.1	18.3	21.6	22.1	-7.07	-5.73	34.88	-2.62
8	26.0	23.7	18.6	21.6	22.1	-8.20	-6.47	42.25	2.18
9	30.1	27.3	19.3	21.6	22.1	-8.88	-6.91	51.59	6.85
10	34.9	31.5	20.1	21.6	22.1	-8.27	-6.76	62.34	12.48
11	37.0	33.9	21.1	21.7	22.1	-7.03	-6.07	58.88	15.82
12	37.9	35.2	22.2	21.9	22.2	-6.27	-5.10	53.35	17.47
13	36.7	36.2	23.3	22.0	22.2	-4.08	-3.54	50.50	18.84
14	38.5	36.7	24.3	22.2	22.3	-1.98	-1.79	43.22	19.37
15	36.6	35.6	25.2	22.4	22.3	0.00	0.10	29.77	17.82
16	33.0	33.2	25.9	22.6	22.4	2.70	1.99	12.14	14.48
17	27.3	29.1	26.4	22.7	22.4	4.93	3.78	-12.97	8.86
18	18.3	22.6	26.6	22.9	22.5	6.79	5.40	-49.65	0.19
19	11.7	16.7	26.2	23.0	22.5	8.57	6.73	-62.85	-7.35
20	9.6	14.2	25.4	23.0	22.5	9.36	7.52	-53.23	-10.47
21	8.0	12.3	24.5	23.0	22.5	8.79	7.55	-49.05	-12.74
22	8.0	11.7	23.5	22.9	22.5	7.73	6.89	-39.76	-13.44
23	7.3	11.0	22.6	22.7	22.4	5.97	5.71	-38.36	-14.26
24	7.2	10.5	21.7	22.5	22.4	4.42	4.22	-33.69	-14.78
Mean	20.2	21.1	22.2	22.2	22.3	-0.20	0.03	-0.36	-1.07

Climatic
(Outdoor)
Chamber

Metering
(Indoor)
Chamber



Legend

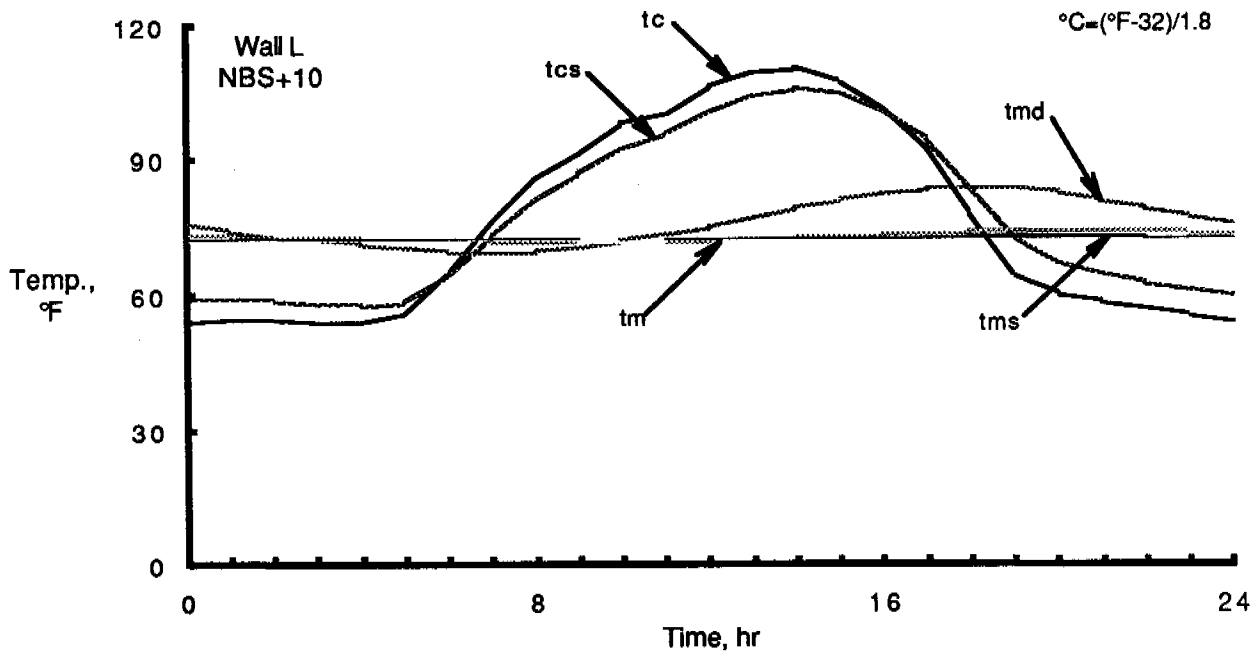
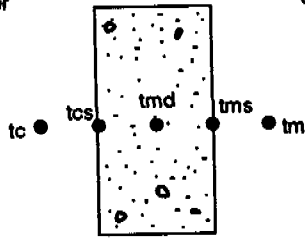


Fig. B4 Measured Temperatures for NBS+10 Test Cycle

Climatic
(Outdoor)
Chamber

Metering
(Indoor)
Chamber



Legend

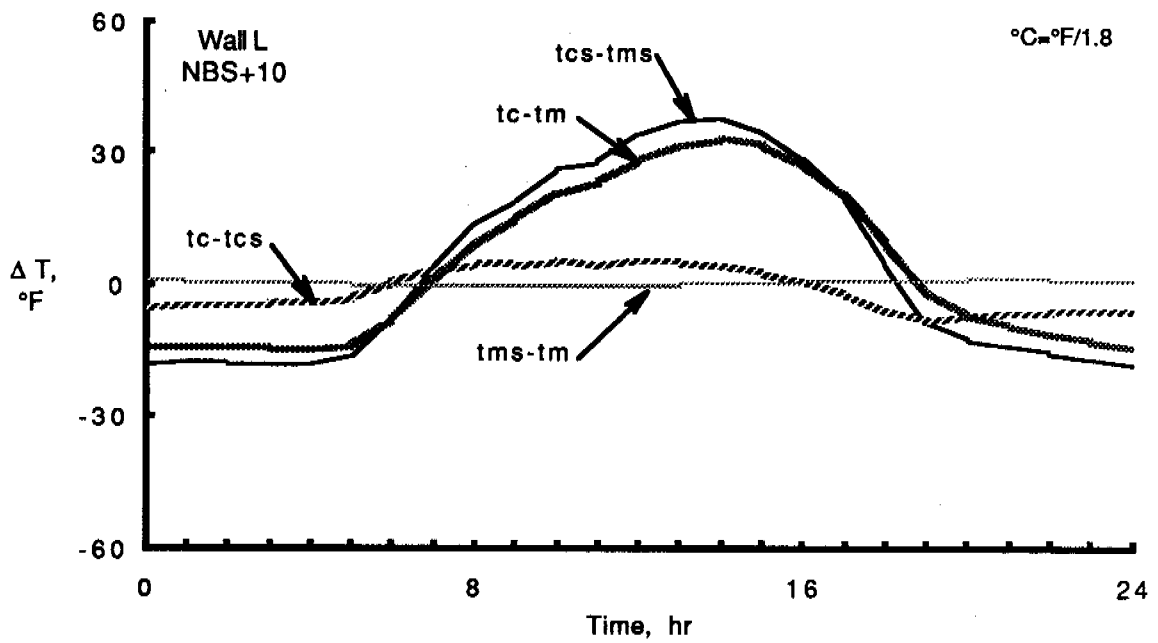


Fig. B5 Temperature Differentials for NBS+10 Test Cycle

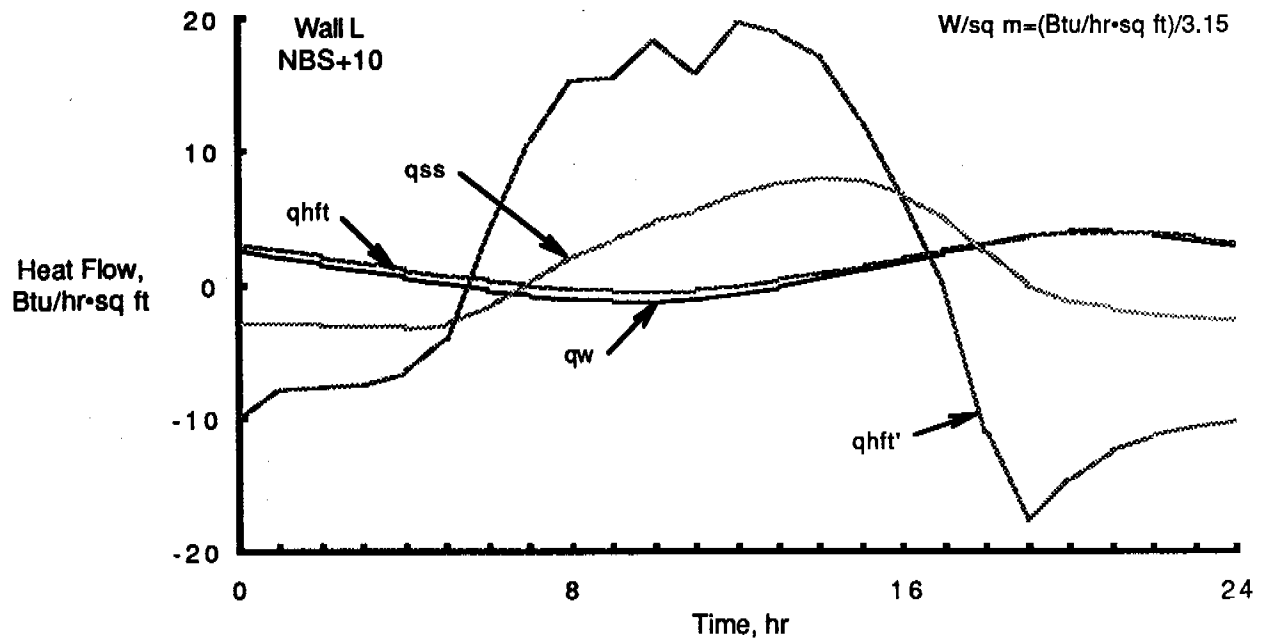


Fig. B6 Heat Flow for NBS+10 Test Cycle

TABLE B2(a) - DYNAMIC (PERIODIC) TEST RESULTS FOR NBS+10 TEMPERATURE CYCLE

Time, hr	Measured Temperatures, °F					Measured Heat Flow, Btu/hr-sq ft			Calculated Heat Flow Btu/hr-sq ft
	tc Climatic Chamber Air	tcs Climatic Surface	tmd Internal Therm.	tms Metering Surface	tm Metering Chamber Air	qw Calib. Hot Box	qhft HFT @ Metering Surface	qhft' HFT @ Climatic Surface	
1	54.7	59.1	74.3	73.1	72.3	2.03	2.57	-7.81	-2.95
2	54.4	58.8	73.1	72.9	72.3	1.48	2.06	-7.61	-2.99
3	53.8	58.1	72.0	72.6	72.2	1.00	1.57	-7.38	-3.15
4	53.8	57.8	71.1	72.4	72.1	0.52	1.09	-6.50	-3.19
5	55.8	58.7	70.2	72.2	72.1	0.01	0.68	-4.13	-2.97
6	65.0	64.4	69.5	72.0	72.0	-0.45	0.32	3.88	-1.70
7	76.3	73.2	69.2	71.8	72.0	-0.83	-0.03	10.73	0.27
8	85.9	81.2	69.6	71.7	72.0	-1.15	-0.29	15.31	2.12
9	91.2	86.8	70.6	71.7	71.9	-1.31	-0.47	15.52	3.46
10	98.1	92.4	72.0	71.7	71.9	-1.30	-0.49	18.33	4.81
11	99.9	95.5	73.6	71.9	72.0	-1.10	-0.35	15.90	5.55
12	106.2	100.5	75.2	72.1	72.0	-0.88	-0.05	19.61	6.77
13	109.3	104.2	77.2	72.4	72.1	-0.22	0.40	18.69	7.67
14	110.3	105.9	79.0	72.7	72.2	0.44	0.86	17.03	8.08
15	107.1	104.5	80.8	73.0	72.3	1.05	1.41	12.24	7.71
16	101.0	100.4	82.2	73.3	72.4	1.74	2.00	6.44	6.66
17	92.1	94.0	83.2	73.6	72.5	2.48	2.58	-0.25	5.07
18	77.5	83.2	83.7	73.9	72.6	3.07	3.12	-11.11	2.47
19	64.2	72.3	83.3	74.0	72.6	3.67	3.57	-17.79	-0.08
20	60.2	67.0	82.2	74.1	72.6	3.94	3.84	-14.51	-1.28
21	58.4	64.6	80.5	74.1	72.6	3.91	3.92	-12.38	-1.81
22	56.8	62.5	78.7	73.9	72.5	3.72	3.79	-11.22	-2.24
23	55.4	60.9	77.0	73.7	72.5	3.16	3.47	-10.54	-2.59
24	54.0	59.3	75.5	73.4	72.4	2.68	3.05	-10.04	-2.92
Mean	76.7	77.7	76.0	72.8	72.2	1.16	1.61	1.35	1.37

Calibrated Hot Box Relative Humidity:
 Metering Chamber - 46%
 Climatic Chamber - 16%

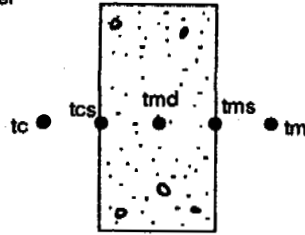
Laboratory Air Temperature:
 Max. - 73 °F
 Min. - 72 °F

TABLE B2(b) - DYNAMIC (PERIODIC) TEST RESULTS FOR NBS-10 TEST CYCLE, SI UNITS

Time, hr	Measured Temperatures °C					Measured Heat Flow, W/sq m			Calculated Heat Flow W/sq m
	tc Climatic Chamber Air	tcs Climatic Surface	tmd Internal Therm.	tms Metering Surface	tm Metering Chamber Air	qw Calib. Hot Box	qhft HFT @ Metering Surface	qhft' HFT @ Climatic Surface	qss Steady- State
1	12.6	15.0	23.5	22.8	22.4	6.41	8.10	-24.65	-9.30
2	12.5	14.9	22.8	22.7	22.4	4.68	6.51	-24.02	-9.45
3	12.1	14.5	22.2	22.6	22.3	3.15	4.94	-23.28	-9.92
4	12.1	14.3	21.7	22.4	22.3	1.65	3.45	-20.52	-10.08
5	13.2	14.8	21.2	22.3	22.3	0.04	2.15	-13.03	-9.38
6	18.3	18.0	20.8	22.2	22.2	-1.43	1.00	12.26	-5.36
7	24.6	22.9	20.7	22.1	22.2	-2.63	-0.09	33.84	0.86
8	30.0	27.3	20.9	22.1	22.2	-3.62	-0.92	48.30	6.69
9	32.9	30.4	21.4	22.0	22.2	-4.12	-1.49	48.99	10.91
10	36.7	33.6	22.2	22.1	22.2	-4.11	-1.55	57.85	15.19
11	37.7	35.3	23.1	22.2	22.2	-3.48	-1.10	50.16	17.51
12	41.2	38.0	24.0	22.3	22.2	-2.15	-0.16	61.87	21.35
13	43.0	40.1	25.1	22.4	22.3	-0.69	1.26	58.97	24.18
14	43.5	41.1	26.1	22.6	22.3	1.40	2.71	53.72	25.50
15	41.7	40.3	27.1	22.8	22.4	3.31	4.46	38.63	24.33
16	38.3	38.0	27.9	23.0	22.4	5.50	6.30	20.33	21.01
17	33.4	34.4	28.5	23.1	22.5	7.84	8.13	-0.79	15.98
18	25.3	28.5	28.7	23.3	22.5	9.70	9.84	-35.04	7.79
19	17.9	22.4	28.5	23.4	22.6	11.59	11.27	-56.13	-0.24
20	15.6	19.4	27.9	23.4	22.6	12.44	12.11	-45.78	-4.04
21	14.7	18.1	26.9	23.4	22.6	12.33	12.37	-39.06	-5.70
22	13.8	17.0	26.0	23.3	22.5	11.75	11.96	-35.41	-7.07
23	13.0	16.0	25.0	23.1	22.5	9.98	10.95	-33.26	-8.16
24	12.2	15.2	24.2	23.0	22.4	8.46	9.62	-31.67	-9.22
Mean	24.8	25.4	24.4	22.7	22.4	3.67	5.08	4.26	4.31

Climatic
(Outdoor)
Chamber

Metering
(Indoor)
Chamber



Legend

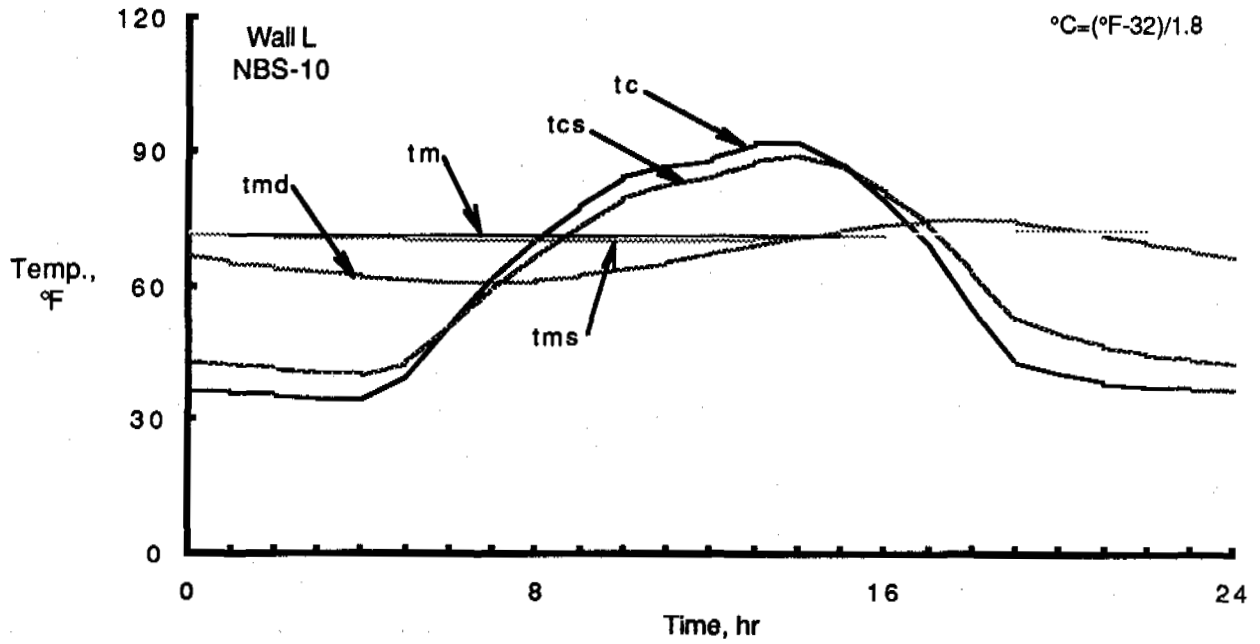
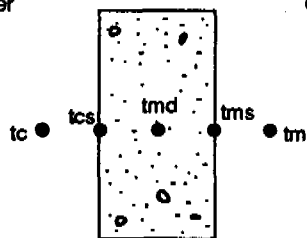


Fig. B7 Measured Temperatures for NBS-10 Test Cycle

Climatic
(Outdoor)
Chamber

Metering
(Indoor)
Chamber



Legend

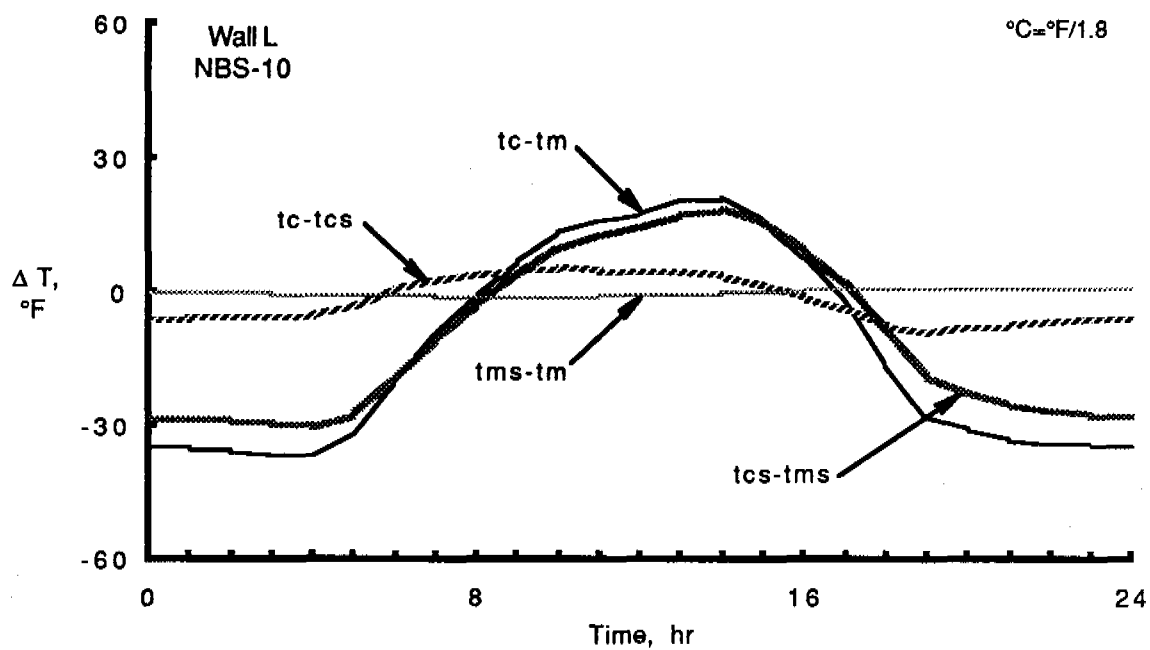


Fig. B8 Temperature Differentials for NBS-10 Test Cycle

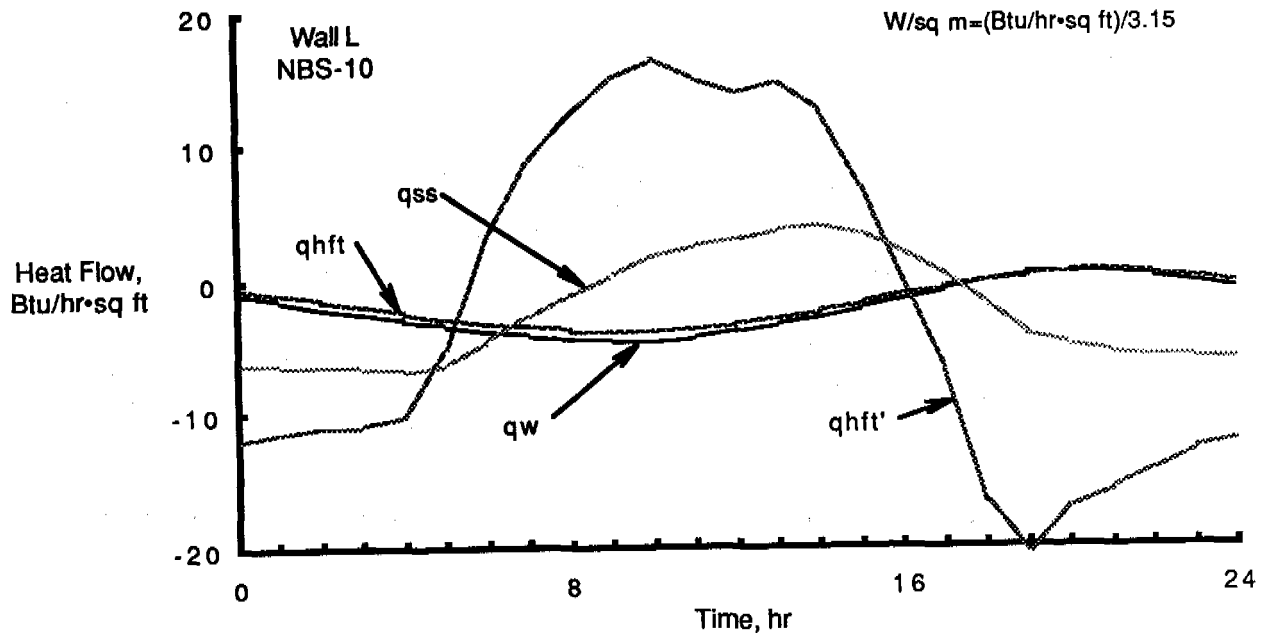


Fig. B9 Heat Flow for NBS-10 Test Cycle

TABLE B3(a) - DYNAMIC (PERIODIC) TEST RESULTS FOR NBS-10 TEMPERATURE CYCLE

Time, hr	Measured Temperatures, °F					Measured Heat Flow, Btu/hr-sq ft			Calculated Heat Flow Btu/hr-sq ft
	tc Climatic Chamber Air	tcs Climatic Surface	tmd Internal Therm.	tms Metering Surface	tm Metering Chamber Air	qw Calib. Hot Box	qhft HFT @ Metering Surface	qhft' HFT @ Climatic Surface	qss Steady-State
1	35.9	42.2	65.2	71.4	71.8	-1.52	-0.99	-11.43	-6.41
2	35.4	41.5	64.0	71.1	71.7	-2.11	-1.49	-11.01	-6.54
3	34.8	40.7	63.0	70.9	71.7	-2.56	-1.96	-10.84	-6.68
4	34.6	40.2	62.1	70.7	71.6	-3.05	-2.42	-10.12	-6.77
5	39.5	42.9	61.2	70.5	71.5	-3.42	-2.82	-5.04	-6.20
6	51.0	50.8	60.6	70.3	71.5	-3.91	-3.22	3.31	-4.55
7	61.8	59.4	60.6	70.1	71.4	-4.23	-3.54	9.00	-2.69
8	70.5	66.8	61.1	70.0	71.4	-4.51	-3.78	12.41	-1.03
9	78.1	73.4	62.3	70.0	71.4	-4.67	-3.91	15.09	0.45
10	84.5	79.5	63.8	70.1	71.5	-4.61	-3.88	16.42	1.85
11	87.0	82.7	65.6	70.3	71.5	-4.35	-3.63	14.98	2.59
12	88.7	84.8	67.5	70.5	71.5	-3.93	-3.33	13.84	3.07
13	92.1	88.0	69.3	70.8	71.6	-3.35	-2.84	14.66	3.81
14	92.4	89.3	71.1	71.2	71.7	-2.83	-2.31	12.57	4.12
15	87.5	86.7	72.8	71.5	71.8	-2.18	-1.72	6.86	3.47
16	79.2	80.8	74.1	71.8	71.9	-1.43	-1.11	-0.19	2.06
17	69.6	73.9	74.8	72.1	72.0	-0.76	-0.54	-6.83	0.43
18	55.2	63.4	74.9	72.4	72.1	-0.12	-0.03	-16.85	-1.94
19	43.2	53.0	74.4	72.5	72.1	0.40	0.36	-20.74	-4.22
20	40.7	49.3	73.0	72.5	72.1	0.57	0.57	-17.16	-5.00
21	38.4	46.4	71.3	72.4	72.1	0.51	0.57	-15.83	-5.59
22	37.4	44.8	69.6	72.2	72.0	0.15	0.34	-14.29	-5.93
23	37.0	43.8	67.9	72.0	71.9	-0.39	-0.02	-12.74	-6.10
24	36.5	43.0	66.5	71.7	71.8	-0.93	-0.49	-12.03	-6.26
Mean	58.8	61.1	67.4	71.2	71.7	-2.22	-1.76	-1.91	-2.25

Calibrated Hot Box Relative Humidity:

Metering Chamber - 41%

Climatic Chamber - 15%

Laboratory Air Temperature:

Max. - 75 °F

Min. - 72 °F

TABLE B3(b) - DYNAMIC (PERIODIC) TEST RESULTS FOR NBS-10 TEST CYCLE, SI UNITS

Time, hr	Measured Temperatures °C					Measured Heat Flow, W/sq m			Calculated Heat Flow W/sq m
	tc Climatic Chamber Air	tcs Climatic Surface	tmd Internal Therm.	tms Metering Surface	tm Metering Chamber Air	qw Calib. Hot Box	qhft HFT @ Metering Surface	qhft' HFT @ Climatic Surface	
1	2.2	5.6	18.4	21.9	22.1	-4.79	-3.11	-36.05	-20.23
2	1.9	5.3	17.8	21.7	22.1	-6.67	-4.70	-34.73	-20.62
3	1.5	4.9	17.2	21.6	22.0	-8.06	-6.19	-34.20	-21.06
4	1.4	4.6	16.7	21.5	22.0	-9.62	-7.63	-31.92	-21.37
5	4.2	6.1	16.2	21.4	22.0	-10.80	-8.90	-15.91	-19.57
6	10.5	10.4	15.9	21.3	21.9	-12.35	-10.16	10.44	-14.35
7	16.6	15.2	15.9	21.2	21.9	-13.36	-11.17	28.40	-8.48
8	21.4	19.4	16.2	21.1	21.9	-14.24	-11.93	39.15	-3.25
9	25.6	23.0	16.8	21.1	21.9	-14.73	-12.34	47.60	1.42
10	29.2	26.4	17.7	21.2	21.9	-14.56	-12.24	51.79	5.83
11	30.5	28.1	18.6	21.3	21.9	-13.72	-11.47	47.26	8.17
12	31.5	29.3	19.7	21.4	22.0	-12.41	-10.50	43.67	9.69
13	33.4	31.1	20.7	21.6	22.0	-10.57	-8.96	46.26	12.03
14	33.6	31.9	21.7	21.8	22.1	-8.92	-7.28	39.65	12.99
15	30.8	30.4	22.7	22.0	22.1	-6.87	-5.42	21.65	10.94
16	26.2	27.1	23.4	22.1	22.2	-4.52	-3.51	-0.61	6.49
17	20.9	23.3	23.8	22.3	22.2	-2.38	-1.70	-21.56	1.35
18	12.9	17.5	23.9	22.4	22.3	-0.37	-0.09	-53.15	-6.13
19	6.2	11.7	23.6	22.5	22.3	1.25	1.14	-65.44	-13.31
20	4.9	9.6	22.8	22.5	22.3	1.79	1.80	-54.13	-15.78
21	3.6	8.0	21.8	22.4	22.3	1.60	1.79	-49.95	-17.64
22	3.0	7.1	20.9	22.3	22.2	0.48	1.08	-45.08	-18.70
23	2.8	6.6	20.0	22.2	22.2	-1.22	-0.08	-40.19	-19.26
24	2.5	6.1	19.1	22.0	22.1	-2.95	-1.55	-37.94	-19.76
Mean	14.9	16.2	19.6	21.8	22.1	-7.00	-5.55	-6.04	-7.11

**CHARACTERIZING THE DYNAMIC THERMAL
PERFORMANCE OF A WALL USING PERIODIC EXCITATION**

Mark P. Modera
Energy Performance of Buildings Group
Applied Science Division
Lawrence Berkeley Laboratory
Berkeley, CA 94720

October 1987

ABSTRACT

The determination of the dynamic thermal performance of walls from laboratory measurements has recently attracted interest as a result of hot-box research at the National Research Council (NRC) in Canada and the National Bureau of Standards (NBS) in the U.S.. This paper describes an alternative measurement/analysis technique for multilayer walls based upon periodic excitation functions, and presents the results of a multi-frequency dynamic test of a single-layer wall performed in a calibrated hot box. The issues surrounding the use of periodic excitations are addressed, as are some of the limitations of hot boxes based upon the data analysis for the single-layer wall. It is shown that even walls with relatively short time constants (≈ 3 h) require either low frequencies (periods longer than 24 h) or high accuracy temperature measurements to extract the dynamic characteristics of a wall using periodic excitations. The interface between different dynamic measurement/analysis techniques and potential yardsticks for comparing dynamic thermal performance is also discussed.

This work was supported by the Assistant Secretary for Conservation and Renewable Energy, Office of Building and Community Systems, Building Systems Division of the U.S. Department of Energy under Contract No. DE-AC03-76SF00098.

INTRODUCTION

The dynamic thermal performance of walls is a subject which has recently evoked interest from several points of view. At present, the three principal points of view are: 1) the prediction of dynamic thermal performance from known material properties and construction details, 2) the verification of predicted performance or characterization of actual performance with laboratory measurements, and 3) the measurement and characterization of dynamic performance in the field.

Concerning the prediction of performance from materials and construction, the theory of dynamic one-dimensional conduction of heat through solids has remained relatively unchanged for the past fifty years, while practical models for incorporating dynamic wall performance into building simulation programs have been in existence for at least ten years. The principal problems remaining in this area are to develop usable models that take into account the multi-dimensional nature of conduction in wall systems, the convection and radiation in wall cavities and insulation, and the interaction between moisture transport and heat transfer through walls.

The determination of thermal performance from laboratory measurements has recently attracted interest for several reasons. First, as the issue of thermal bridges in wall systems has attracted attention, the possibility of measuring the overall performance of a wall system in a hot box has been discussed. Secondly, research at the National Research Council (NRC) in Canada (Stephenson 1987) and at the National Bureau of Standards (NBS) in the U.S. (Burch 1987), has significantly increased interest in dynamic measurements on wall systems in hot boxes. The laboratory measurements are an attempt to examine the validity of applying standard one-dimensional heat conduction algorithms to actual walls, and to develop a means for comparing the performance of wall systems with thermal bridges or non-conductive heat transfer, as well as novel wall systems, with that of simple multilayer walls.

The third point of view, that of characterizing dynamic performance from field measurements stems from a desire to verify the performance of actual field installations, and to characterize the performance of installations of unknown construction. This problem is similar to that posed in the laboratory, except that these measurements suffer from the additional difficulties associated with any field measurements.

This paper focuses on the second point of view, laboratory characterization of dynamic performance, describing an alternative measurement/analysis technique for multilayer walls based upon periodic excitation functions and non-intrusive measurements, as well as the results of a dynamic test of a single-layer wall in a calibrated hot box. The objectives of the paper are to examine the use of periodic excitations to extract the dynamic thermal characteristics of a wall, to provide a feel for some of the limitations of hot boxes based upon data analysis for a simple single-layer wall, and to discuss the interface between different measurement/analysis techniques and potential yardsticks for comparing dynamic

thermal performance. As recent publications contain detailed descriptions of techniques developed by NRC Canada and NBS for high-accuracy hot boxes, the use of periodic driving functions in these techniques is not discussed in detail. To narrow the scope of the discussion, complications resulting from thermal bridges and/or non-conductive heat transfer, although important issues, are not discussed.

MEASUREMENT/ANALYSIS TECHNIQUES FOR DYNAMIC THERMAL PERFORMANCE

Exact solutions to the differential equation for one-dimensional thermal conduction between parallel planes are well known (Carslaw and Jaeger, 1959). The solutions for transient and periodic boundary conditions completely characterize the heat transfer through a single-layer wall with only two parameters, the conductance (U) and time constant (τ). For periodic boundary conditions, the solution is:

$$\begin{pmatrix} J_1 \\ T_1 \end{pmatrix} = \begin{pmatrix} \frac{\cosh(i\pi^2\omega\tau)^{\frac{1}{2}}}{\text{what}} & \frac{-\sinh(i\pi^2\omega\tau)^{\frac{1}{2}}}{U(i\pi^2\omega\tau)^{\frac{1}{2}}} \\ -U(i\pi^2\omega\tau)^{\frac{1}{2}} \sinh(i\pi^2\omega\tau)^{\frac{1}{2}} & \cosh(i\pi^2\omega\tau)^{\frac{1}{2}} \end{pmatrix} \begin{pmatrix} J_2 \\ T_2 \end{pmatrix} \quad (1)$$

where the time constant τ in Equation 1 is defined as:

$$\tau = \frac{l^2}{\pi^2\alpha} \quad (2)$$

and:

- α is the thermal diffusivity of the material [m^2/s],
- l is the thickness of the material [m], and
- ω is the excitation frequency [rad/s].

To obtain the dynamic thermal characteristics of a wall from measured surface fluxes and temperatures, Equation 1 has to be solved for U and τ . This can be accomplished using the fourier transform of the measured flux and temperature data, the amplitude and phase relationship at each frequency expressed as:

$$\begin{aligned} J_1(\omega) &= A_{J_1}(\omega) e^{i\omega t + \Phi_{J_1}(\omega)} \\ J_2(\omega) &= A_{J_2}(\omega) e^{i\omega t + \Phi_{J_2}(\omega)} \\ T_1(\omega) &= A_{T_1}(\omega) e^{i\omega t + \Phi_{T_1}(\omega)} \\ T_2(\omega) &= A_{T_2}(\omega) e^{i\omega t + \Phi_{T_2}(\omega)} \end{aligned} \quad (3)$$

Substituting two temperatures and one flux from Equation 2 into either the top or bottom half of Equation 1 and equating the real and imaginary parts yields an equation for τ in terms of the two measured surface temperatures, and an additional equation involving U , τ , the measured temperatures, and the measured flux. However, to avoid introducing the error in τ into the computation of U , it should be determined directly from the average temperature difference across the wall and the average heat flux through the wall. Thus, the wall can be completely characterized from measured data by calculating U from the DC component (i.e., $\omega=0$) of the heat transfer, and τ at a single frequency.

The time constant can be determined by searching for the single parameter a to optimize:

$$\frac{\sinh(a)\cos(a)+\sin(a)\cosh(a)}{\sinh(a)\cos(a)-\sin(a)\cosh(a)} = \frac{T_{1r}\cosh(a)\cos(a)+T_{1i}\sin(a)\sinh(a)-T_{2r}}{T_{1r}\cosh(a)\cos(a)-T_{1i}\sin(a)\sinh(a)-T_{2i}} \quad (4)$$

where:

$$a = \sqrt{\frac{\pi^2\omega\tau}{2}} \quad (5)$$

and:

$$\begin{aligned} T_{j,i}(\omega) &= |T_j(\omega)| \sin(\phi_j(\omega)) \\ T_{j,r}(\omega) &= |T_j(\omega)| \cos(\phi_j(\omega)) \end{aligned} \quad (6)$$

where:

$T_{j,i}(\omega)$ is the imaginary component of the temperature on side j at frequency ω [K],

$T_{j,r}(\omega)$ is the real component of the temperature on side j at frequency ω [K], and

ϕ_j is the phase angle of the temperature on side j relative to the flux on side 1 at frequency ω , $\Phi_{T_j} - \Phi_{J_1}$ [rad].

From the point of view of signal-to-noise, the choice of frequency at which to determine τ can be rather important (Modera 1984). There will be very little phase lag or amplitude reduction at frequencies (ω) much lower than $4/\pi^2\tau$, implying that the signal-to-noise ratio will be reduced significantly at those frequencies. Similarly, at frequencies much higher than $4/\pi^2\tau$, the amplitude ratio across the wall tends to zero. For this reason the chosen wall excitation frequency should be close to $4/\pi^2\tau$.

Multi-layer Walls

The exact solution for surface heat transfer on a multilayer wall submitted to periodic boundary conditions is often expressed in a matrix formalism similar to

Equation 1:

$$\begin{pmatrix} J_1 \\ T_1 \end{pmatrix} = \begin{pmatrix} a_1 b_1 \\ c_1 d_1 \end{pmatrix} \begin{pmatrix} a_2 b_2 \\ c_2 d_2 \end{pmatrix} \cdots \begin{pmatrix} a_n b_n \\ c_n d_n \end{pmatrix} \begin{pmatrix} J_n \\ T_n \end{pmatrix} \quad (7)$$

In Equation 7, the a's, b's, c's and d's are the transfer functions involving hyperbolic trigonometric functions in U and τ found in Equation 1, where subscripts refer to the wall layer. However, the frequency domain analysis of measured data is not so straightforward for a multilayer wall. Although Equation 7 could theoretically be solved for the U 's and τ 's for each layer, the number of layers is unknown. An approximate technique for characterizing multilayered walls from measured data was examined by Sherman. This technique involves adding some additional parameters into the transfer functions for a single layer wall (Sherman 1981). These additional parameters were intended to account for the non-uniform distribution of mass in a multilayer wall. The parameters must be determined with a non-linear search routine, which was found to be susceptible to error (Modera 1984).

Another means of using Equation 7 to characterize a multilayer wall from measured temperature and flux data is to approximate the number of layers in the wall. The argument for assuming that all walls can be approximated by three layers is as follows. First, few walls have more than three functional layers, three functional layers being a very common wall construction. Furthermore, if a wall which has less than three layers is measured, the three layer model can collapse directly into a two- or even one-layer model. This occurs simply by the analysis program assigning the same U and τ (corrected for dimensions) to two or three layers. If a wall with four layers were measured, some blurring of wall layer properties would have to occur in the analysis of the measured data. The resulting parameters would depend to a certain extent on the choice of driving side. However, unlike the problem of modeling a three-layer wall with two layers, the characteristics of the two surfaces could be separated from the characteristics of the center of the wall.

Assuming that a three-layer model is an adequate approximation for most walls, a measurement and analysis technique based on Equation 7 can be developed. First, substituting the a, b, c and d for each of the three layers into Equation 7, two equations relating the measured heat fluxes and surface temperatures can be obtained by performing the matrix multiplication. These two equations are actually four equations, as both the real and imaginary parts of each equation must be equal. This implies four equations in six unknowns, $U_1, \tau_1, U_2, \tau_2, U_3, \tau_3$. One means of treating this situation is to excite the wall at multiple frequencies and use a χ^2 minimization routine to find the best-fitting parameters, an analysis technique similar to that used by Sherman.

To improve this analysis, a direct determination of overall conductance of the wall from the DC components of the temperatures and fluxes can be performed,

where:

$$U = \frac{1}{\frac{1}{U_1} + \frac{1}{U_2} + \frac{1}{U_3}} \quad (8)$$

The best-fit solution can be improved further by performing an additional measurement. This measurement would determine the overall thermal mass of the wall, and thereby provide a further constraint on the χ^2 minimization routine. One means of making this measurement is by integrating the heat flux leaving the wall on both sides after changing the temperature of the entire wall. This can be accomplished by holding both sides of the wall at equal temperature until the heat flux into or out of the wall goes to zero, and then changing the temperature on both sides of the wall and integrating the resulting heat flux. This implies:

$$\tau_1 U_1 + \tau_2 U_2 + \tau_3 U_3 = l_1 \rho_1 c_1 + l_2 \rho_2 c_2 + l_3 \rho_3 c_3 = \frac{\int_{t_{init}}^{t_{final}} (Q_A + Q_D) dt}{T_{final} - T_{init}} \quad (9)$$

The final set of six equations to be solved includes Equations 8, 9 and 10.

$$\begin{aligned} J_1 &= A J_2 + B T_2 \\ T_1 &= C J_2 + D T_2 \end{aligned} \quad (10)$$

where:

$$A = a_1 a_2 a_3 + b_1 c_2 a_3 + a_1 b_2 c_3 + b_1 a_2 c_3$$

$$B = a_1 a_2 b_3 + b_1 c_2 b_3 + a_1 b_2 a_3 + b_1 a_2 a_3$$

$$C = c_1 a_2 a_3 + a_1 c_2 a_3 + c_1 b_2 c_3 + a_1 a_2 c_3$$

$$D = c_1 a_2 b_3 + a_1 c_2 b_3 + c_1 b_2 a_3 + a_1 a_2 a_3$$

$$a_j = \cosh(i\pi^2 \omega \tau_j)^{\frac{1}{2}}$$

$$b_j = \frac{-\sinh(i\pi^2 \omega \tau_j)^{\frac{1}{2}}}{-U_j (i\pi^2 \omega \tau_j)^{\frac{1}{2}}}$$

$$c_j = -U_j (i\pi^2 \omega \tau_j)^{\frac{1}{2}} \sinh(i\pi^2 \omega \tau_j)^{\frac{1}{2}}$$

There are two major disadvantages in attempting to characterize a wall from measured data via Equations 8, 9, and 10. The first is the sheer complexity of Equation 10, which precludes separating the variables algebraically. The second is that the wall will have to be excited over a large range of frequencies, as Equation 10 does not provide any direct guidance on choice of frequency. In summary, using a simplified model for a multilayer wall based upon three layers is a potential means for characterizing the dynamic thermal performance of a wall from

surface measurements, although the analysis error propagation and the robustness of the parameters determined will have to be investigated.

EXPERIMENTAL INVESTIGATION — A SINGLE-LAYER WALL

To test the use of periodic excitations to determine wall characteristics in a commercial calibrated hot box, a single-layer lightweight concrete wall was tested. The experiment was performed at Construction Technologies Laboratory (CTL) in Skokie, IL. The wall tested was a 2.6 m (8.6 ft) square section of 20 cm (8 inch) thick lightweight structural concrete (MacroliteTM ceramic spheres) wall.

For the CTL facility, the cold side operating temperature range is -23 °C to 54 °C and the hot side operating range is 18-27 °C. For this test the warm side was maintained at 19.9 C, while the cold side was driven at three frequencies around a steady-state temperature of 2.0 C. The three frequencies were 0.26 rad/h (one cycle every 24 hours), 0.52 rad/h (one cycle every 12 hours), and 1.05 rad/h (one cycle every 6 hours). The surface temperature, measured with thermocouples, has a specified uncertainty of ± 0.03 °C. The heat flux on the warm side surface of the wall is determined from a heat balance on the warm-side box. The specified precision of the heat flux is 0.15 W/m^2 , and the specified accuracy 2.2 W/m^2 .

The DC temperature difference and the DC component of the heat flux were used to compute the U-value of the wall to be $1.23 \text{ W/m}^2 \text{ }^\circ\text{C}$. This value is within 9% of 1.13, the value computed from the thermal conductivity measured at CTL according to ASTM standard C177. The temperature amplitudes at each frequency, the phase lag between the warm and cold side temperatures, and the results of the analysis based upon the solution of Equation 4 are presented in Table 1.

Cycle Period [h]	$T_{cold}(\omega)$ [K]	$T_{warm}(\omega)$ [K]	$\phi_{warm-cold}$ [degrees]	τ [h]	α [m^2/h]
24	12.25	0.569	-109.4	2.94	0.0014
12	11.07	0.273	-165.5	4.99	0.00084
6	10.21	0.067	-241.7	1.04	0.0040

Looking first at the temperature amplitudes at each of the frequencies in Table 1, it is clear that very little of the cold-side temperature oscillations is propagated across to the warm side of the wall. As expected, the amplitude fraction traversing the wall decreases as the frequency increases. However, all frequencies seem to be too high, as even for the 24 hour cycle the amplitude ratio is very small. This result indicates that even for a wall with a 3 h time constant, frequencies longer than diurnal are required to accurately extract the dynamic

characteristics.

Considering the minimal amplitudes of the temperature fluctuations on the warm side at higher frequencies, the 24-hour cycle is likely to provide the most accurate estimate of the time constant. Assuming this to be the case, the 12-hour value is 70% high, and the 6-hour value 65% low. As a check on these values, the diffusivities computed from the wall time constants can be compared with values based upon laboratory tests of the material properties. These measurements, made by CTL, resulted in two distinct values for two different measurement techniques. Direct diffusivity measurements based upon U.S. Army Corps of Engineers Specification CRD-C36-73 (U.S. Army) yielded a value of $0.96 \times 10^{-3} \text{ m}^2/\text{h}$, whereas diffusivities determined from measured conductivities, specific heats and densities ranged between 2.4×10^{-3} and $3.4 \times 10^{-3} \text{ m}^2/\text{h}$. Although the best estimate of diffusivity based upon the wall tests falls in between the laboratory estimates, this comparison is not confidence inspiring, as the laboratory values differ from each other by more than a factor of three.

Another check on the time constants in Table 1 can be made by assuming that the dynamic heat fluxes on the warm side are negligible. This is not an unrealistic assumption, as the measured dynamic temperature variations and heat fluxes on the warm side were both extremely small. Based on this assumption, a solution for τ based solely upon the phase difference between the dynamic temperature variations can be used. This solution is obtained from the solution in Carslaw and Jaeger for a single-layer wall submitted to symmetric periodic boundary conditions on both faces. In this case the phase difference between the center (where the heat flux is zero) and surfaces of the wall is:

$$\phi = \arg \left\{ \frac{1}{\cosh \left((1+i) \left[\frac{\omega l^2}{2\alpha} \right]^{\frac{1}{2}} \right)} \right\} \quad (12)$$

In Equation 12, l is half the width of the wall, which corresponds to the entire thickness of our wall, so that Equation 12 can be rewritten as:

$$\tanh(a) \tan(a) = \tan(-\phi_{\text{warm-cold}}) \quad (13)$$

Thus Equation (13) can be solved for the time constant of the wall from $\phi_{\text{warm-cold}}$ at each frequency. The results of this computation are presented in Table 2.

Table 2. Phase-Angle Analysis of Single-Layer Wall.			
Cycle Period [h]	$\phi_{warm-cold}$ [degrees]	τ [h]	α [m ² /h]
24	-109.4	2.79	0.0015
12	-165.5	3.23	0.0013
6	-241.7	3.44	0.0012

The time-constant and diffusivity results for different frequencies are surprisingly consistent in Table 2, and are on average within 7% of the value obtained in the above analysis for the 24-hour cycle. The interpretation of this result is that although the accuracy at which the amplitudes of the measured temperatures on the warm side of the wall is not sufficient at higher frequencies, the phase relationship between the surface temperatures is measured relatively accurately at these frequencies.

DISCUSSION

Having derived a potential methodology for extracting the dynamic thermal characteristics of a wall from its measured response to periodic excitation, and having tested the simplest use of periodic excitation to extract the dynamic thermal characteristics of a single-layer wall, several observations can be made.

First, the use of periodic excitations to extract the dynamic characteristics of a wall seems to require either very long test times, or prohibitively accurate measurements. From the single-layer wall test, it is clear that very long test periods are required to obtain measurable temperature data for the time constant. For a wall with a three-hour time constant, a 24-hour cycle induced warm-side temperature variations with barely enough amplitude to provide an accurate measure of the time constant. This result has important ramifications for any tests using periodic excitation to obtain dynamic characterization parameters for walls, including those employed by Stephenson. This effect is also illustrated in Figures 1 and 2 (from Burch 1987), in which a outdoor cycle with a 24-hour component of approximately 10°C (Figure 1) induces an inside surface heat flux of only 15 Watts for a 14 m² insulated concrete wall section (Figure 2).

The second observation concerns the comparison of measured wall response with that predicted from measured material properties. The most surprising results are the large discrepancy between the material diffusivities measured using two different laboratory measurement techniques, and the consistency of the diffusivity determined from the three different wall excitation frequencies (Table 2). The first result implies a large uncertainty associated with using laboratory-measured material properties for predicting the dynamic thermal performance of lightweight concrete walls. This result, if confirmed, indicates a need for developing a standard methodology for measuring the diffusivity of materials such as

lightweight concrete. The second result, although preliminary, could be used to develop an alternative technique for estimating diffusivity.

Before closing this discussion, some attention should be given to the question of how to compare the dynamic performance of wall systems based on either measured or predicted performance. Intuitively, one would like to have a single parameter similar to the U-value (or R-value) to characterize the dynamic thermal performance of a wall. In fact, no such analogous parameter exists. Thus one is posed with the problem of either using a single intuitive parameter as a yardstick for comparing dynamic thermal performance, or to use the requisite number of parameters required to completely describe the performance of the wall. The τ 's for each layer used to characterize the wall from periodic excitations, despite the fact that they should provide a complete description of the wall performance, do not lend themselves readily to use as yardsticks for comparing walls. Similarly, the transfer function coefficients or response factors determined by Burch or Stephenson provide a relatively complete description of the wall performance (depending upon the time-step used), but do not readily lend themselves to use as yardsticks of performance.

Two potential yardsticks which have been suggested as a means for comparing walls are the phase relationship and the amplitude ratio at some characteristic frequency (Subbarao 1985, Subbarao 1985a). One advantage of this characterization is that it does not require extensive experimental effort or equipment. The parameters in this type of characterization are easy to determine experimentally, both in the laboratory and in the field. In the lab, the wall need simply be submitted to a sinusoidal boundary condition on one side while measuring the response on both sides. In the field, the measured surface temperatures and fluxes must be fourier transformed, after which the phase lag and amplitude ratio at any of the existing frequencies can be determined directly. Another argument in favor of this type of characterization is that in most applications a single frequency, the diurnal (24-hour) cycle, is clearly the dominant excitation at which dynamic response is desired.

CONCLUSIONS

There are two conclusions that can be drawn from the experimental study of a single-layer wall. The first conclusion stems from the quantification of the excitation frequencies required to extract the dynamic characteristics of the wall. The fact that exciting a three-hour-time-constant wall with a 24-h cycle gives a temperature amplitude reduction of more than 20 implies that hot boxes will have to be cycled very slowly to extract the dynamic characteristics of many walls. This implies that any standardization of the methodologies developed at NRC Canada or NBS should take the implied test-period/sensor-accuracy considerations into account. In particular, the NRC procedure (Stephenson, 1987) is directly affected by such considerations. The second conclusion concerns the observed reduction in uncertainty associated with using phase angle rather than amplitude ratio to extract the wall characteristics with periodic excitations. This result suggests that

the test-period/sensor-accuracy constraints described above could be relaxed if phase angle were used instead of amplitude ratio or complete response. Considering the potential reductions in experimental effort associated with such a substitution, it appears that a more careful examination of this possibility is warranted.

REFERENCES

D.M. Burch, R.R. Zarr, T.K. Faison, B.A. Licitra, C.E. Arnold, "A Procedure for Measuring the Dynamic Thermal Performance of Wall Specimens Using a Calibrated Hot Box", *ASHRAE Trans.* Vol. 93 Part I, January 1987.

H.S. Carslaw and J.C. Jaeger, **Conduction of Heat in Solids**, Second Edition, Oxford University Press, Oxford England, 1959.

M.P. Modera, M.H. Sherman, and S.G. de Vinuesa, "In-Situ Measurement of Wall Thermal Performance: Data Interpretation and Apparatus Design Recommendations", ASTM Special Technical Publication STP 922, *Thermal Insulation Materials and Systems*, Dallas, TX, December, 1984, Lawrence Berkeley Laboratory Report, LBL-17773.

M.H. Sherman, J.W. Adams, R.C. Sonderegger, "Simplified Thermal Parameters: A Model of the Dynamic Performance of Walls", ASTM STP-789, *Thermal Insulation, Materials and Systems for Energy Conservation in the 80's*, Lawrence Berkeley Laboratory Report, LBL-13503, December 1981.

D. G. Stephenson, Ouyang Kunze, "An Experimental Procedure for Determining the Dynamic Thermal Characteristics of Walls Using a Calibrated Hot Box", NRC Canada 613-993-1421, 1987.

K. Subbarao, J. Burch, E. Hancock, H. Jeon, "Measurement of Effective Thermal Capacitance in Buildings", ASHRAE SP 49, Conference Proceedings - Thermal Performance of the Exterior Envelopes of Buildings III, December 2-5, 1985, Clearwater Beach, Florida.

K. Subbarao, J. Burch, "A Unified Framework for Dynamic Thermal Testing of Building Components", Presented at ASME Winter Annual Meeting, 85-WA/SOL-8, November 1985a.

U.S. Army, **Handbook for Concrete and Cement**, U.S. Army Waterways Experimental Station, Vicksburg, MS, 1987.

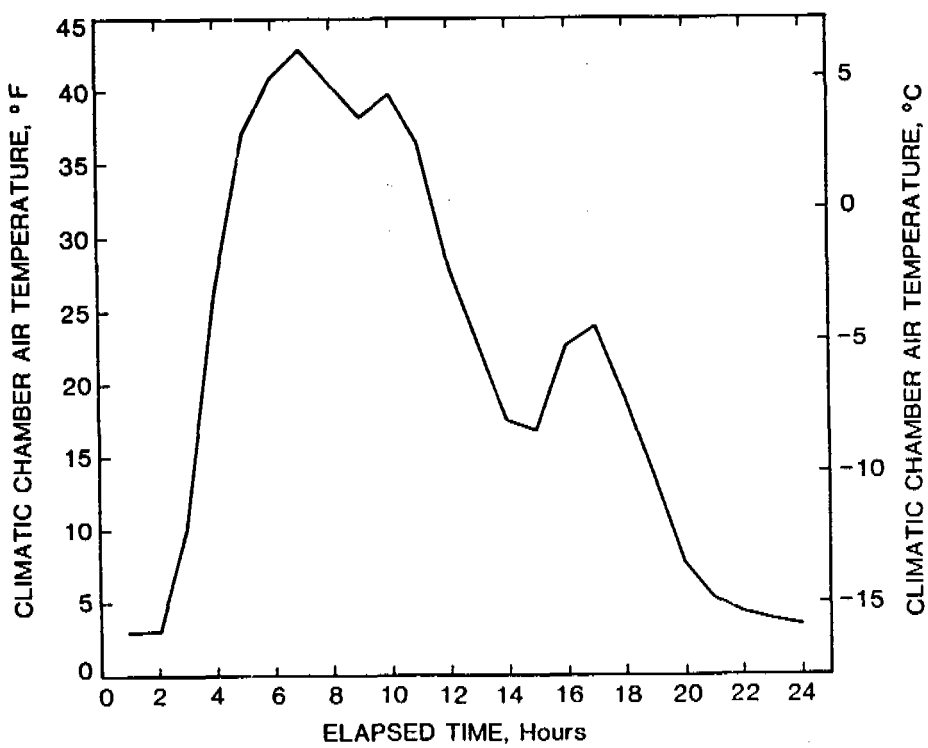


Figure 1: NBS hot-box climatic chamber temperature profile (from Burch 1987).

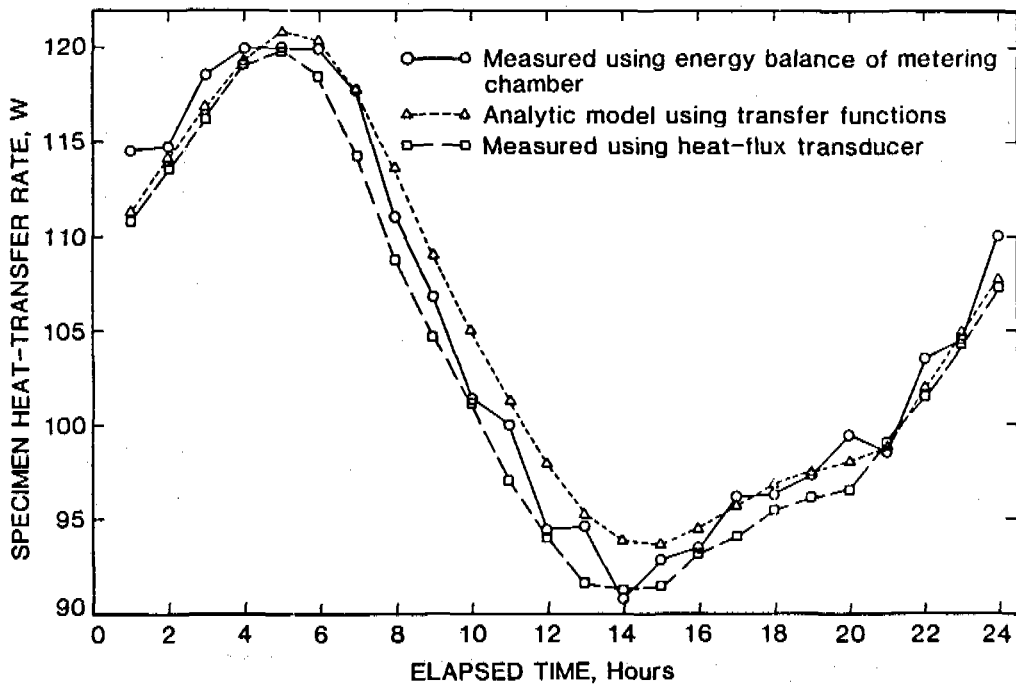


Figure 2: NBS hot-box metering chamber heat transfer rate through an insulated concrete wall submitted to climatic temperature profile in Figure 1 (from Burch 1987).

APPENDIX D - TRANSIENT TEMPERATURE TEST RESULTS

Measured temperatures, temperature differentials, and heat flow for transient temperature tests on Walls L and S are presented in Figs. D1 through D6 and listed in Tables D1 and D2. Data for Wall L are presented first, followed by data for Wall S.

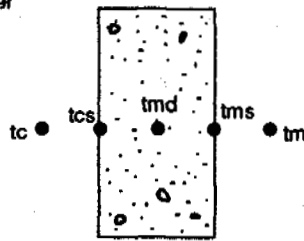
Tables D1 and D2 denoted (a) and (b), respectively, list hourly test data in IP and SI units.

Symbols used in these figures and tables are described in detail in the "Test Results" portion of the "Dynamic (24-Hr Periodic) Calibrated Hot Box Tests" section of this report.

Measured temperatures for Walls L and S, respectively, are listed in Tables D1 and D2, and shown as a function of time in Figs. D1 and D4. Air-to-air (t_c-t_m), surface-to-surface ($t_{cs}-t_{ms}$), and surface-to-air (t_c-t_{cs} , $t_{ms}-t_m$) temperature differentials for Walls L and S, respectively, are illustrated in Figs. D2 and D5. Measured and calculated heat flows for Walls L and S, respectively, are listed in Tables D1 and D2, and shown as a function of time in Figs. D3 and D6.

Climatic
(Outdoor)
Chamber

Metering
(Indoor)
Chamber



Legend

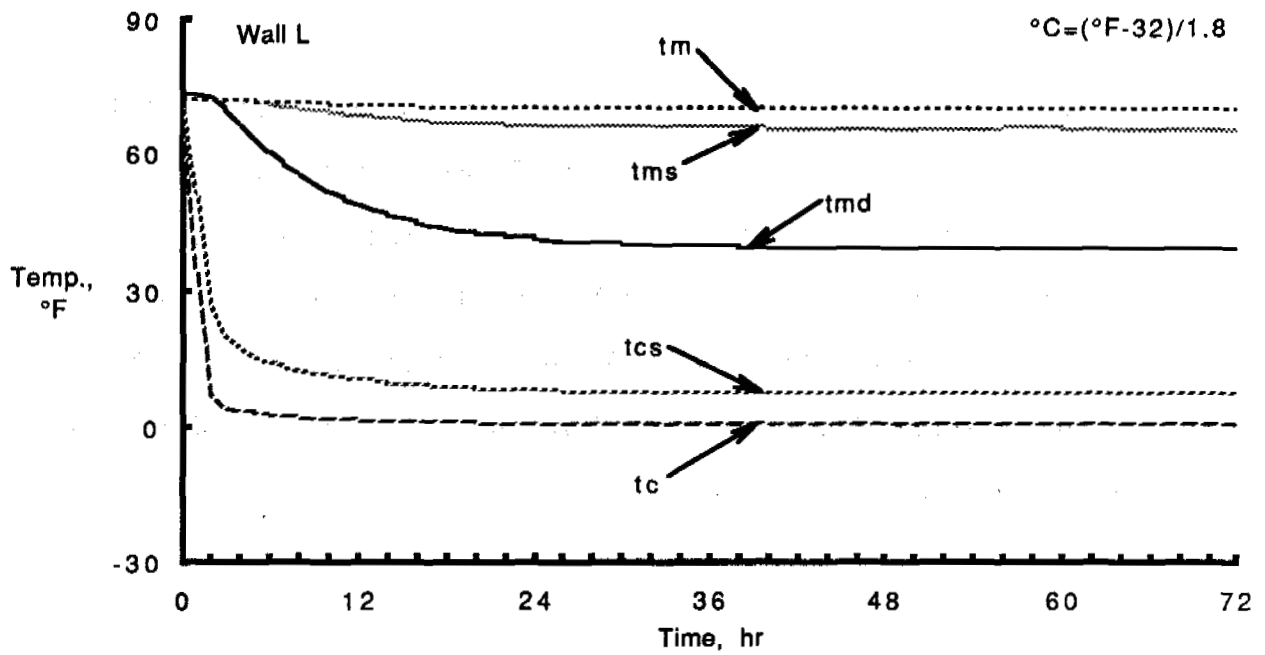
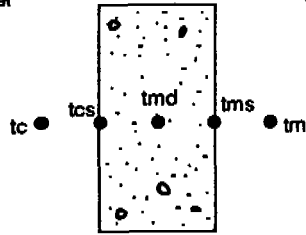


Fig. D1 Measured Temperatures for Transient Test on Wall L

Climatic
(Outdoor)
Chamber

Metering
(Indoor)
Chamber



Legend

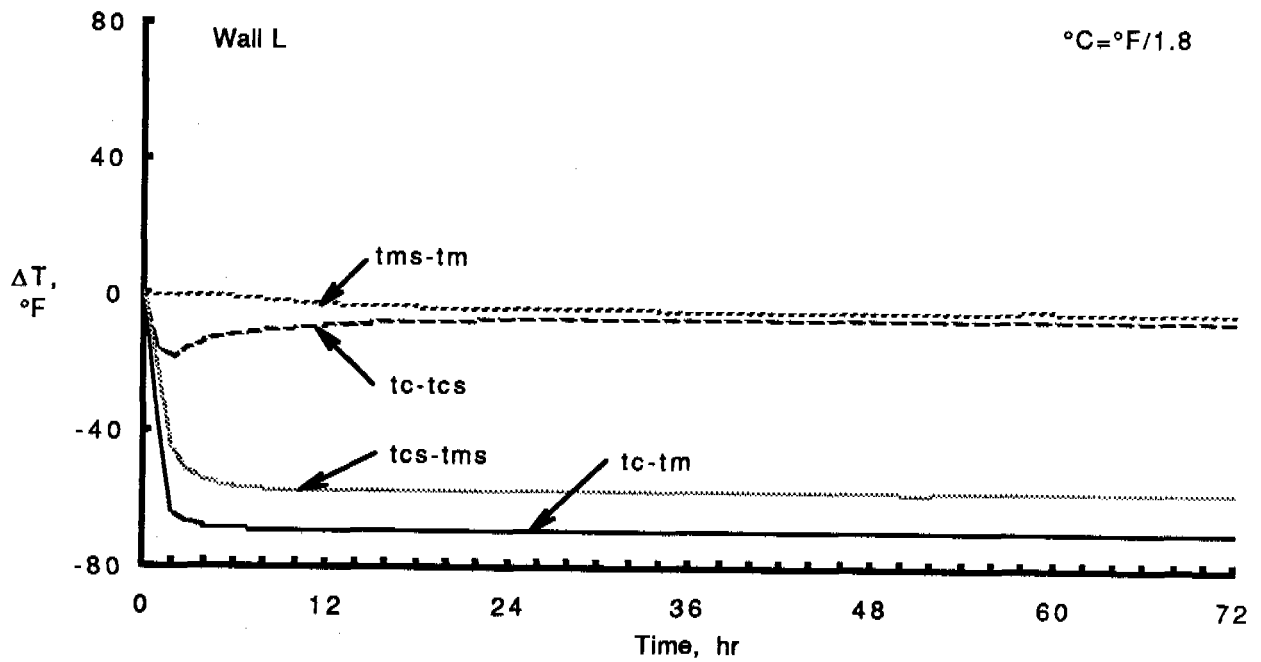


Fig. D2 Temperature Differentials for Transient Test on Wall L

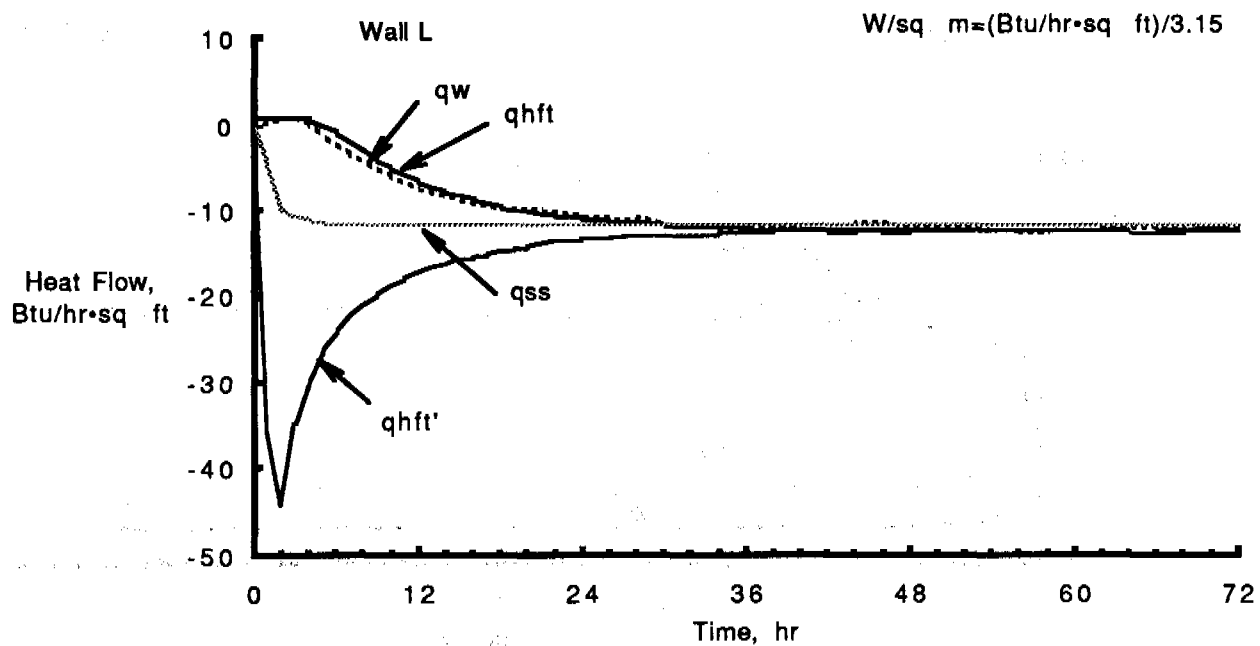


Fig. D3 Heat Flow for Transient Test on Wall L

TABLE D1(a) - TRANSIENT TEST RESULTS FOR WALL L

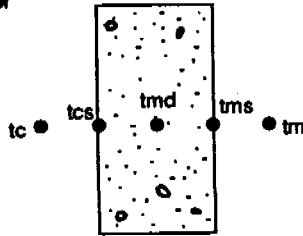
Time, hr	Measured Temperatures, °F					Measured Heat Flow, Btu/hr-sq ft			Calculated Heat Flow, Btu/hr-sq ft
	tc Outdoor Air	tcs Outdoor Surface	tmd Internal Indoor	tms Indoor Surface	tm Indoor Air	qw Calib. Hot Box	qhft HFT @ In. Surf.	qhft' HFT @ Out. Surf.	
0	72.1	73.3	73.6	72.3	72.1	0.19	0.69	0.62	0.21
1	34.4	51.2	73.5	72.3	72.1	0.28	0.70	-35.74	-4.65
2	7.4	26.4	72.7	72.3	72.1	0.52	0.70	-44.50	-9.69
3	4.4	20.0	69.9	72.3	72.0	0.51	0.65	-34.81	-10.91
4	3.5	17.2	66.5	72.1	72.0	-0.28	0.35	-29.89	-11.40
5	2.9	15.4	63.2	71.6	71.9	-1.37	-0.29	-26.20	-11.63
6	2.6	14.1	60.2	71.1	71.7	-2.42	-1.17	-24.09	-11.75
7	2.3	13.1	57.7	70.6	71.6	-3.55	-2.18	-22.22	-11.80
8	2.1	12.5	55.5	70.1	71.5	-4.35	-3.19	-20.86	-11.81
9	1.9	11.8	53.5	69.6	71.3	-5.35	-4.21	-19.70	-11.82
10	1.8	11.3	51.7	69.2	71.2	-6.12	-5.10	-18.66	-11.82
11	1.7	10.8	50.1	68.8	71.1	-6.88	-5.93	-17.98	-11.82
12	1.6	10.5	48.8	68.4	71.0	-7.69	-6.68	-17.34	-11.81
13	1.5	10.1	47.6	68.1	70.9	-7.96	-7.36	-16.68	-11.80
14	1.4	9.8	46.6	67.8	70.8	-8.39	-7.90	-16.29	-11.79
15	1.3	9.5	45.7	67.5	70.7	-8.81	-8.36	-15.58	-11.78
16	1.2	9.3	44.9	67.3	70.7	-9.17	-8.90	-15.39	-11.78
17	1.2	9.2	44.2	67.2	70.7	-9.49	-9.23	-15.17	-11.77
18	1.2	9.0	43.6	67.0	70.7	-9.80	-9.68	-14.63	-11.77
19	1.1	8.8	43.0	66.7	70.7	-9.82	-10.03	-14.47	-11.74
20	1.0	8.6	42.6	66.7	70.6	-9.65	-10.21	-14.19	-11.76
21	1.0	8.5	42.2	66.6	70.6	-10.12	-10.54	-13.85	-11.76
22	0.9	8.4	41.8	66.5	70.5	-10.14	-10.67	-13.54	-11.75
23	0.9	8.3	41.5	66.4	70.5	-10.45	-10.90	-13.53	-11.76
24	0.9	8.2	41.2	66.4	70.5	-10.69	-11.14	-13.30	-11.76
26	0.8	8.0	40.7	66.2	70.4	-10.95	-11.32	-13.36	-11.77
28	0.7	7.9	40.4	66.1	70.3	-10.70	-11.52	-12.83	-11.76
30	0.8	7.9	40.1	66.2	70.4	-11.84	-11.87	-12.84	-11.77
32	0.9	7.9	40.0	66.2	70.5	-12.11	-11.95	-12.79	-11.77
34	0.9	7.9	39.9	66.1	70.5	-12.21	-12.09	-12.65	-11.77
36	0.8	7.9	39.8	66.1	70.5	-12.04	-12.15	-12.56	-11.76
38	0.8	7.8	39.7	66.1	70.5	-11.93	-12.25	-12.43	-11.76
40	0.8	7.8	39.6	66.0	70.4	-11.82	-12.30	-12.24	-11.75
42	0.8	7.8	39.6	66.0	70.4	-11.75	-12.27	-12.48	-11.76
44	0.7	7.7	39.6	65.9	70.4	-11.49	-12.23	-12.35	-11.76
46	0.7	7.7	39.5	65.9	70.3	-11.34	-12.33	-12.51	-11.76
48	0.7	7.7	39.5	65.9	70.3	-12.04	-12.43	-12.24	-11.76
50	0.8	7.6	39.4	65.9	70.4	-12.02	-12.43	-12.33	-11.77
52	0.8	7.7	39.4	65.9	70.4	-12.05	-12.46	-12.38	-11.76
54	0.8	7.7	39.4	66.0	70.4	-12.36	-12.43	-12.35	-11.77
56	0.9	7.8	39.5	66.0	70.5	-12.63	-12.42	-12.27	-11.77
58	0.8	7.8	39.5	66.0	70.4	-12.42	-12.40	-12.27	-11.76
60	0.8	7.8	39.5	66.0	70.4	-12.19	-12.39	-12.32	-11.76
62	0.8	7.7	39.4	65.9	70.4	-11.95	-12.40	-12.30	-11.76
64	0.8	7.7	39.5	65.9	70.4	-11.95	-12.48	-12.48	-11.76
66	0.8	7.7	39.5	65.9	70.4	-11.91	-12.44	-12.46	-11.76
68	0.7	7.7	39.4	65.9	70.4	-11.77	-12.37	-12.43	-11.75
70	0.8	7.7	39.5	66.0	70.4	-11.77	-12.40	-11.95	-11.76
72	0.8	7.7	39.4	66.0	70.4	-12.12	-12.44	-12.30	-11.77

TABLE D1(b) - TRANSIENT TEST RESULTS FOR WALL L, SI UNITS

Time, hr	Measured Temperatures, °C					Measured Heat Flow, W/sq m			Calculated Heat Flow, W/sq m
	tc Outdoor Air	tcs Outdoor Surface	tmd Internal Therm.	tms Indoor Surface	tm Indoor Air	qw Calib. Hot Box	qhft HFT @ In. Surf.	qhft' HFT @ Out. Surf.	
0	22.3	22.9	23.1	22.4	22.3	0.80	2.19	1.94	0.65
1	1.3	10.7	23.1	22.4	22.3	0.88	2.22	-112.74	-14.67
2	-13.7	-3.1	22.6	22.4	22.3	1.64	2.21	-140.40	-30.57
3	-15.3	-6.7	21.1	22.4	22.2	1.62	2.05	-109.84	-34.41
4	-15.9	-8.3	19.2	22.3	22.2	-0.87	1.12	-94.30	-35.95
5	-16.2	-9.2	17.3	22.0	22.1	-4.31	-0.91	-82.65	-36.70
6	-16.4	-9.9	15.7	21.7	22.1	-7.62	-3.68	-76.01	-37.06
7	-16.5	-10.5	14.3	21.4	22.0	-11.19	-6.89	-70.09	-37.23
8	-16.6	-10.9	13.0	21.1	21.9	-13.72	-10.07	-65.83	-37.27
9	-16.7	-11.2	11.9	20.9	21.9	-16.89	-13.28	-62.16	-37.28
10	-16.8	-11.5	10.9	20.6	21.8	-19.31	-16.08	-58.86	-37.30
11	-16.8	-11.8	10.1	20.4	21.7	-21.71	-18.71	-56.74	-37.29
12	-16.9	-12.0	9.3	20.2	21.7	-24.25	-21.07	-54.71	-37.25
13	-17.0	-12.2	8.7	20.0	21.6	-25.12	-23.23	-52.62	-37.22
14	-17.0	-12.3	8.1	19.9	21.6	-26.47	-24.93	-51.38	-37.21
15	-17.1	-12.5	7.6	19.7	21.5	-27.78	-26.37	-49.15	-37.16
16	-17.1	-12.6	7.1	19.6	21.5	-28.93	-28.07	-48.55	-37.16
17	-17.1	-12.7	6.8	19.5	21.5	-29.93	-29.14	-47.87	-37.12
18	-17.1	-12.8	6.5	19.5	21.5	-30.93	-30.55	-46.17	-37.12
19	-17.2	-12.9	6.1	19.3	21.5	-30.97	-31.64	-45.67	-37.03
20	-17.2	-13.0	5.9	19.3	21.4	-31.08	-32.22	-44.78	-37.09
21	-17.2	-13.0	5.7	19.2	21.4	-31.94	-33.26	-43.71	-37.11
22	-17.3	-13.1	5.4	19.2	21.4	-32.00	-33.68	-42.71	-37.08
23	-17.3	-13.2	5.3	19.1	21.4	-32.98	-34.39	-42.68	-37.09
24	-17.3	-13.2	5.1	19.1	21.4	-33.72	-35.14	-41.97	-37.11
26	-17.3	-13.4	4.8	19.0	21.3	-34.54	-35.72	-42.14	-37.14
28	-17.4	-13.4	4.7	19.0	21.3	-33.77	-36.33	-40.47	-37.10
30	-17.3	-13.4	4.5	19.0	21.3	-37.36	-37.45	-40.52	-37.14
32	-17.3	-13.4	4.4	19.0	21.4	-38.20	-37.70	-40.35	-37.14
34	-17.3	-13.4	4.4	18.9	21.4	-38.53	-38.15	-39.90	-37.12
36	-17.3	-13.4	4.3	18.9	21.4	-37.97	-38.32	-39.63	-37.09
38	-17.3	-13.4	4.3	18.9	21.4	-37.83	-38.65	-39.22	-37.11
40	-17.3	-13.4	4.2	18.9	21.3	-37.29	-38.80	-38.62	-37.08
42	-17.3	-13.5	4.2	18.9	21.3	-37.07	-38.73	-39.38	-37.10
44	-17.4	-13.5	4.2	18.9	21.3	-36.25	-38.59	-38.97	-37.09
46	-17.4	-13.5	4.2	18.9	21.3	-35.77	-38.91	-39.46	-37.10
48	-17.4	-13.5	4.1	18.8	21.3	-37.98	-39.20	-38.62	-37.10
50	-17.4	-13.5	4.1	18.9	21.3	-37.92	-39.20	-38.89	-37.12
52	-17.3	-13.5	4.1	18.9	21.3	-38.01	-39.30	-39.04	-37.10
54	-17.3	-13.5	4.1	18.9	21.3	-38.99	-39.22	-38.97	-37.12
56	-17.3	-13.5	4.1	18.9	21.4	-39.85	-39.19	-38.72	-37.12
58	-17.3	-13.5	4.2	18.9	21.3	-39.18	-39.13	-38.73	-37.11
60	-17.3	-13.5	4.2	18.9	21.3	-38.45	-39.08	-38.88	-37.09
62	-17.3	-13.5	4.1	18.9	21.3	-37.71	-39.12	-38.81	-37.09
64	-17.4	-13.5	4.2	18.9	21.3	-37.70	-39.37	-39.38	-37.10
66	-17.4	-13.5	4.2	18.9	21.3	-37.58	-39.24	-39.32	-37.09
68	-17.4	-13.5	4.1	18.8	21.3	-37.14	-39.01	-39.21	-37.09
70	-17.4	-13.5	4.1	18.9	21.3	-37.13	-39.11	-37.71	-37.10
72	-17.4	-13.5	4.1	18.9	21.3	-38.25	-39.24	-38.81	-37.13

Climatic
(Outdoor)
Chamber

Metering
(Indoor)
Chamber



Legend

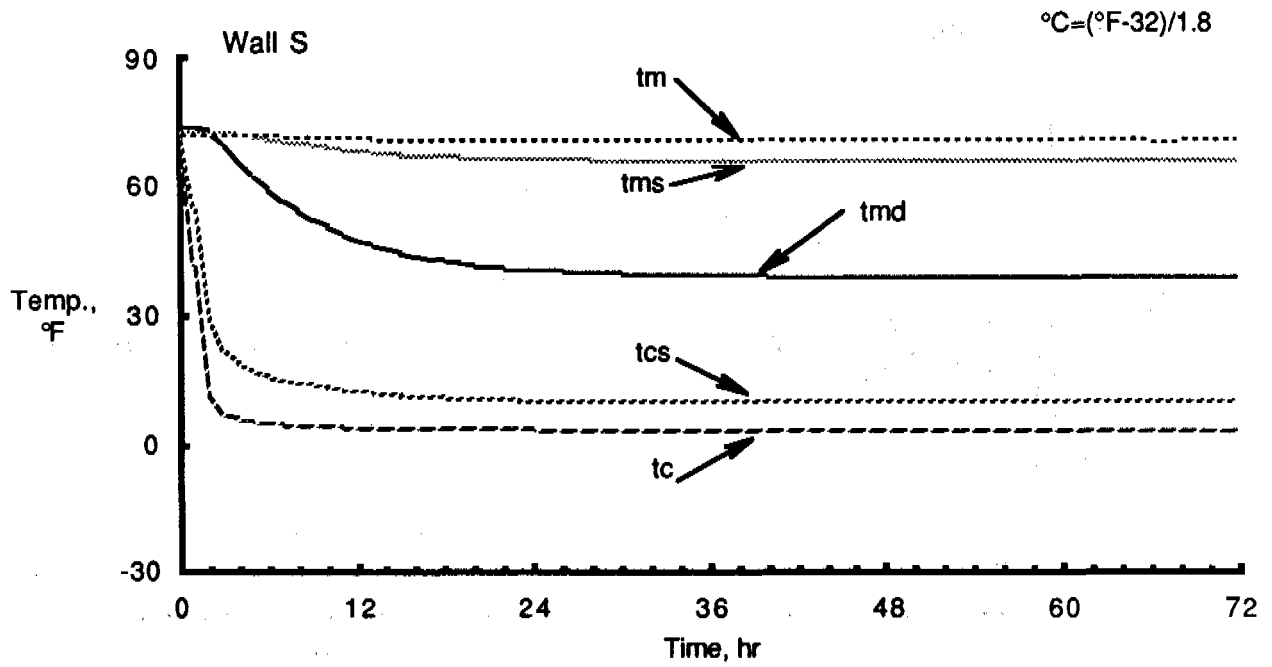
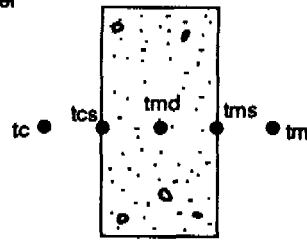


Fig. D4 Measured Temperatures for Transient Test on Wall S

Climatic
(Outdoor)
Chamber

Metering
(Indoor)
Chamber



Legend

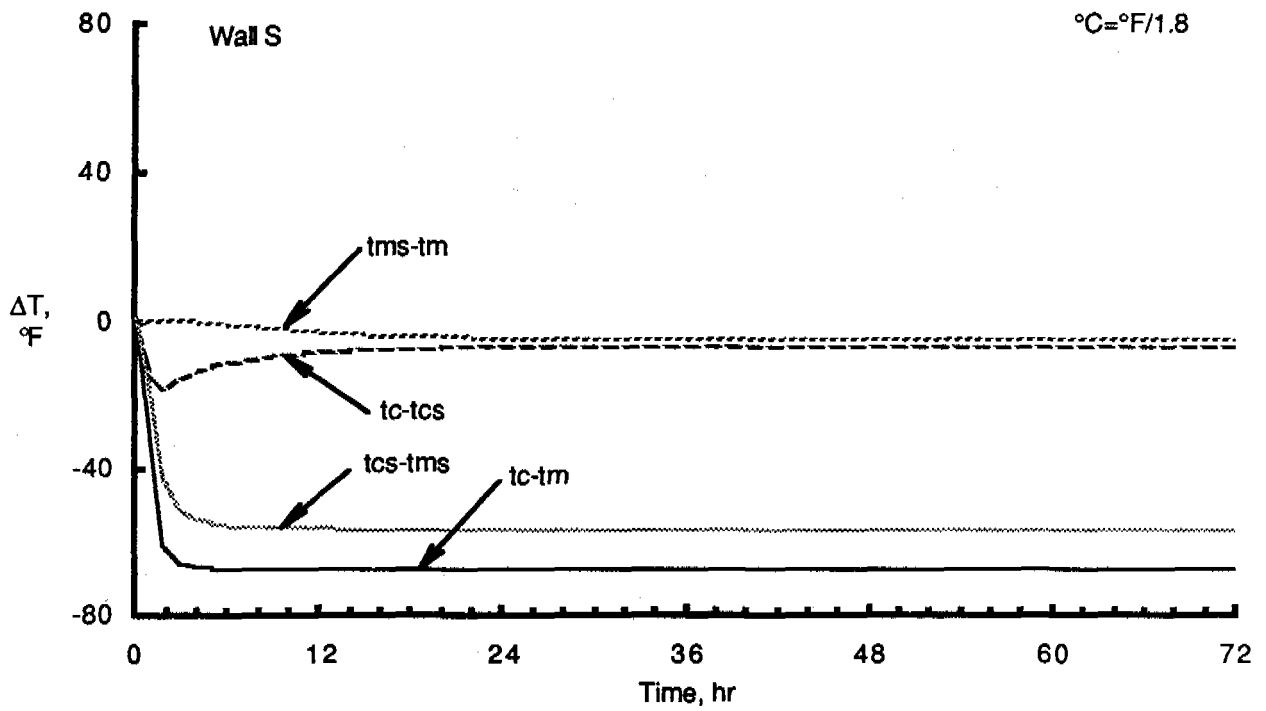


Fig. D5 Temperature Differentials for Transient Test on Wall S

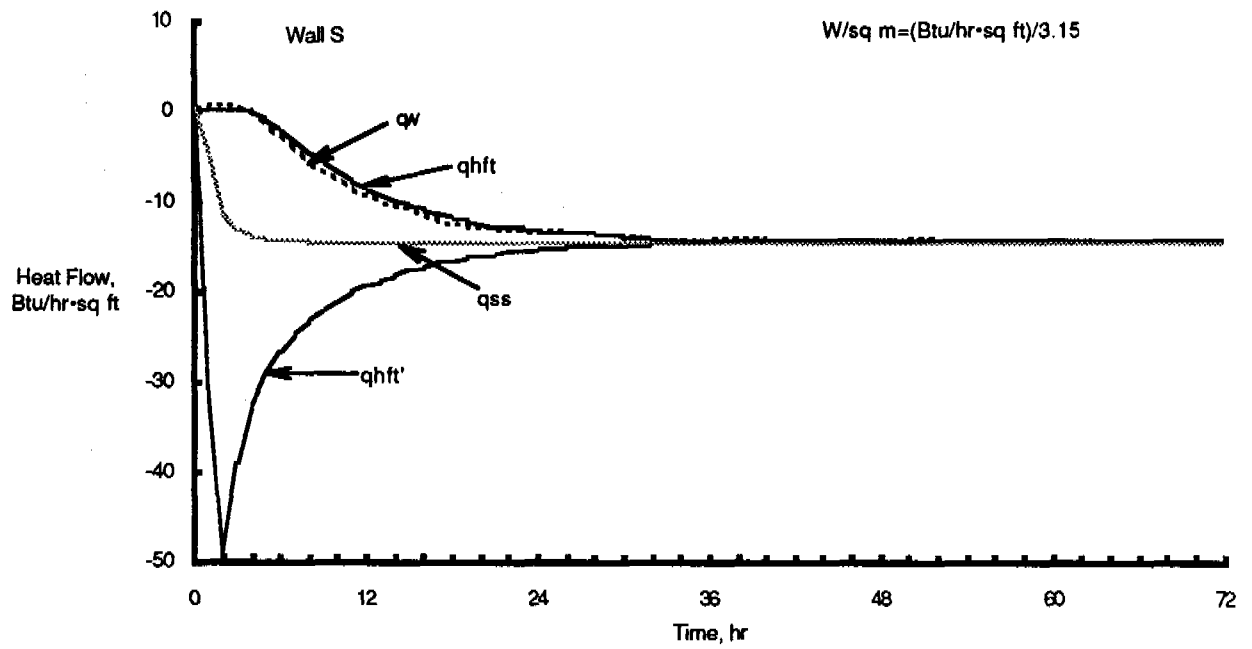


Fig. D6 Heat Flow for Transient Test on Wall S

TABLE D2(a) - TRANSIENT TEST RESULTS FOR WALL S

Time, hr	Measured Temperatures, °F					Measured Heat Flow, Btu/hr-sq ft			Calculated Heat Flow, Btu/hr-sq ft
	tc Outdoor Air	ics Outdoor Surface	imd Internal Indoor	ims Indoor Surface	tm Indoor Air	qw Calib. Hot Box	qhft HFT @ In. Surf.	qhft' HFT @ Out. Surf.	
0	73.5	74.1	73.8	72.9	72.5	0.42	0.17	0.02	0.32
1	41.6	55.5	73.8	72.9	72.4	0.67	0.19	-32.15	-4.53
2	11.1	29.3	72.7	72.8	72.4	0.68	0.18	-48.73	-11.20
3	6.6	21.5	69.6	72.7	72.4	0.47	0.11	-38.74	-13.15
4	5.7	18.6	65.9	72.3	72.3	-0.21	-0.19	-32.40	-13.78
5	5.1	16.9	62.3	71.8	72.1	-1.50	-1.00	-28.86	-14.07
6	4.9	15.7	59.3	71.2	72.0	-2.82	-2.10	-26.39	-14.22
7	4.6	14.8	56.6	70.6	71.8	-4.32	-3.35	-24.50	-14.30
8	4.4	14.0	54.3	70.1	71.7	-5.67	-4.61	-23.10	-14.34
9	4.3	13.4	52.3	69.6	71.6	-6.64	-5.72	-21.95	-14.35
10	4.2	12.9	50.5	69.1	71.5	-7.55	-6.69	-20.80	-14.35
11	4.0	12.5	48.9	68.7	71.4	-8.61	-7.68	-19.90	-14.36
12	4.0	12.1	47.5	68.3	71.3	-9.26	-8.52	-19.07	-14.35
13	3.8	11.8	46.4	68.0	71.2	-9.96	-9.23	-18.54	-14.36
14	3.8	11.5	45.4	67.7	71.1	-10.45	-9.87	-18.06	-14.36
15	3.7	11.3	44.5	67.5	71.1	-10.97	-10.44	-17.33	-14.36
16	3.7	11.1	43.8	67.3	71.0	-11.48	-11.01	-17.07	-14.36
17	3.6	10.9	43.1	67.1	71.0	-12.00	-11.39	-16.64	-14.36
18	3.5	10.7	42.6	67.0	71.0	-12.40	-11.88	-16.49	-14.37
19	3.5	10.6	42.1	66.9	71.0	-12.66	-12.03	-16.04	-14.38
20	3.5	10.4	41.7	66.8	70.9	-12.75	-12.36	-15.88	-14.37
21	3.5	10.3	41.3	66.7	70.9	-12.92	-12.66	-15.65	-14.38
22	3.5	10.3	41.0	66.6	70.8	-13.13	-12.81	-15.28	-14.38
23	3.5	10.2	40.8	66.6	70.8	-13.42	-13.01	-15.23	-14.38
24	3.4	10.1	40.6	66.5	70.9	-13.15	-13.20	-15.02	-14.37
26	3.4	10.0	40.1	66.4	70.7	-13.44	-13.40	-14.82	-14.38
28	3.4	9.9	39.8	66.3	70.7	-13.52	-13.67	-14.73	-14.38
30	3.3	9.9	39.6	66.2	70.7	-13.66	-13.84	-14.67	-14.38
32	3.3	9.8	39.4	66.2	70.8	-14.21	-14.06	-14.43	-14.37
34	3.3	9.8	39.3	66.1	70.7	-14.12	-14.09	-14.35	-14.37
36	3.3	9.8	39.3	66.1	70.7	-13.95	-14.12	-14.43	-14.37
38	3.3	9.8	39.2	66.1	70.7	-13.96	-14.12	-14.26	-14.37
40	3.3	9.8	39.2	66.1	70.7	-14.05	-14.08	-14.24	-14.37
42	3.3	9.7	39.2	66.1	70.7	-14.32	-14.30	-14.19	-14.38
44	3.2	9.7	39.1	66.1	70.7	-14.35	-14.18	-14.23	-14.38
46	3.2	9.7	39.1	66.1	70.7	-14.45	-14.29	-14.16	-14.39
48	3.3	9.7	39.1	66.1	70.7	-14.20	-14.23	-14.24	-14.39
50	3.3	9.7	39.1	66.1	70.7	-13.94	-14.36	-14.23	-14.38
52	3.3	9.7	39.0	66.0	70.7	-14.07	-14.27	-14.18	-14.37
54	3.3	9.7	39.0	66.0	70.6	-14.08	-14.33	-14.09	-14.36
56	3.2	9.7	39.0	66.0	70.7	-14.27	-14.30	-14.13	-14.37
58	3.2	9.7	39.0	66.0	70.8	-14.11	-14.26	-14.19	-14.37
60	3.3	9.7	39.0	66.0	70.7	-14.09	-14.33	-14.17	-14.36
62	3.3	9.7	39.0	66.0	70.7	-14.09	-14.28	-14.10	-14.35
64	3.2	9.7	39.0	66.0	70.7	-14.15	-14.15	-14.18	-14.36
66	3.3	9.7	39.0	66.0	70.6	-14.20	-14.26	-14.04	-14.36
68	3.3	9.7	39.1	66.0	70.7	-14.08	-14.24	-14.11	-14.36
70	3.3	9.7	39.0	66.0	70.7	-14.18	-14.30	-14.14	-14.36
72	3.3	9.7	39.0	66.1	70.7	-14.43	-14.41	-14.15	-14.38

TABLE D2(b) - TRANSIENT TEST RESULTS FOR WALL S, SI UNITS

Time, hr	Measured Temperatures, °C					Measured Heat Flow, W/sq m			Calculated Heat Flow, W/sq m
	tc Outdoor Air	tcs Outdoor Surface	tmd Internal Therm.	tms Indoor Surface	tm Indoor Air	qw Calib. Hot Box	qhft HFT @ In. Surf.	qhft' HFT @ Out. Surf.	
0	23.1	23.4	23.2	22.7	22.5	1.33	0.55	0.05	1.02
1	5.3	13.0	23.2	22.7	22.5	2.12	0.60	-101.44	-14.30
2	-11.6	-1.5	22.6	22.7	22.5	2.14	0.58	-153.75	-35.32
3	-14.1	-5.8	20.9	22.6	22.4	1.49	0.33	-122.22	-41.49
4	-14.6	-7.4	18.8	22.4	22.4	-0.67	-0.59	-102.23	-43.48
5	-14.9	-8.4	16.8	22.1	22.3	-4.72	-3.16	-91.06	-44.39
6	-15.1	-9.1	15.1	21.8	22.2	-8.91	-6.61	-83.27	-44.87
7	-15.2	-9.6	13.7	21.5	22.1	-13.64	-10.56	-77.29	-45.10
8	-15.3	-10.0	12.4	21.1	22.1	-17.89	-14.54	-72.87	-45.23
9	-15.4	-10.3	11.3	20.9	22.0	-20.94	-18.05	-69.26	-45.29
10	-15.5	-10.6	10.3	20.6	21.9	-23.81	-21.09	-65.62	-45.28
11	-15.5	-10.8	9.4	20.4	21.9	-27.17	-24.23	-62.79	-45.30
12	-15.6	-11.1	8.6	20.2	21.8	-29.21	-26.87	-60.17	-45.28
13	-15.7	-11.2	8.0	20.0	21.8	-31.41	-29.13	-58.49	-45.32
14	-15.7	-11.4	7.4	19.8	21.7	-32.97	-31.14	-56.96	-45.30
15	-15.7	-11.5	6.9	19.7	21.7	-34.60	-32.93	-54.68	-45.30
16	-15.7	-11.6	6.5	19.6	21.7	-36.23	-34.75	-53.86	-45.31
17	-15.8	-11.7	6.2	19.5	21.7	-37.85	-35.93	-52.49	-45.32
18	-15.8	-11.8	5.9	19.5	21.7	-39.13	-37.50	-52.02	-45.34
19	-16.8	-11.9	5.6	19.4	21.6	-39.94	-37.95	-50.61	-45.37
20	-15.9	-12.0	5.4	19.3	21.6	-40.21	-38.98	-50.10	-45.35
21	-15.9	-12.0	5.2	19.3	21.6	-40.76	-39.93	-49.37	-45.37
22	-15.9	-12.1	5.0	19.2	21.6	-41.44	-40.43	-48.21	-45.36
23	-15.9	-12.1	4.9	19.2	21.6	-42.34	-41.05	-48.04	-45.36
24	-15.9	-12.1	4.8	19.2	21.6	-41.49	-41.65	-47.37	-45.35
26	-15.9	-12.2	4.5	19.1	21.5	-42.39	-42.29	-46.77	-45.37
28	-15.9	-12.3	4.3	19.0	21.5	-42.66	-43.14	-46.47	-45.36
30	-15.9	-12.3	4.2	19.0	21.5	-43.08	-43.65	-46.27	-45.35
32	-15.9	-12.3	4.1	19.0	21.5	-44.83	-44.36	-45.51	-45.35
34	-15.9	-12.3	4.1	19.0	21.5	-44.55	-44.45	-45.27	-45.35
36	-15.9	-12.4	4.0	18.9	21.5	-44.01	-44.55	-45.52	-45.34
38	-15.9	-12.4	4.0	18.9	21.5	-44.04	-44.53	-44.98	-45.34
40	-16.0	-12.4	4.0	18.9	21.5	-44.34	-44.43	-44.92	-45.34
42	-16.0	-12.4	4.0	18.9	21.5	-45.20	-45.13	-44.77	-45.37
44	-16.0	-12.4	4.0	19.0	21.5	-45.29	-44.73	-44.91	-45.37
46	-16.0	-12.4	4.0	19.0	21.5	-45.57	-45.10	-44.69	-45.41
48	-16.0	-12.4	4.0	19.0	21.5	-44.81	-44.89	-44.94	-45.39
50	-16.0	-12.4	3.9	18.9	21.5	-43.97	-45.30	-44.91	-45.36
52	-16.0	-12.4	3.9	18.9	21.5	-44.40	-45.02	-44.75	-45.33
54	-16.0	-12.4	3.9	18.9	21.5	-44.43	-45.21	-44.44	-45.31
56	-16.0	-12.4	3.9	18.9	21.5	-45.01	-45.11	-44.59	-45.32
58	-16.0	-12.4	3.9	18.9	21.5	-44.50	-44.98	-44.76	-45.35
60	-16.0	-12.4	3.9	18.9	21.5	-44.47	-45.22	-44.71	-45.29
62	-16.0	-12.4	3.9	18.9	21.5	-44.47	-45.06	-44.48	-45.28
64	-16.0	-12.4	3.9	18.9	21.5	-44.64	-44.64	-44.75	-45.29
66	-16.0	-12.4	3.9	18.9	21.5	-44.79	-44.98	-44.29	-45.30
68	-16.0	-12.4	3.9	18.9	21.5	-44.42	-44.94	-44.53	-45.30
70	-16.0	-12.4	3.9	18.9	21.5	-44.75	-45.13	-44.61	-45.31
72	-16.0	-12.4	3.9	18.9	21.5	-45.51	-45.45	-44.64	-45.37